Effects of Per-and Polyfluoroalkyl Substances (PFAS) on the Freshwater Gastropod (*Planorbella pilsbryi*) in the Laboratory and *in situ* Integrating a Multi-omic Approach

by

Almira Khan

A thesis submitted to the
School of Graduate and Postdoctoral Studies in partial
fulfillment of the requirements for the degree of

Master of Science in Applied Bioscience

Biology | Ontario Tech University | Science

University of Ontario Institute of Technology (Ontario Tech University)

Oshawa, Ontario, Canada
September 2023

THESIS EXAMINATION INFORMATION

Submitted by: **Almira Khan**

Masters of Science in Applied Bioscience

Thesis title: Effects of Per-and Polyfluoroalkyl Substances (PFAS) on the Freshwater Gastropod (*Planorbella pilsbryi*) in the Laboratory and *in situ* integrating a Multi-omic Approach

An oral defense of this thesis took place on September 14, 2023 in front of the following examining committee:

Examining Committee:

Chair of Examining Committee	Dr. Dario Bonetta
Research Supervisor	Dr. Denina Simmons
Research Co-supervisor	Dr. Ève Gilroy
Examining Committee Member	Dr. Andrea Kirkwood
Thesis Examiner	Dr. Robert Bailey, Ontario Tech University

The above committee determined that the thesis is acceptable in form and content and that a satisfactory knowledge of the field covered by the thesis was demonstrated by the candidate during an oral examination. A signed copy of the Certificate of Approval is available from the School of Graduate and Postdoctoral Studies.

ABSTRACT

Per- and polyfluoroalkyl substances (PFAS) are anthropogenic chemicals that are globally used in consumer and industrial applications. Specifically, perfluorooctane sulfonate (PFOS) has been under scrutiny due to its environmental persistence, toxicity, bioaccumulation potential, and long-range transport. PFOS can enter waterways and have adverse impacts on aquatic life through a broad range of toxic effects. In order to gain insight on how PFAS affects freshwater invertebrates, we conducted an *in situ* and laboratory exposure. For 28-days, we caged freshwater snails in a documented PFAS contaminated site and exposed snails in the laboratory at three different PFOS concentrations (0.1 -1000 µg/L). To understand PFAS affects, we examined survival, growth, and reproduction. Untargeted proteomics and metabolomics analyses were conducted on the laboratory data to examine the differences in protein and metabolite profiles. The laboratory multi-omic analyses indicated that PFOS significantly altered the abundance of various proteins and metabolites.

Keywords: PFAS; PFOS; proteomics; metabolomics; ecotoxicology

AUTHOR'S DECLARATION

I hereby declare that this thesis consists of original work of which I have authored. This is a true copy of the thesis, including any required final revisions, as accepted by my examiners.

I authorize the University of Ontario Institute of Technology (Ontario Tech University) to lend this thesis to other institutions or individuals for the purpose of scholarly research. I further authorize University of Ontario Institute of Technology (Ontario Tech University) to reproduce this thesis by photocopying or by other means, in total or in part, at the request of other institutions or individuals for the purpose of scholarly research. I understand that my thesis will be made electronically available to the public.

_____ ALMIRA KHAN

STATEMENT OF CONTRIBUTIONS

Two external collaborators assisted in PFAS analyses for this project. Each provided summarized results and methods to be included in this thesis. Dr. Amy Rand at Carleton University, Department of Chemistry (Ottawa, ON) conducted PFAS analyses of water, sediment, and snail tissue samples collected from the field exposure. Dr. Amila De Silva at Canada Centre for Inland Waters (CCIW), Environment and Climate Change Canada (ECCC) (Burlington, ON) conducted the PFAS analyses for the laboratory exposure. This included analysis of water and snail tissue samples. Lastly, John Toito at CCIW, ECCC (Burlington, ON) identified the spectral peaks for the metabolomic samples. This entailed running the metabolomic snail samples on the Orbitrap IDX Tribrid mass spectrometer. I would like to thank each of these contributors for their assistance in making this project possible.

I hereby certify that I am the sole author of this thesis and that no part of this thesis has been published or submitted for publication. I have used standard referencing practices to acknowledge ideas, research techniques, or other materials that belong to others. Furthermore, I hereby certify that I am the sole source of the creative works and/or inventive knowledge described in this thesis.

ACKNOWLEDGEMENTS

I would like to express my gratitude to my supervisors Dr. Denina Simmons and Dr. Ève Gilroy for being the most amazing mentors! You have both taken your time to share your valuable knowledge, enthusiasm, and time to mentor me for the past two years. Thank you both, for being such an inspiration for women in STEM. I am eternally grateful for your guidance, support, and patience.

Thank you to the Environment Canada Snail Lab and the Aquatic Omics Lab for supporting and uplifting me throughout my research, this would not be possible without each and every one of you. To David McNabney, Jeanne St-Laurent-Guérin, Maria Villela, Urvi Pajankar, Amy Delvechio, and Simon Pollard I am so grateful to have met and worked with each of you. I can't wait to keep growing alongside each of you!

To my family - Mom, Dad, Gibran, and Safiyah, thank you. Thank you for always believing in me even in times when I didn't believe in myself. Your unwavering support, sacrifice, constant encouragement, and endless cups of tea were always appreciated. I would not have been able to do this without you all, you are the greatest joys of my life and I am so proud to be a first generation Master's Graduate. I love you all ♥

TABLE OF CONTENTS

LIST OF TABLES

CHAPTER 3

LIST OF FIGURES

CHAPTER 3

LIST OF ABBREVIATIONS AND SYMBOLS

6:2 FTS	6:2 fluorotelomer sulfonates
AB	Ammonium Bicarbonate
ADAM	A Disintegrin and Metalloproteinases
ADAMTS	A Disintegrin and Metalloproteinase with Thrombospondin motifs
AFFF	Aqueous Film Forming Foam
ALRF	Aquatic Life Research Facility
ANOVA	Analysis of Variance
BCF	Bioconcentration factors
BTB	Blood-testis barrier
CCIW	Canada Centre for Inland Waters
CMP	Chemicals Management Plan
CTD	Comparative Toxicogenomic Database
Ctrl.	Control
DLCO	Diffusion capacity of the lungs for carbon monoxide
ECCC	Environment and Climate Change Canada
ERK1/2	Extracellular signal-regulated kinase 1/2
FAD	Flavin Adenine Dinucleotide
FMN	Flavin Mononucleotide
FWQG	Federal Water Quality Guideline
GO	Gene Ontology
HPLC	High-performance Liquid Chromatography
JNK	c-Jun N-terminal kinase
LC-MS/MS	Liquid Chromatography Tandem Mass Spectrometry
LOEC	Lowest Observable Effect Concentration
MAPK	Mitogen-activated protein kinases
MMP	Matrix metalloproteinases
MS/MS	Tandem mass spectrometry
NRTK	Non-receptor tyrosine protein kinase
p38MAPK	p38 MAPK pathway
PCA	Principal Component Analysis
PFAA	perfluoroalkyl acid
PFAS	Per - and polyfluoroalkyl substance
PFBA	Perfluorobutanoic acid
PFBS	Perfluorobutane sulfonic acid
PFDA	Perfluorodecanoic acid
PFDoDA	Perfluorododecanoic acid
PFDS	Perfluorodecane sulfonic acid
PFHpA	Perfluoroheptanoic acid

PFHxA	Perfluorohexanoic acid
PFHxDA	Perfluorohexadecanoic acid
PFHxS	Perfluorohexane sulfonic acid
PFNA	Perfluorononanoic acid
PFOA	perfluorooctanoic acid
PFOcDA	Perfluorooctadecanoic acid
PFOS	perfluorooctanesulfonic acid
PFPeA	Perfluoropentanoic acid
PFTeDA	Perfluorotetradecanoic acid
PFTrDA	Perfluorotridecanoic acid
PFUnDA	Perfluoroundecanoic acid
PPAR	Peroxisome Proliferator-Activated Receptors
PTK	Protein Tyrosine Kinases
Q-TOF	Quadrupole Time-of- Flight
RTKs	Receptor tyrosine kinase
SPE	Solid Phase Extraction
U.S EPA	United States Environmental Protection Agency
WW	Wet Weight

Chapter 1. Introduction

1.1 Significance

Per - and polyfluoroalkyl substances (PFAS) are widely used in industrial and consumer applications such as nonstick cookware, personal care products, disposable food packaging, stain resistant coatings, as well as in firefighting formulations (Glüge et al., 2020). Pathways into the environment include: surface runoff, product degradation, and wastewater effluent drainage which has led to the contamination of aquatic environments (J. W. Lee et al., 2020). These compounds are notoriously environmentally persistent due to the chemical stability of their fluorocarbon (C-F) bonds. The chemical stability diminishes the potential for chemical, biological, or thermal degradation, leading to accumulation within the environment (Lei, Tian, Sobhani, Naidu, & Fang, 2020). Aquatic organisms are therefore threatened due to PFAS exposure and its subsequent bioaccumulation (Flynn et al., 2019).

Initially, there was little concern regarding environmental fate and health impacts of PFAS, as they were thought to be inert and non-toxic. However, PFAS have become a global health concern worldwide (Sinclair, Long, & Jones, 2020). PFAS have a broad range of toxic effects on aquatic organisms, affecting growth, development, reproduction, mobility and survival (J. W. Lee et al., 2020). Furthermore, PFAS are reported endocrine disruptors in fish, causing reduced fecundity, increased malformations, and overall increased mortality in fish larvae (O'Connor, Partridge, Fielder, Woolley, & Palanisami, 2020). Although the health risks associated with the effects of PFAS in vertebrate species have been previously explored, it is imperative to further investigate the effects of

environmental contaminants on non-model species, particularly the many invertebrate species which play vital roles in aquatic ecosystem health. *Planorbella pilsbryi* is found in lakes, ponds, and streams of Canada (Prosser, Rodriguez-Gil, Solomon, Sibley, & Poirier, 2017). Importantly, these snails and their eggs are a vital source of food for many aquatic invertebrates and fish, making them an ecologically relevant species (Prosser et al., 2017). A recent study found that exposure to PFAS in snails induced significant oxidative stress with an increase in bioactive molecules such as peroxidases and catalases (Rijnders et al., 2021). However, very little is known about the molecular effects of PFAS on snails in response to exposure. Understanding molecular-level responses in snails such as changes in abundance of proteins and metabolites will help deduce the mechanisms behind whole-organism effects such as growth and development.

This thesis will focus on *P. pilsbryi* exposed to PFAS both in laboratory and *in situ*. This research will focus on studying the effects of PFAS on a lower-level aquatic species by studying specific endpoints, PFAS burden, and non-targeted proteomics and metabolomics. This will build upon the current knowledge of PFAS and further explore specific proteins, metabolites, and biological pathways that are affected by PFAS exposure.

1.2 Background Information

PFAS are a family of compounds that includes over 4000 individual anthropogenic chemicals (9). The 3M company is a known global manufacturer of PFAS, which began production in the late 1940s (Armitage et al., 2006; Sunderland et al., 2019). PFAS are chemicals composed of a chain of varying lengths of carbon with at least one or more fluorinated carbon within the chain (Buck et al., 2011). In addition, the compounds contain

a charged functional group which is commonly a carboxylic or sulfonic acid. PFAS can further be distinguished as either long or short chain compounds. Long chain compounds are perfluoroalkyl carboxylates with eight or more carbons and perfluoroalkyl sulfonates with six or more carbons (OECD, 2013). In comparison, short chain compounds are perfluoroalkyl carboxylates with seven or less carbons and perfluoroalkyl sulfonates with five or less carbons (OECD, 2013).

These chemicals are now classified as emerging contaminants, a class of contaminants that were previously not of concern nor monitored, but are now considered a concern, as they have the potential to cause adverse effects (Milley et al., 2018). Due to a prior lack of knowledge and monitoring of these chemicals, there is now widespread contamination. Unfortunately, there are knowledge gaps and a need for scientific understanding especially at the molecular level (Milley et al., 2018).

1.2.1 PFAS Bioaccumulation

PFAS have been measured in fish, birds, mammals, and even humans (DeWitt, 2015). Due to PFAS being proteinophilic these substances show an affinity for albumin, fatty acid binding proteins located in the liver, and organic ion transporters in the kidney (Martin, Mabury, Solomon, & Muir, 2013). In fish, PFAS are known to be stored in protein rich tissue such as the liver or blood (Martin et al., 2013). The Government of Canada has determined that PFOS has the ability to bioaccumulate in the tissue of organisms and biomagnify through the food chain in marine and terrestrial mammals as well as piscivorous birds (CEPA, 2018). The biomagnification of PFAS is dependent on interspecies variability, congener characteristics, and environment (George, Baker, &

Baker, 2023). Since invertebrates play a vital role in the food chain it is pertinent to investigate PFAS accumulation to gain an understanding of the trajectory of PFAS.

1.2.2 PFAS Sources

Both point and non-point sources contribute to PFAS pollution. Point sources of PFAS include manufacturing plants, landfills, PFAS applications (eg. aqueous film forming foam (AFFF)) and sewage treatment plants (Huset et al., 2008; Schultz et al., 2006). Examples of non-point sources include wet and dry atmospheric deposition released from original sources and contaminated runoff (K. L. Davis, Aucoin, Larsen, Kaiser, & Hartten, 2007; Huset et al., 2008; Schultz et al., 2006). It is evident that there are a wide variety of applications releasing PFAS into aquatic environments that further degrade and partition, thus posing a risk to aquatic organisms and habitats. Between 1951 and 2004, the total global emissions of PFAS, specifically that of perfluoroalkyl carboxylates, ranged between 3200 tons and 7300 tons (Prevedouros, Cousins, Buck, & Korzeniowski, 2006). It was reported that more than 95% of the total emissions are directly released into aquatic environments while less than 5% of emissions are released within the atmosphere (Paul, Jones, & Sweetman, 2009; Prevedouros et al., 2006). Once in the aquatic environment, PFAS are subjected to various partitioning, pathway degradation and global transport (Ahrens, 2011).

1.2.3 Aqueous Film Forming Foam

A key point source of PFAS into the environment is through the release of AFFF, a synthetic mixture used to coat the fuel layer of fires to suppress combustion (Milley et al., 2018). AFFF utilizes perfluoroalkyl acid (PFAA) additives as they act as a vapor sealant

to prevent the re-ignition of fuel and solvents (Alm & Stern, 1992; Kissa, 2001). AFFFs have been widely used at Canadian military and commercial airports for firefighting training (Milley et al., 2018). 3M was the major manufacturer of AFFF, which contained large proportions of PFAS, specifically, perfluorooctanesulfonic acid (PFOS) and perfluorooctanoic acid (PFOA); however both of these additives were removed from manufacturing in the early 2000s and 1976, respectively (Backe, Day, & Field, 2013; Place & Field, 2012; Prevedouros et al., 2006). The manufacturing industry then turned to an increase in production of fluorotelomers – a type of PFAS, predominantly 6:2 fluorotelomer sulfonates (6:2 FTS) (Gonzalez, Thompson, Quinones, Dickenson, & Bott, 2021). 6:2 FTS degradation pathways result in final products of short-chain PFAAs (Gonzalez et al., 2021). Short-chain PFAS are less studied and further research is needed to evaluate their environmental impacts.

AFFFs elicit environmental contamination during handling, storage, and usage (de Solla, De Silva, & Letcher, 2012). The Lester B. Pearson International Airport (Toronto, Canada) was responsible for accidentally releasing 22,000 L of AFFF into Etobicoke Creek in June 2000 (Moody, Martin, Kwan, Muir, & Mabury, 2002). Another incident occurred at the Lester B Pearson airport in 2005, when 48,000 L of AFFF was released to extinguish a fire (de Solla et al., 2012). A study by de Solla et al., (2012) noted that both of these incidents showed evidence of oxidative stress in fish found downstream of the airport. There is a lack of large-scale screening of Canadian Airports to estimate PFAS burden from the use of AFFF, in published scientific literature (Milley et al., 2018). This is a concern, as it is highly likely there are many more contaminated sites, but the number of which are

unknown to the general public, and therefore we have no way to estimate what levels of risk mitigation or clean-up are needed (Milley et al., 2018).

1.2.4 John C. Munro International Airport

John C. Munro International Airport is a known source of PFAS contamination in downstream waters. This airport contains a firefighting training area in the southwest quadrant of the airport property indicating the operational use of AFFF (Milley et al., 2018). Lake Niapenco, located in Binbrook, Ontario, is an artificial lake downstream of John C. Munro International Airport, which receives no wastewater treatment plant effluent discharge or runoff from nearby industries (de Solla et al., 2012). A study reported PFAS contamination due to the use of AFFF, and past activities at the airport (de Solla et al., 2012). Knowing Lake Niapenco is a documented contaminated PFAS site makes it a site of interest for *in-situ* studies.

1.2.5 Test Organism: P. pilsbryi

P. pilsbryi is a freshwater pulmonate snail that is a native Canadian species and is a simultaneous hermaphrodite (Clarke, 1981). In addition, this aquatic snail dominates the benthic zone and is the principal grazer that influences algal primary productivity (Hawkins & Furnish, 1987; Huryn, Benke, & Ward, 1995; Johnson et al., 2013). This species plays a pivotal role in the food web and assists with nutrient cycling in aquatic ecosystems (Covich, Palmer, & Crowl, 1999). These non-predatory species are often nestled in the benthic zone with direct exposure to potentially contaminated sediments, groundwater and other forms of pollution including runoff, untreated sewage and more (Johnson et al., 2013). *P. pilsbryi* is an ideal test organism as they are in constant contact with the substrate,

require low maintenance, and grow to large enough sizes to yield sufficient tissue for multi-omic and PFAS analysis.

1.3 Proteomics and Metabolomics

Non-targeted proteomics and metabolomics aim to detect as many molecules as possible in one analysis, to reduce bias, and capture universal information. Proteomic and metabolomic technologies have been developed to identify and quantify proteins and metabolites present in complex mixtures of biological samples. Over the last two decades, these technologies have been increasingly used to study the effects of chemicals on biological and molecular pathways in aquatic and terrestrial organisms (Horgan & Kenny, 2011; Martyniuk & Simmons, 2016).

Proteomics is a large-scale study of the proteins that are defined by a specific proteome (Patterson & Aebersold, 2003). This approach is a useful tool in environmental toxicology as it allows for adverse molecular responses in aquatic organisms to be observed (Simmons, Cowie, Koh, Sherry, & Martyniuk, 2019). Liquid chromatography tandem mass spectrometry (LC-MS/MS) based proteomics can utilize a bottom-up approach also referred to as shotgun proteomics (Martyniuk & Simmons, 2016). This approach focuses on identifying proteins by characterizing peptide sequences from complex mixtures following chemical or enzymatic digestion (Martyniuk & Simmons, 2016). Combining these proteomic technologies with bioinformatics allows for identification of organism responses observed through changes in protein abundance after an environmental exposure (Liang, Martyniuk, & Simmons, 2020). These observed changes can assist in identifying specific pathways being affected, and then extrapolated to understand the health status of the organisms.

Metabolomics focuses on metabolites which are the intermediate and final chemical products produced by living organisms during metabolism (Martyniuk & Simmons, 2016). The goal of metabolomics is to study the metabolome which is the entirety of endogenous metabolites within a biological sample through multiple analyses (Martyniuk & Simmons, 2016). The metabolome is dynamic and dependent on factors such as tissue type and the environment. More specifically, the metabolome is responsive to chemical effects which can be observed through changes in metabolite abundance (Martyniuk & Simmons, 2016). Various instrumental approaches can be used in metabolomics studies such as Nuclear Magnetic Resonance, LC-MS/MS, and gas-chromatography mass spectrometry (Martyniuk & Simmons, 2016).

1.4 Research Contribution

The estimated $2 billion PFAS industry is reaping the economic benefits, but is failing to take responsibility for the long-term costs associated with environmental exposures (Milley et al., 2018). However, contaminated site clean-up has been progressing, and the government recognizes a future liability cost of an estimated $5.8 billion dollars (Schultz et al., 2006). By investigating the effects of PFAS on lesser studied, ecologically relevant aquatic organisms such as *P. pilsbryi* will provide a wider scope of risks posed by this class of contaminants. Furthermore, chronic level toxicity testing of specific PFAS compounds will contribute to the assessment of environmental risks, as most biological effects at environmentally relevant concentrations are seen after longer durations of exposure. Using proteomic and metabolomic approaches as a tool to investigate PFAS toxicity is promising as it is able to detect all possible responses to contamination induced

at the molecular level. The data generated from this thesis will help to predict the potential adverse effects of PFAS on aquatic invertebrates, potentially leading to policies that help to prevent increased PFAS pollution and environmental impacts.

The Chemicals Management Plan (CMP) was created by the Government of Canada in 2006 to aid in the protection of human and environmental health by managing risks posed by chemical substances (Easton, 2008). By assessing if substances in Canada are harmful to the environment and Canadians through scientific research, the government can further decide on risk management and enforcement guideline implementation (Easton, 2008). This research will contribute to the CMP by providing information on the potential impact of PFAS on aquatic ecosystems and organisms. We not only evaluated observable outcomes pertaining to survival, growth, and reproduction that are referred to as apical endpoints, but also investigated at the molecular level. This research will help deepen the understanding of how PFAS play a role at environmentally relevant and sublethal concentrations.

1.5 Research Objectives

The goal of this thesis is to examine the effects of PFAS on the freshwater *P. pilsbryi* through the investigation of apical endpoints and toxicological effects on the proteome and metabolome of freshwater snails. In order to achieve these goals two research objectives were proposed.

Objective 1. *To investigate the chronic toxicity of PFAS on snails within a laboratory setting.* This research objective entailed conducting a 28-day PFOS exposure to adult snails to observe if PFOS affects survival, growth, and reproduction. In addition, this objective will allow for the proteome and metabolome of snails to be studied in response to PFOS.

Changes in protein and metabolite expression are observed to potentially identify biomarkers of exposure and biological pathways affected.

Objective 2. To a*ssess the in situ effects of PFAS at environmentally relevant concentrations on apical endpoints.* This research objective focuses on deploying snails in Lake Niapenco, an environmentally relevant area. Survival, growth, and reproduction as well as bioconcentration was recorded and analyzed. This objective assists in understanding how environmentally relevant levels of PFAS mixtures are affecting aquatic organisms in real aquatic environments.

Chapter 2. Methods

2.1 Test Organism: *P. pilsbryi*

A continuous culture of *P. pilsbryi* was established and used in the Aquatic Life Research Facility (ALRF), Canada Centre for Inland Waters, located in Burlington, Ontario. This culture was initially established by the Ministry of the Environment, Conservation and Parks (Etobicoke, Ontario). The snail culture located in the ALRF is held in 75 L aquaria maintained at a light period of 16 hours of light to 8 hours of dark at ~22°C. The aquaria are filled with ALRF water supplemented with $CaCO_3$, to optimize growth conditions for freshwater snails. The snails' diet consists of organic spinach and whole shrimp pellets (Omega One Catfish Pellets). Once a week, the aquaria filters and aquaria are cleaned, including manual removal of detritus from the filters and syphoning.

2.2 Field Study

2.2.1 Field Sites

Two field sites were chosen based on proximity to the John C. Munro International Airport. The first site was located at 43°06’41.9” N, 079°52’52.2” W and represented the contaminated site, known as the Binbrook Conservation Area. The second site was located at 43°09’18.4” N, 079°51’14.2” W and represented the reference site, known as Twenty-Mile Creek. These sites were visited and inspected in October 2021 and again in May 2022 to determine if the water conditions were acceptable and accessible by wading into the water. During the initial visits, sufficient dissolved oxygen and biodiversity including: snails, fish and crustaceans were observed. Both sites were deemed acceptable for the field study to be conducted in June 2022.

2.2.2 Experimental Design

Three days prior to the field deployment, 180 adult snails from the ALRF culture were inspected to ensure they were healthy and fit for caging conditions. A digital field scale was used to measure the weight (wet weight (g)) and digital callipers measured the length (mm) of each snail. In order to acclimate the snails and assess fertility, a total of 36 - 1L mason jars with 5 snails in each were set up for 3 days. The snails were fed 3 g of fresh organic spinach and ¼ tsp of shrimp pellets. After the three days, fertility was measured by counting the number of egg masses produced per jar, including egg masses on the spinach leaves and on the snails.

A stratified randomization was used to control variation within the experiment. The experimental groups included: floating cages, sinking cages, reference site and contaminated site (n = 45 per experimental group). This randomization was completed in order to account for the difference in fertility amongst the snails. More specifically, it helped to ensure there was an even distribution between the replicates of the treatments. Due to low survival of snails exposed in the sinking cages, only the data from the floating cages were analyzed. A possible explanation for the low survival rate could be due to low dissolved oxygen in the water.

2.2.3 Field Set-up

On the day of the deployment, snails were transferred from the acclimation jars to field cages and transported in aerated coolers filled with $CaCO_3$-supplemented ALRF water. The cages were constructed using transparent acrylic tubes with 300 μm Nitex net on each side; this design is adapted from to increase cage size for an approximate volume

of 1L. Each sealed field cage was approximately 1L and consisted of 5 adult snails per cage, 3 g of fresh organic spinach and ¼ tsp of shrimp pellets. Food was replenished weekly and cages were deployed for a duration of four weeks.

A total of 18 cages were deployed at each site - 9 cages were submerged (sinking) and 9 cages were floating. The floating cages were equipped with fragments of pool noodles to enable flotation. All of the cages were secured using 10 lb weights (3 sinking cages and 3 floating cages per weight) and stainless-steel wire. In order to avoid movement of the cages, the weights were secured to a fixed landmark along the shore.

Water quality parameters were measured using a YSI Probe deployed at each site. Measurements were collected every 30 minutes throughout the exposure duration. Continuous data on pH, temperature, dissolved oxygen, and depth were collected (YSI data and water chemistry can be found in Appendix A and Appendix B). However, measurement recordings were inconsistent near the end of the experiment. This is due to equipment error and resulted in fewer readings being recorded. This issue could be potentially due to mud and debris disrupting the data collecting sensor.

2.2.4 Weekly Evaluation

Once a week the sites were visited to feed the snails, perform health checks, and record observations. Each cage was evaluated for fertility and survival, as the cages were opened, the number of egg masses were counted, and any dead snails were removed. Snails were then transferred to clean cages, with each transfer being tracked by recording the cage identification number. Algae and food would clog the mesh sides of the cages, potentially decreasing water and oxygen flow, therefore new cages were used weekly. Flotation devices were also replaced to maintain the flotation integrity.

2.2.5 Whole Tissue Collection

After the completion of the *in-situ* exposures, the cages were retrieved and transferred to aerated coolers containing site-specific water and transported back to the ALRF – CCIW (ECCC – Burlington, ON). Once the snails were returned to the ALRF, weight, length, and fertility were recorded as the final measurements. Digital callipers were used to measure the snails shell length, a digital field scale was used to measure the weight, and egg masses were counted to evaluate fertility. The shell of the snails were removed and the snail tissues were transferred to individual pre-labelled cryogenic vials where the snails were flash frozen in liquid nitrogen. The vials were then stored at -80°C to be used for analysis at a later date.

2.2.6 Analysis of PFAS Concentrations in Field Samples (water, tissue and sediment)

For the in-field exposure, water and sediment were collected at the conclusion of the 28-day deployment. At each site, surface water was collected in 1L polyethylene bottles. In addition, a Ponar Grab Sampler was used to collect 3 replicates of sediment per site. The sediment samples were collected in 500mL glass jars. The water and sediment samples were brought back to CCIW where they were then stored in a -20 freezer.

Later, water, sediment, and snail whole-body tissue were sent to Dr. Amy Rand's laboratory at Carleton University - Ottawa, Ontario for PFAS analysis. The samples were shipped from Burlington to Ottawa in an insulated foam container containing ice packs. Previously established methods of solid phase extraction and LC-MS/MS were utilized for analysis of the samples (EPA, 2021; ISO, 2019)

2.3 Laboratory Study

2.3.1 Chemical Test Solution Preparation

Heptadecafluorooctanesulfonic Acid Potassium Salt ($C_8F_{17}KO_3S$), purity ≥ 95%, was obtained from Toronto Research Chemicals (Toronto, Ontario) in a solid state. Control and stock solutions were prepared using ALRF water and $CaCO_3$. The stock solution (1000 µg/L) was prepared by dissolving PFOS salt in a solid state using a heat-plate and stirrer. Once the PFOS salt was in solution and at room temperature, $CaCO_3$ was added. A series of dilutions were performed to obtain the other treatment concentrations (0.1, 1, 10, 100 µg/L). Treatment solutions were made in two - 12 L batches. The first batch was used for day zero and seven water renewals and the second batch was used for day 14 and 21 water renewals. For this study a control, low, medium, and high treatment with a concentration of 0, 1, 10, and 1000 µg/L respectively were used.

2.3.2 Experimental Design

Acclimation of adult snails took place in 1L plastic jars in order to prevent PFOS from accumulating onto glass surfaces. There were 180 adult freshwater snails from the continuous culture selected based on size. The initial weight (g) and length (mm) of each snail was recorded using digital callipers and a scale; these measurements represented day -3 of the experiment. 1L plastic jars housed 5 snails, 3 grams of fresh organic spinach and ¼ tsp of whole-shrimp pellets. The snails were left for three days in order to assess fertility. At the end of the acclimation period, the egg masses produced in the jar, on the spinach, and on the snails were counted.

2.3.3 Adult Chronic Exposure Study

A 28-day chronic laboratory exposure to PFOS was performed on 180 adult *P. pilsbryi* . Following a three-day acclimation period, five adult snails were placed into clear round wide-mouth polystyrene - 32 oz plastic jars (Model No. S-9937) containing ALRF water using a stratified randomization. As previously explained, this randomization was used to allow for an even distribution of fertility between the replicates of treatments.

Water renewals occurred once a week on days 7, 14, and 21. Food was replenished twice a week and consisted of ~0.1g of ground shrimp pellets (Omega One Catfish Pellets) and 1 organic spinach leaf per jar. Fertility and survival were assessed throughout the exposure period, with fertility being evaluated twice a week on days 3, 7, 10, 14, 17, 21, 24, and 28, and any dead snails were removed from the study. Fertility assessment included counting the egg masses produced on the jar, spinach, and snail shells. Egg masses produced on the jar were circled and colour coded to keep track of egg masses produced per assessment. Egg masses on the spinach leaves were counted, then the spinach leaf was removed. Furthermore, the egg masses produced on the snail shells were removed using a Kimwipe in order to avoid counting the same egg masses twice.

2.3.4 Whole Tissue Collection

Concluding the 28-day exposure, the snails were taken to a procedure room located in the ALRF to record length and weight parameters and collect the whole-body tissue for analysis. In order to obtain the whole snail tissue, the shells of the snails were removed, and the snail tissue was gently dried on filter paper. The individual whole snail tissue was then inserted into pre-labelled cryogenic vials which were then flash frozen using liquid

nitrogen. The vials were then stored at -80°C for preservation awaiting omic and PFAS analyses.

2.3.5 Analysis of PFAS Concentrations in Laboratory Water Samples

The stock solutions were collected prior to laboratory exposure and the composite residues were collected after seven days of laboratory exposure. Water samples were analyzed for PFAS in Dr. Amila De Silva's laboratory at CCIW, ECCC (Burlington, Ontario). Samples were diluted with 50/50 methanol water and spiked with isotopically labelled standard. No peaks were detected in method blanks and most controls. Method detection limit is based on S:N of 3 multiplied by dilution factor. Analytes were detected in the lowest treatment but did not agree well with the nominal. Therefore, the low-level treatments were also analyzed using solid phase extraction.

Control samples and media at the 0.1 and 1 µg/L treatment were subjected to solid phase extraction (SPE) to enhance the signal and accuracy of quantitation. Briefly, the weak anion exchange cartridge (OASIS WAX) was conditioned using 5 mL 0.2% ammonia methanol, followed by 5 ml of polished High-performance liquid chromatography (HPLC) grade water. A subsample of 8.5 ml media was spiked with 30 µl of internal standard and then loaded on the SPE by gravity. The cartridge was dried under a strong vacuum for 30 min and eluted using 5 ml of 0.2% NH_4OH in methanol. The extract was concentrated to dryness using N_2 gas and reconstituted in 1.0 ml 50/50 methanol water. Analytes were not detected in the cartridge blanks. Therefore, the method detection limit for SPE samples were based on the S:N 3 and the concentration factor (8.5). Due to these lower detection limits, we occasionally detected PFOA and PFOS at trace levels. Recovery of the internal standard in SPE extracts corresponded to 65 ± 4.9 M3PFOS and 68 ± 5.7% M4PFOA based

on peak area compared to the calibration curve. SPE method detection limits were 0.00485 ug/L PFBA, 0.001197 ug/L PFHxA, 0.001615 ug/L PFOA, 0.000768 ug/L PFBS, 0.001247 ug/L PFHxS, and 0.001725 ug/L PFOS. For all samples that were handled both with SPE and dilution, the SPE data is considered more accurate because it doesn't require a calibration curve extrapolation.

2.3.6 Analysis of PFAS Concentrations in Laboratory Tissue Samples

Subsamples of 0.28 g, wet weight of whole-body snails were cut into small pieces using stainless steel forceps and scissors and accurately weighed for extraction into a 15 ml conical polypropylene tube. Samples were spiked with 30 μL of an isotopically labelled standard mix. Extraction was conducted by vortex, ultrasonication, and mechanical shaker into 5 ml acetonitrile, twice. Both extracts were combined and concentrated to 1.0 ml using nitrogen. The extract was subjected to a dispersive carbon clean-up and then concentrated to 0.5 ml. For optimal chromatography, 0.5 ml of SPE-polished HPLC-grade water was added to ensure the final extract volume was 1.0 ml and the concentration of isotopically labelled standards was 1.0 ng/ml. The extracts were analyzed by ultra-performance liquid chromatography - tandem mass spectrometer using a Thermo Vanquish Altis system. An 18-level calibration curve was employed ranging from 0.012 ng/ml to 30 ng/ml of C4 to C14 PFCA and C4 to C10 PFSA (R2>0.99). QA/QC consisted of spike and recovery using control snail tissue, five method blanks, and analysis of National Institute of Standards and Technology (NIST) Lake Superior 1946 SRM (R).

2.4 Field and Laboratory Post-Experimental Applications

2.4.1 Whole Snail Tissue Omics Extraction

Whole snail tissues were removed from a -80°C freezer and thawed on ice. Upon complete thaw, the entire tissue samples were weighed in pre-weighed 2-mL reinforced homogenization tubes. Five times the volume:mass of 100 mM ammonium bicarbonate buffer (AB buffer) was added to the tubes. Samples were homogenized using 4 - 2.4mm stainless steel beads and a mill (Bead Mill 24 Homogenizer, Fisherbrand™).

Ice cold HPLC-grade methanol was used to quench each homogenate at a ratio of 200 µL:400 µL. The modified Bligh-Dyer liquid-liquid phase extraction method was executed herein; samples were sonicated five times for one second, and then we sequentially added 200 µL of chloroform, 200 µL of MilliQ H2O, followed by 50 µL of chloroform with a 20 s vortex to mix between each addition. Samples were then centrifuged (5000 SERIES MICRO, OHAUS) at 5000 rpm for 30 min at 4°C, which yielded three visually distinct layers: an upper aqueous phase layer containing amino acids and polar metabolites, a lower organic phase layer containing lipids and non-polar metabolites, and a middle layer containing a disk of precipitated proteins.

2.4.2 Whole Snail Tissue Amino Acid Metabolomics

250 µL of the aqueous phase was pipetted into a clean low retention tube. Eight pooled composite samples were created using 5 µL per 10 samples to serve as a quality control parameter. The composite samples and blanks were spiked using 5 µL of the L-Leucine-5,5,5-d3(Sigma-Aldrich, CAS:87828-86-2) internal standard. All samples were evaporated using a centrifugal evaporator (AES2000-220 Automatic Environmental

SpeedVac with Vapornet, Savant) to obtain a near-dryness state. All samples were then re-suspended in 55 µL of 90% acetonitrile (ACN) 10% H_2O (for HILIC metabolomics) solution, and vortexed. The entire volume of the re-suspended samples was then transferred into glass HPLC vials equipped with PPE spring-bottom inserts.

2.4.3 HPLC Metabolomics Method

Separation of the samples were performed using an Agilent 1260 Infinity II LC coupled to a Thermo Scientific Orbitrap IDX Tribrid mass spectrometer (gradient conditions shown in Appendix C). Solvent A consisted of 90% Acetonitrile:10% Water, 10mM ammonium formate, 0.1% formic acid and solvent B consisted of 10mM ammonium formate 0.1% formic acid. The chromatographic column used was a SeQuant ZIC cHILIC (Thermo Scientific™, 3µm,100Å 100 x 2.1 mm, PEEK LINED) operated at a flow rate of 0.5 mL/min at 50°C. The injection volume of each sample was 5 µL.

Mass spectral data were obtained using the Orbitrap full-scan mode from 100 - 1000 m/z at a resolution of 120,000 the full width at half maximum. The pooled samples were run in data-dependent Orbitrap high energy c-trap dissociation MS2 mode (ddMS2 OT HCD) operated in electrospray positive mode for feature/metabolite identification and annotation. Further MS setup data can be found in Appendix C.

Individual Thermo Fisher Scientific raw MS/MS (Tandem mass spectrometry) spectra files were analyzed for untargeted metabolomics. The files were converted to. mzML format using MSConvertGUI (64-bit). Metabolomic data analysis was completed using online MetaboAnalyst version 5.0. The liquid chromatography – mass spectrometry Spectra Processing module was used, which allows for raw liquid chromatography – mass

spectrometry spectra to be processed through the optimized MetaboAnalyst - OpticLCMS workflow (OptiLCMS (1.0.5)).

2.4.4 Whole Snail Tissue Proteomics

Protein disks were resuspended in 50 µL of 100 mM AB buffer with gentle vortex. After this, proteins were reduced with the addition of 2.65 µL of 100 mM of tris (2-carboxyethyl) phosphine in 100 mM AB buffer, mixed using gentle vortex, and allowed to incubate at room temperature for 45 min. Proteins were then alkylated with the addition of 2.8 µL of 200 mM iodoacetamide in 100 mM AB buffer, vortexed gently, and incubated in the dark at room temperature for 45 min. At the end of the second incubation, 50 µL of chemical digestion solution (20% formic acid v/v) was added to each sample and vortexed for 5 s. The tubes were capped with lid locks, and incubated at 115°C for 30 min in a heating block (VWR 96 place heating block). Samples were dried in a centrifugal evaporator (SpeedVac, Thermo-Fisher) for 40 min. Dried samples were stored at 4°C overnight, and then resuspended in 20 µL of 95% H_2O, 5% acetonitrile, and 0.1% formic acid. Samples were vortexed until dried pellets were completely dissolved, and then centrifuged for 10 min at 14000 × g. 20 µL of the sample supernatant were added to 2 mL screw thread HPLC vials (Chromatographic Specialties, 12 × 32 mm) containing 250 µL pp. bottom spring inserts (Canadian Life Sciences, 6 × 29 mm). Samples were stored at 4°C until instrumental analysis.

2 µL of the peptide solution from each sample were injected and then separated by reverse phase liquid chromatography using a Zorbax, 300SB-C18, 1.0 × 50 mm 3.5 µm column (Agilent Technologies Canada Inc., Mississauga, ON) using an Agilent 1260

Infinity Binary LC. The Agilent 6545 Accurate-Mass Quadrupole Time-of- Flight (Q-TOF) was used as the detector in tandem with the Agilent 1200 series liquid chromatography system. Samples were separated with a gradient using solvent A (95% H_2O 5% acetonitrile and 0.1% formic acid) and Solvent B (5% H2O 95% acetonitrile and 0.1% formic acid).

Spectral files for each sample were analyzed using Spectrum Mill Software (Version B.04.01.141). Peptides were searched against a concatenated Uniprot Reference Proteome for *Homo sapiens* (humans) and *Biomphalaria glabrata* (Bloodfluke planorb - Freshwater snail) (ID: UP000005640; ID: UP000076420, downloaded January 2022). Proteins were then manually validated and accepted when at least one peptide had a peptide score (quality of the raw match between the observed spectrum and the theoretical database spectrum) greater than 6 and a %SPI (Scored peak intensity; the percentage of the spectral peak-detected ion current explained by the search interpretation) greater than 70% (these settings are recommended by the manufacturer for validating results obtained with an Agilent Q-TOF mass spectrometer).

After peptides were sequenced and identified by Spectrum Mill at the MS/MS level, quantification at the MS1 level was performed using the data dependent acquisition workflow in Skyline 20.2 (MacCoss Lab Software) with a score of 0.9, retention time window of 5 mins, and 5 missed cleavages with transition settings for TOF (Pino, Just, MacCoss, & Searle, 2020).

In order to classify the human gene symbols for the original Uniprot accession numbers, a python script utilizing the Basic Local Alignment Search Tool was used to find the closest human protein ortholog and official gene symbol. This tool compares protein

sequences and statistical significance of matches in order to confidently identify similar sequences in proteins. Further data consolidation occurred in Excel (2016) using the official gene symbols in order to remove duplicate values. Additionally, values less than or equal to 2000 were removed and replaced with a blank value so that they could be replaced with ⅓ of the detection limit in subsequent statistical analyses.

2.5 Statistical Analysis

2.5.1 Field and Laboratory Endpoint Analysis

All apical endpoint data including survival, growth and reproduction were analyzed in Graph Pad Prism 9.5.1. In addition, all jars/cages were analyzed using unpaired t-tests or Analysis of Variance (ANOVA) to test for differences between mason jar or cage effects ($p < 0.05$). An Analysis of Covariance (ANCOVA) was used to analyze survival of the field and laboratory exposures independently. Reproduction parameters were statistically analyzed based on the number of egg masses laid per number of snails alive per jar or cage. For the field exposure, an unpaired Welch t-test was performed to determine potential significance between the two field sites. For the laboratory exposure a repeated measure ANOVA and Tukey's multiple comparisons tests were used. Furthermore, T-test and ANOVA testing were performed to determine if there was a significant difference between field sites and laboratory exposure concentrations, respectively. A two-way ANOVA was used to compare differences between initial (day 0) and final (day 28) measurements followed by Tukey's multiple comparisons tests.

2.5.2 Field and Laboratory Sample Analysis

Graph Pad Prism 9.5.1 was used to analyze the measured PFAS within water, sediment and tissue data. For the field data, unpaired t-tests were used to determine if there was a significant difference ($p < 0.05$) between the reference and contaminated site. In terms of the laboratory data, ANOVA tests were used to determine if there was a significant difference between the nominal, stock solution, and residue concentrations. Lastly, bioconcentration factors (BCF) were calculated by dividing the mean tissue concentration by the mean concentration of the aqueous media.

2.5.3 Proteomics Lab Data

Statistical analysis of the laboratory data was performed with Metaboanalyst 5.0 (Xia, Psychogios, Young, & Wishart, 2009). Missing values were replaced with 1/5 of the limit of detection, normalized using median, square root transformation and range scaling, and then ANOVA (Fisher's LSD post-hoc) Principal Component Analysis (PCA), and heatmaps were created with the normalized data and top proteins from the ANOVA results. A PCA was used to help identify potential outliers and heatmaps were created to show visual differences in protein abundances.

2.5.4 Metabolomics Lab Data

Statistical analysis of the laboratory data was performed using Metaboanalyst 5.0 (Xia et al., 2009). Missing values were replaced with 1/5 of the limit of detection, features were filtered based on relative standard deviation and the data were normalized using median, cube root transformation and range scaling. PCA and ANOVA (Fisher's LSD

post-hoc test) were conducted with the normalized data to identify potential outliers within the dataset.

2.5.5 Significant Proteins/Metabolites and Pathway Analysis

Due to the large dataset undergoing multiple pairwise comparisons, I opted to use the raw p-value (< 0.05) after ANOVA without BH-FDR correction to identify proteins and metabolites with significantly different abundance among exposure groups. Proteins and metabolites that had a p-value of <0.05 were identified and combined into a smaller list which represented all significantly changed proteins or metabolites. These smaller lists were used for further analyses, including identifying biological and molecular pathways affected, as well as related diseases. Significant proteins ($p < 0.05$) were analyzed using Gene Ontology (GO) enrichment analysis. GO biological process, molecular function, cellular component, protein class, and reactome pathways were manually chosen based on significance and number of genes related to a specific ontology. The Comparative Toxicogenomic Database (CTD) set analyzer and MyGeneVenn tool as well as g: Profiler's functional enrichment analysis were used for data analysis. Significant proteins ($p< 0.05$) were analyzed for tissue and disease-related specificity and selected based on the number of proteins related to specific gene sets. For the metabolomic data, putatively annotated metabolites (Level 2) were uploaded to Metaboanalyst's Enrichment Analysis tool to determine the top 25 enriched processes.

Chapter 3. Results

3.1 Apical Field Endpoints

There were no differences between the slopes of the progression of survival over time ($p = 0.878$) (Figure 3.1). Statistical analysis revealed the final length ($p = 0.207$) and weight ($p = 0.905$) did not vary significantly between the two field sites. Among the snails that did survive to the end of the 28-day field exposure, there was a significant increase in both length (Figure 3.2) and weight (Figure 3.3) between day 0 and day 28 measurements ($p < 0.0001$). Overall, significant differences in reproduction were not observed within the first three weeks. However, after four weeks, there were significant differences in the number of egg masses produced between the reference and contaminated site, with more egg masses produced in the contaminated site ($p = 0.000234$) (Figure 3.4).

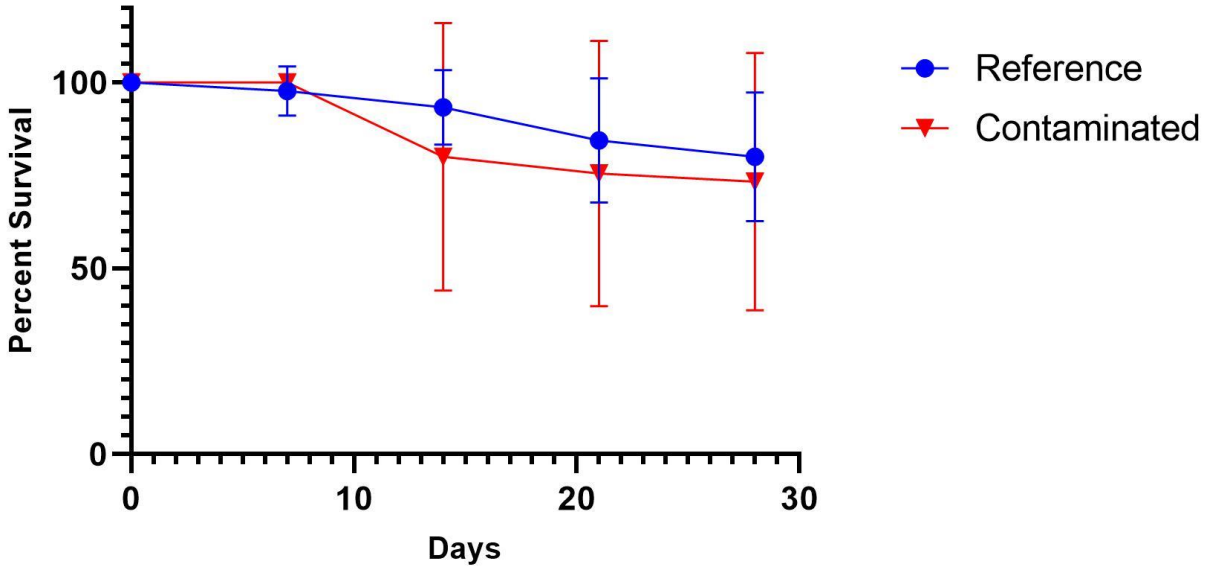

Figure 3. 1. Survival curves of *P. pilsbryi* deployed at two field sites. An ANCOVA determined there was no significant difference between the slopes of each curve (p = 0.878). The reference site is represented by a blue circle symbol and the contaminated site represented by a red upside down triangle symbol.

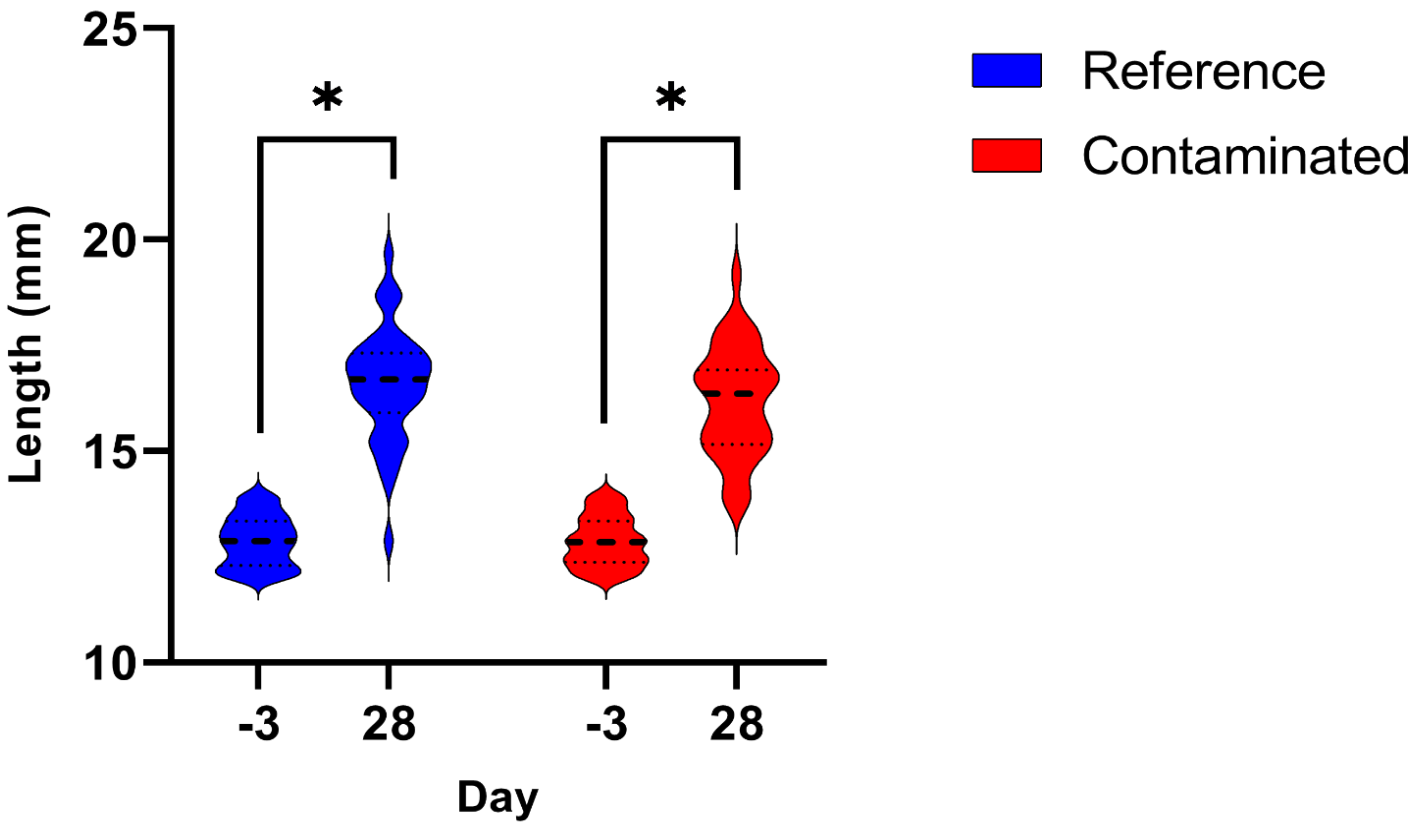

Figure 3. 2. Average initial and final snail shell length of *P. pilsbryi* deployed at two field sites for 28 days. The initial and final length measurements were acquired on day -3 and day 28 respectively. Final snail lengths were significantly larger than the initial lengths ($p < 0.0001$), but did not differ between sites ($p = 0.239$).

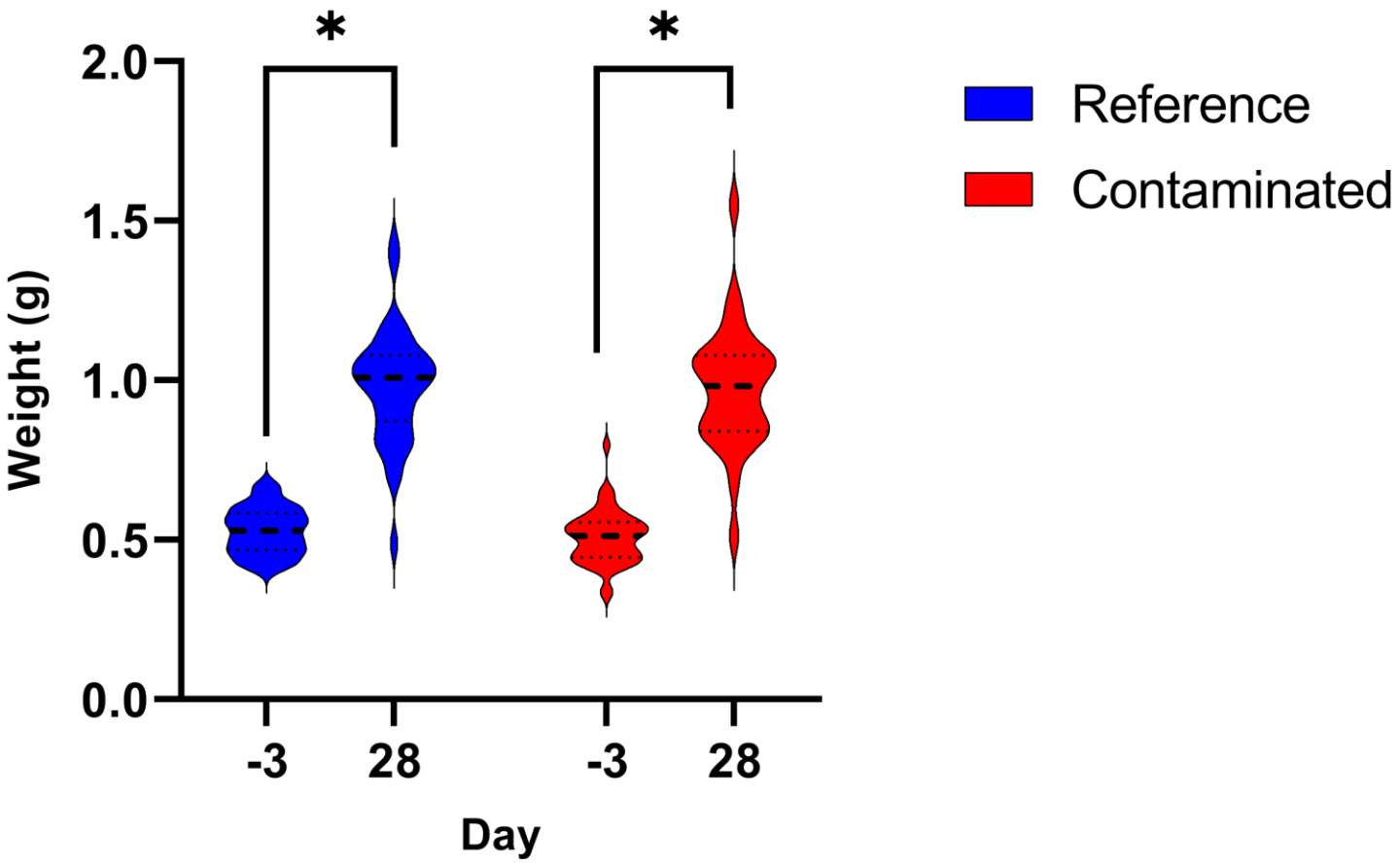

Figure 3. 3. **Average initial and final snail weight of *P. pilsbryi* deployed at two field sites for 28 days.** The initial and final weight measurements were acquired on day -3 and day 28, respectively. Final snail weights were significantly larger than the initial lengths ($p < 0.0001$), but did not differ between sites ($p = 0.521$).

.

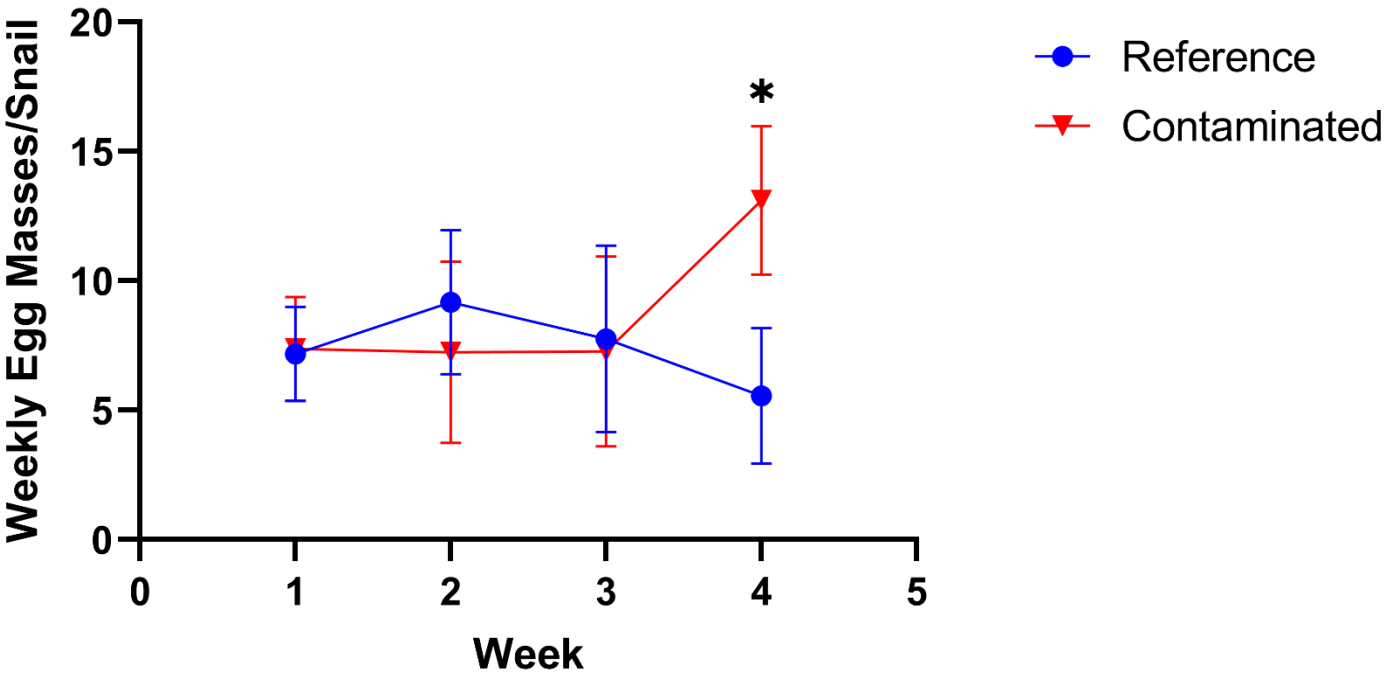

Figure 3. 4. Average weekly egg masses produced per snail alive per cage of *P. pilsbryi* deployed at two field sites for 28 days. There is a significant difference between the reference and contaminated site at week four ($p < 0.05$). The reference site is represented by a blue circle symbol and the contaminated site represented by a red upside down triangle symbol.

3.2 Apical Laboratory Endpoints

Snail survival was not affected by PFOS concentration in the laboratory exposure, There were no differences between the slopes of the progression of survival over time ($p = 0.796$) (Figure 3.5). Throughout the 28-day laboratory exposure, all snails survived except for one snail within the medium treatment that died on day three. This death was likely due to chance variation among the snail population. Our toxicity testing methods are based on previously established methods, which follow the criterion that the mean control should not exceed 20% mortality in order for the test to be valid (OECD, 2016). This confirms the validity of our test as the mortality of the control group was 0.33%. Final length ($p = 0.261$) (Figure 3.6) and final weight ($p = 0.412$) (Figure 3.7) did not differ significantly between the exposure concentrations. However, the surviving snails displayed a significant difference in length and weight between day 0 and day 28 of the 28-day laboratory exposure ($p < 0.0001$) (Figure 3.8). Overall, varying PFOS concentrations did not affect the reproductive output of the snails ($p = 0.265$).

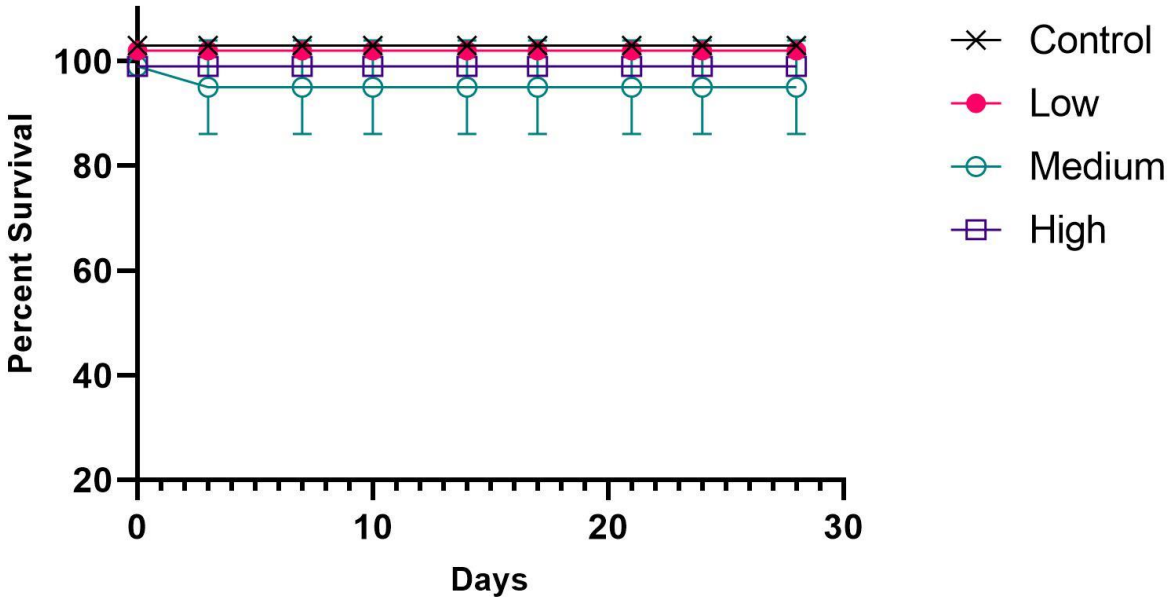

Figure 3. 5. Survival curves of *P. pilsbryi* exposed to PFOS for 28 days. An ANCOVA determined there was no significant difference between the slopes of each curve (p = 0.796). Each concentration is represented by a specific colour and patterned line. The data for the control, low, and high treatments represent 100% survival, data units were incremented along the Y – axis to avoid overlap.

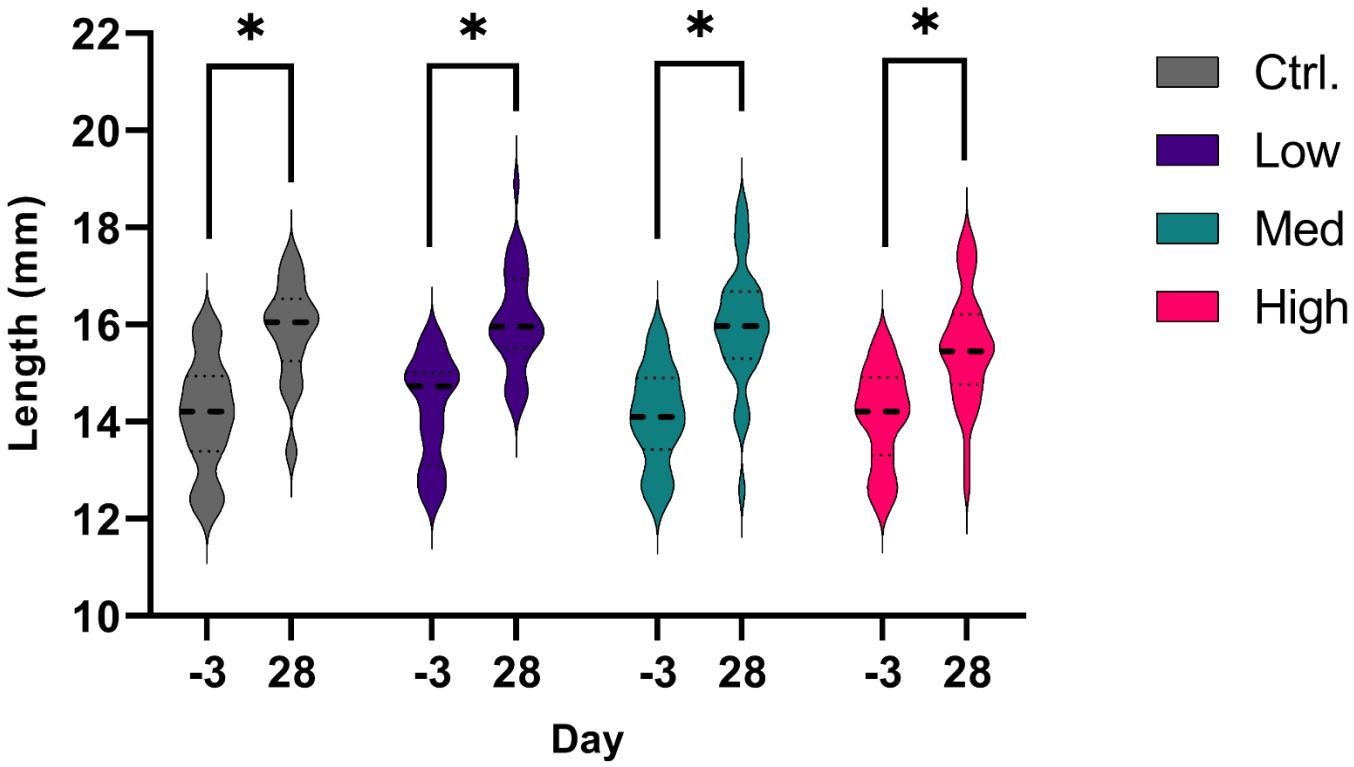

Figure 3. 6. Average initial and final snail shell length of *P. pilsbryi* exposed to 3 differing concentrations for 28 days. The initial and final length measurements were acquired on day -3 and day 28 respectively. Snail final lengths were significantly larger than the initial lengths ($p < 0.0001$), but did not differ between treatments ($p = 0.353$).

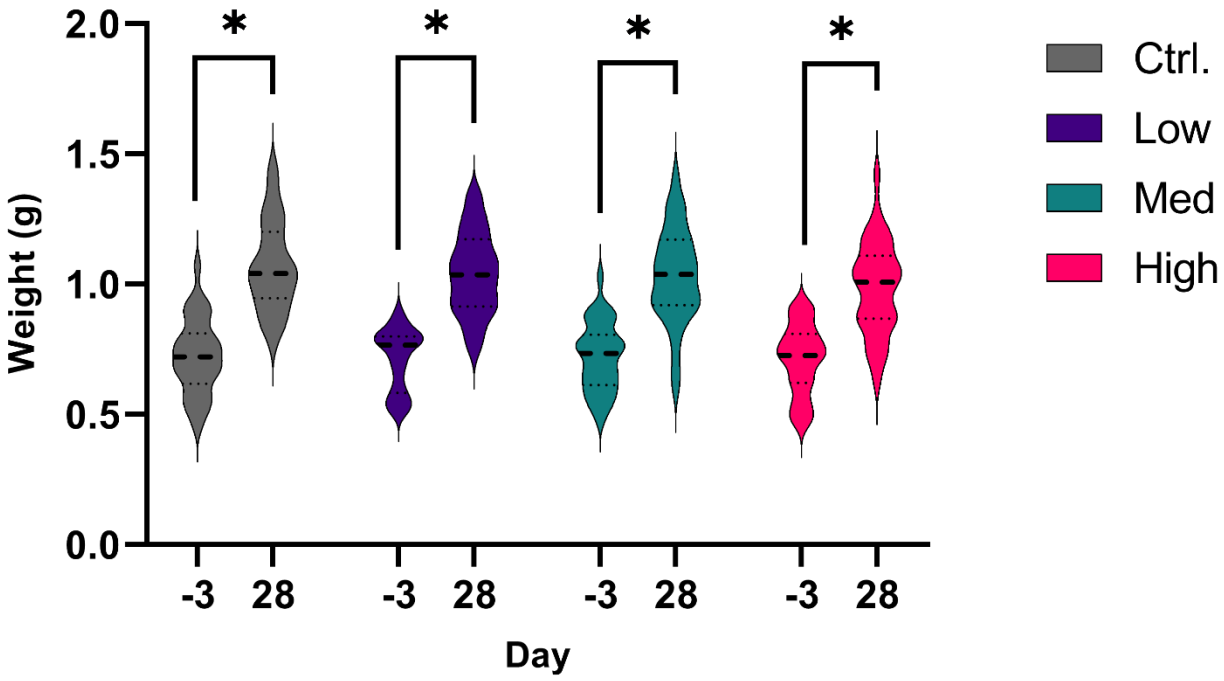

Figure 3. 7. Average initial and final snail weight of *P. pilsbryi* exposed to 3 differing concentrations for 28 days. The initial and final weight measurements were acquired on day -3 and day 28 respectively. Final snail lengths were significantly larger than the initial lengths ($p < 0.0001$), but did not differ significantly between treatments ($p = 4.52$).

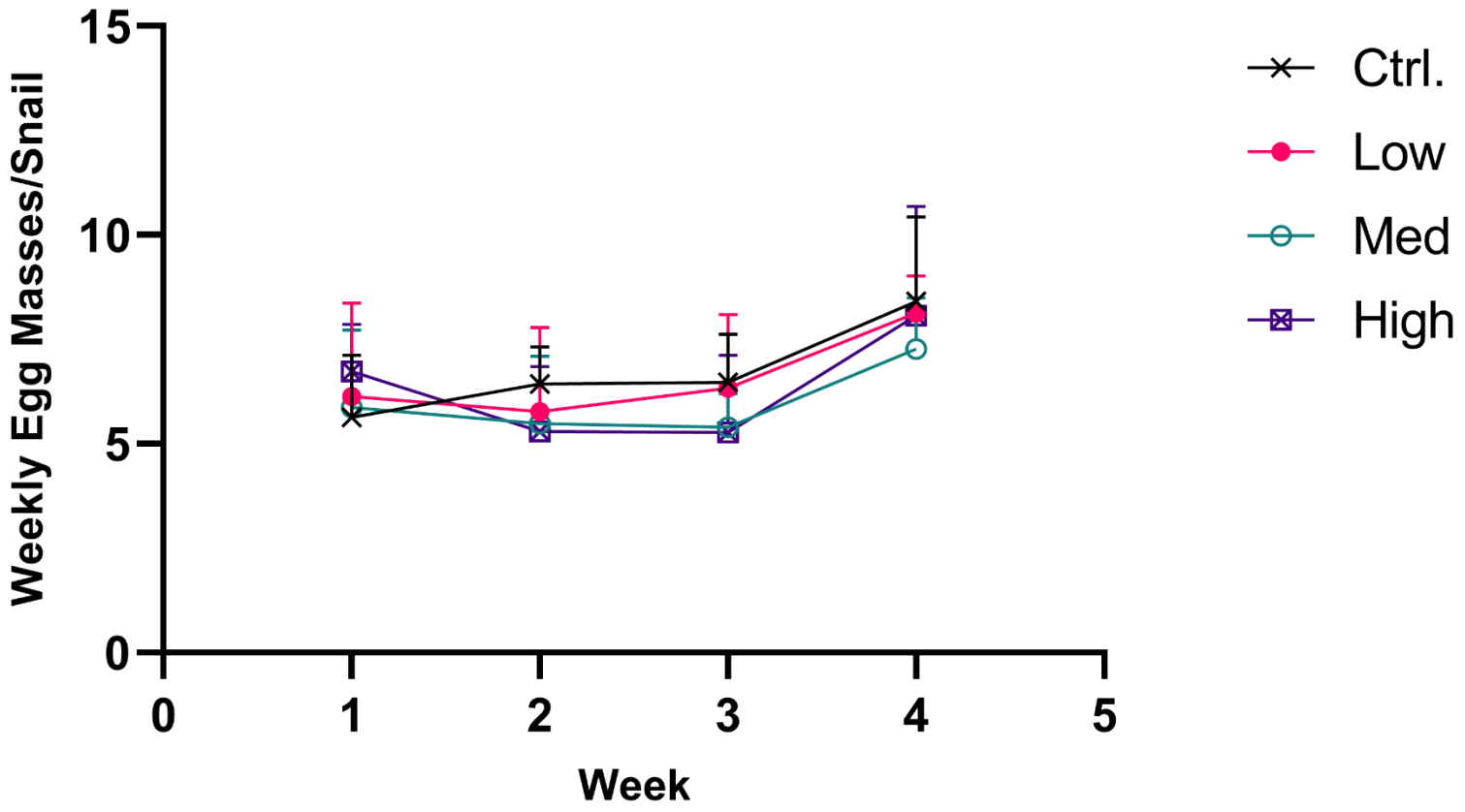

Figure 3. 8. Average weekly egg masses produced per the amount of snails alive per jar of *P. pilsbryi* exposed to 3 differing concentrations for 28 days. Each concentration is represented by a different colour and symbol.

3.3 PFAS Analysis of Field Samples

All samples collected during the 28-day field exposure, including water, sediment, and tissue samples, were tested for a suite of 17 PFAS chemicals. The specific chemicals include PFBA, PFPeA, PFBS, PFHxA, PFHpA, PFHxS, PFOA, PFNA, PFOS, PFDA, PFUnDA, PFDS, PFDoDA, PFTrDA, PFTeDA, PFHxDA, and PFOcDA. These chemical structures include both carboxylate or sulfonate functional group congeners. They also range from the 4-carbon short-chained structures to the 18-carbon long-chained structures. The overall trend indicated that there were higher levels of PFAS in the contaminated site compared to the reference site (Figure 3.9).

The water samples from both the reference and contaminated sites found 8 types of PFAS including: PFBA, PFPeA, PFHxA, PFHpA, PFHxS, PFOA, PFNA, and PFOS. A significant difference can be observed for PFPeA ($p= 0.000199$), PFHxA ($p = 0.00254$), PFHpA ($p = 0.000006$), PFHxS ($p = 0.000043$), PFOA ($p = 0.000003$), PFNA ($p = 0.000308$), and PFOS ($p = 0.000091$), all with higher concentrations in the contaminated site compared to the reference site (Figure 3.9). Within the sediment samples, 17 types of PFAS were detected in both the reference and contaminated sites, the mean and standard deviation are shown in Table 3.1. Statistical analysis indicated that there were no significant differences between sites. Although there is not a significant difference ($p < 0.05$) it can be visually observed that there are higher concentrations of PFHxA, PFOS, and PFOcDA in the contaminated site (Table 3.1). The mean and standard deviation of PFAS concentrations measured in whole body snail tissues are shown in Table 3.2. Twelve PFAS were found in both the reference and contaminated sites including: PFBA, PFBS, PFHxA, PFHpA, PFOA, PFNA, PFOS, PFDA, PFUnDA, PFDoDA, PFHxDA, and PFOcDA.

Statistically significant differences were only found for PFHxA ($p = 0.002408$) which was over 1000% higher in the tissue samples from the contaminated site exposure.

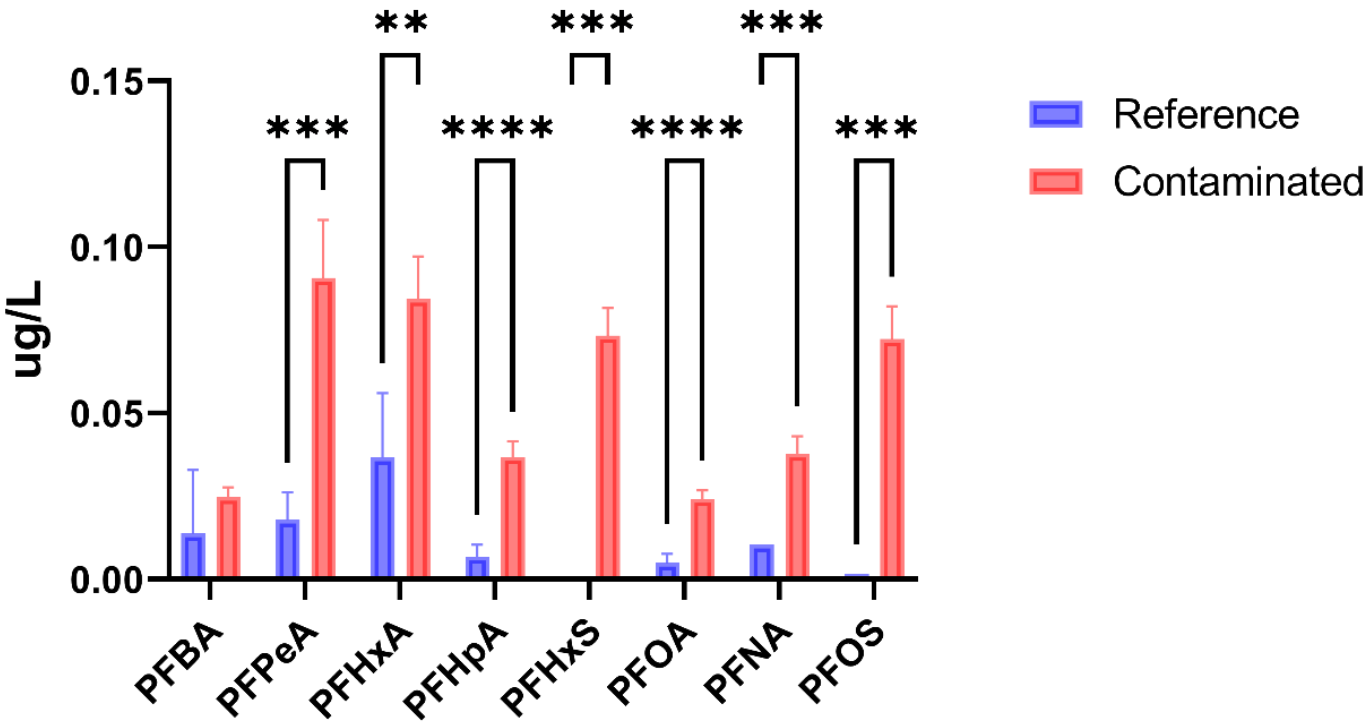

Figure 3. 9. Mean concentration of PFAS in water samples collected at the field sites. Error bars represent standard deviation. Asterisk (*) represents level of significance: ** $p \leq 0.01$, *** $p \leq 0.001$, **** $p \leq 0.0001$.

Table 3. 1. Measured PFAS concentrations in sediment after a 28-day field exposure (mean ± standard deviation). Sediment samples were collected concluding the test (n=3).

Measured PFAS (ng/g wet weight)

	n	PFBA	PFPeA	PFBS	PFHxA	PFHpA	PFHxS	PFOA	PFNA	PFOS	PFDA	PFUnDA	PFDS	PFDoDA	PFTrDA	PFTeDA	PFHxDA	PFOcDA
Reference	3	0.179[a]	ND	0.023	2.688 ± 1.147	0.132 ± 0.026	0.056 ± 0.042	1.146 ± 0.273	0.141 ± 0.062	1.124 ± 0.286	0.338 ± 0.215	0.121 ± 0.053	0.022	0.327 ± 0.244	0.247 ± 0.09	0.075 ± 0.086[b]	ND	0.762 ± 0.79[b]
Contaminated	3	0.053[a]	0.104 ± 0.058[b]	0.145[a]	6.138 ± 1.829	0.176 ± 0.107	0.573 ± 0.271	1.003 ± 0.395	0.242 ± 0.108	6.811 ± 7.096	0.458 ± 0.32	0.181 ± 0.13	0.034 ± 0.014	0.409 ± 0.385	0.127 ± 0.064	0.056 ± 0.01[b]	0.037 ± 0.023	6.362 ± 10.93

* = Significance

ND = Non-detection

[a] = n=1. Other two samples were non-detects

[b] = n=2. The other sample was a non-detect.

Table 3. 2. Measured PFAS concentrations in snail whole-body tissue after a 28-day field exposure (mean ± standard deviation). Tissue samples were collected at the end of the test (n=5).

		Measured PFAS (ng/g wet weight)											
	n	**PFBA**	**PFBS**	**PFHxA***	**PFHpA**	**PFOA**	**PFNA**	**PFOS**	**PFDA**	**PFUnDA**	**PFDoDA**	**PFHxDA**	**PFOcDA**
Reference	5	12.231 ± 2.397	2.885 ± 0.26	1.475 ± 1.584	3.363 ± 0	3.379 ± 2.33	3.657 ± 1.433	16.062 ± 20.42	4.443 ± 2.046	2.92 ± 1.421	3.913 ± 0	0.935 ± 1.399	2.347 ± 0
Contaminated	5	59.246 ± 31.047	4.565 ± 3.093	16.201 ± 5.336	5.089 ± 2.12	31.313 ± 41.451	6.584 ± 3.994	82.668 ± 52.78	10.006 ± 8.907	9.088 ± 7.913	9.888 ± 4.753	1.758 ± 2.61	7.789 ± 4.6

3.4 Nominal and Measured PFOS of Laboratory Samples

Laboratory water samples were collected at two different time points during this experiment and subjected to PFAS analysis. The stock solutions were collected prior to exposure to the snails, and composite residues (pooled replicates) were collected after seven days of exposure. Analysis of the stock solutions proved that the low and high treatments were less than the desired nominal concentration (60% and 56% respectively) (Table 3.3). The lower measured PFOS concentrations could possibly be due to potential analytical scale and equipment errors during solution preparation. The medium treatment closely represented the desired nominal concentration, with 108% of the nominal concentration (Table 3.3). In the water residue samples, all measured concentrations were lower than the nominal concentration. Specifically, the low, medium, and high concentrations had 65%, 52%, and 89% of the nominal concentrations, respectively (Table 3.3). Bioconcentration factors (BCFs) of 10.14 L/kg (medium treatment) and 4.68 L/kg (high treatment) were calculated for PFOS in whole-body tissues (Table 3.3).

Table 3. 3. Nominal and measured concentrations of PFOS at day 0 (stock solution) and day 7 (residue) of the 28-day exposure. Percent of nominal is calculated as the percent difference between the nominal and measured concentrations. The mean tissue concentration of PFOS in *P. pilsbryi* is reported in ng/g. The calculated bioconcentration factor (BCF) is reported in L/kg wet weight (WW) and was calculated by dividing the mean tissue concentration by the mean water concentration.

	Ctrl.	**Low**	**Medium**	**High**
Nominal (µg/L)	0	0.1	10	1000
Stock Water (µg/L)	0.0047	0.060	10.8	564
Percent of Nominal (%)	-	60	108	56
Composite residue Water (µg/L)	0.0158	0.065	5.2	888
Percent of Nominal	-	65	52	89
Mean of Water (µg/L)		0.062 ± 0.004	7.979 ± 3.938	726.141 ± 228.883

Mean of Tissue (ng/g)	-	-	80.899 ± 55.696	3397.545 ± 428.849
BCF (L/kg WW)	-	-	10.139± 6.98	4.679± 0.591

3.5 Laboratory Whole Snail Tissue Proteomics

The 28-day laboratory exposure to PFOS had an effect on protein abundance. Through LC-MS/MS, 4246 proteins were identified, and changes in protein abundance were observed in 289 proteins (ANOVA, Fisher's LSD post-hoc, p-value < 0.05). The treatment differences in the 289 significantly altered proteins can be visualized in the heatmap (Figure 3.10).

A Principal Component Analysis (PCA) plot representing all ordinal treatments visually showed that there were two outliers for the control group and one outlier for the medium group (Figure 3.11). This is normal since the PCA represented the entire large proteomic dataset, where a large number of proteins did not experience changes in abundance. Thus, little variation in the entire proteome was observed.

Significant proteins were combined into a smaller list and then uploaded and analyzed to the CTD using the MyGeneVenn tool to compare my list of proteins to proteins associated with the chemical PFOS. Among the 271 proteins uploaded, 148 were recognized, and 123 of those recognized proteins were also known to be affected by PFOS

in other studies (Figure 3.12). Furthermore, among the 123 proteins, there was a known top-interacting protein: Acyl-CoA Thioesterase 2 (Acot2). The Acot2 protein found in the significant proteins list is among the top 10 genes that interact with PFOS in the CTD database. Furthermore, the Acot2 protein found in our laboratory dataset increased in abundance in the high treatment (ANOVA, Fisher's LSD post-hoc, p-value = 0.027) (Figure 3.13).

GO enrichment analysis was used to evaluate what processes were associated with the 289 significant proteins. The biological processes that were related to these significantly altered proteins included peptidyl-tyrosine autophosphorylation, mitogen-activated protein kinase (MAPK), activation of p38 MAPK pathway (p38MAPK), extracellular signal-regulated kinase 1/2 (ERK1/2) cascade, c-Jun N-terminal kinase (JNK), acrosomal reaction, and calcium pathways. Peptidyl-tyrosine autophosphorylation was the most significant biological process affected with 5 out of the 18 proteins related to this process being significantly altered. Furthermore, two enriched protein classes were identified, which were non-receptor tyrosine protein kinase (NRTK) and matrix metalloproteinases (MMP). A public web server - g:Profiler's functional enrichment analysis was used to investigate tissue specificity of the significant proteins. From the 289 significant proteins g:Profiler classified, 127 are associated with nasopharynx respiratory epithelial cells and 128 to bronchus respiratory epithelial cells (Table 3.4, Table 3.5).

Changes in protein abundance were observed within significant proteins associated with the p38MAPK pathway (Figure 3.14). Specifically, glutamate metabotropic receptor 1 (Grm1) and glutamate metabotropic receptor 5 (Grm5) followed the same trend with high protein abundances found in the control and medium treatment while the low and high

treatments had low protein abundances. Bone morphogenetic protein 2 (Bmp2), dual specificity phosphatase 22 (Dusp22), and mitogen-activated protein kinase kinase 1(Map2k1), displayed an overall decrease in protein abundance. In contrast, Janus kinase 2 (Jak2) and zinc finger MYND-type containing 11(Zmynd11) increased in protein abundance. Arachidonate 12-lipoxygenase, 12R type (Alox12b), ABL proto-oncogene 1, non-receptor tyrosine kinase (Abl1), and interleukin 1 alpha (Il1a), anti-Mullerian hormone (Mif), formyl peptide receptor 2 (Fpr2), and protein tyrosine kinase 2 beta (Ptk2b) experienced an increase in protein abundance within the low treatment. The medium and high treatments were either similar to the control group or experienced a slight decrease.

A heatmap (Figure 3.15) illustrates the abundance changes for proteins related to the ERK1/2 cascade. Il1a and ABL proto-oncogene 1 (Abl1) in the low group had similar abundance levels to that of the control and experienced a decrease in the medium and high groups. Fpr2, argininosuccinate synthase 1 (Ass1), Map2k1, and Ptk2b all displayed a decrease in the low and medium group but the high group represented similar abundance levels to the control. Bmp2, and Mif overall decreased in abundance across all treatments compared to the control. In contrast, Map3k15, only increased in abundance in the high treatment whereas, Adamts7 and Ppp5c noted increase in the low and high treatment. Arhgef6 and Sele increased in the low and medium groups only. Lastly, Jak2, and Zmynd11 distinguished increases in the medium and high treatments.

There are six proteins associated with the JNK pathway (Figure 3.16). Bmp2 indicated a high protein abundance in the control group but low abundance across all other treatments. Dusp22 showed a decrease of protein abundance in the low and medium groups. In contrast, Ptk2b displayed high protein abundance in the high treatment and lower

abundances were noted in all other groups. Zmynd11 displayed an increase in the medium and high group, while Arhgef6 increased in abundance in the low and medium group. Lastly, Il1A only experienced an increase in the low treatment. Overall, the proteins related to the JNK pathway did not experience a specific trend-wise change across all treatments, instead individual treatments experienced protein abundance changes.

Two proteins related to calcium-regulated pathways experienced significantly altered abundances. PFOS exposure resulted in an overall decrease of Calcyphosine 2 (Caps2) and an increase in Synaptotagmin 1 (Syt1) (Figure 3.17). Lastly, only one protein related to acrosomal reaction was significantly altered: Polycystin Family Receptor for Egg Jelly (Pkdrej). An increase in protein abundance in the low and medium groups can be visualized in a boxplot (Figure 3.18).

The two enriched protein classes are NRTK and MMPs which had five and eight significantly different related proteins, respectively. In terms of NRTK, Abl1 and Ptk2b decreased in protein abundance in the medium and high groups (Figure 3.19). While Src-Related Kinase Lacking C-Terminal Regulatory (Srms), Jak2, and Lymphocyte Cell-Specific Protein-Tyrosine Kinase (Lck) experienced an abundance increase in the various treatments (Figure 3.19). Proteins corresponding to MMPs visually displayed distinct trends of protein abundance changes. Specifically, Adamts7, Membrane Metalloendopeptidase (Mme), A Disintegrin-Like and Metalloprotease (Reprolysin Type) With Thrombospondin Type 1 Motif, 18 (Adamts18), and A Disintegrin-Like and Metalloprotease (Reprolysin Type) With Thrombospondin Type 1 Motif, 9 (Adamts9) decreased in protein abundance across all treatments (Figure 3.20). Contrastingly, Meprin A Subunit Beta (Mep1b), Ubiquinol-Cytochrome C Reductase Core Protein 2 (Uqcrc2),

Inositol Polyphosphate-5-Phosphatase E (Inpp5e), and Nardilysin Convertase (Nrdc) increase in protein abundance in the high treatment (Figure 3.20).

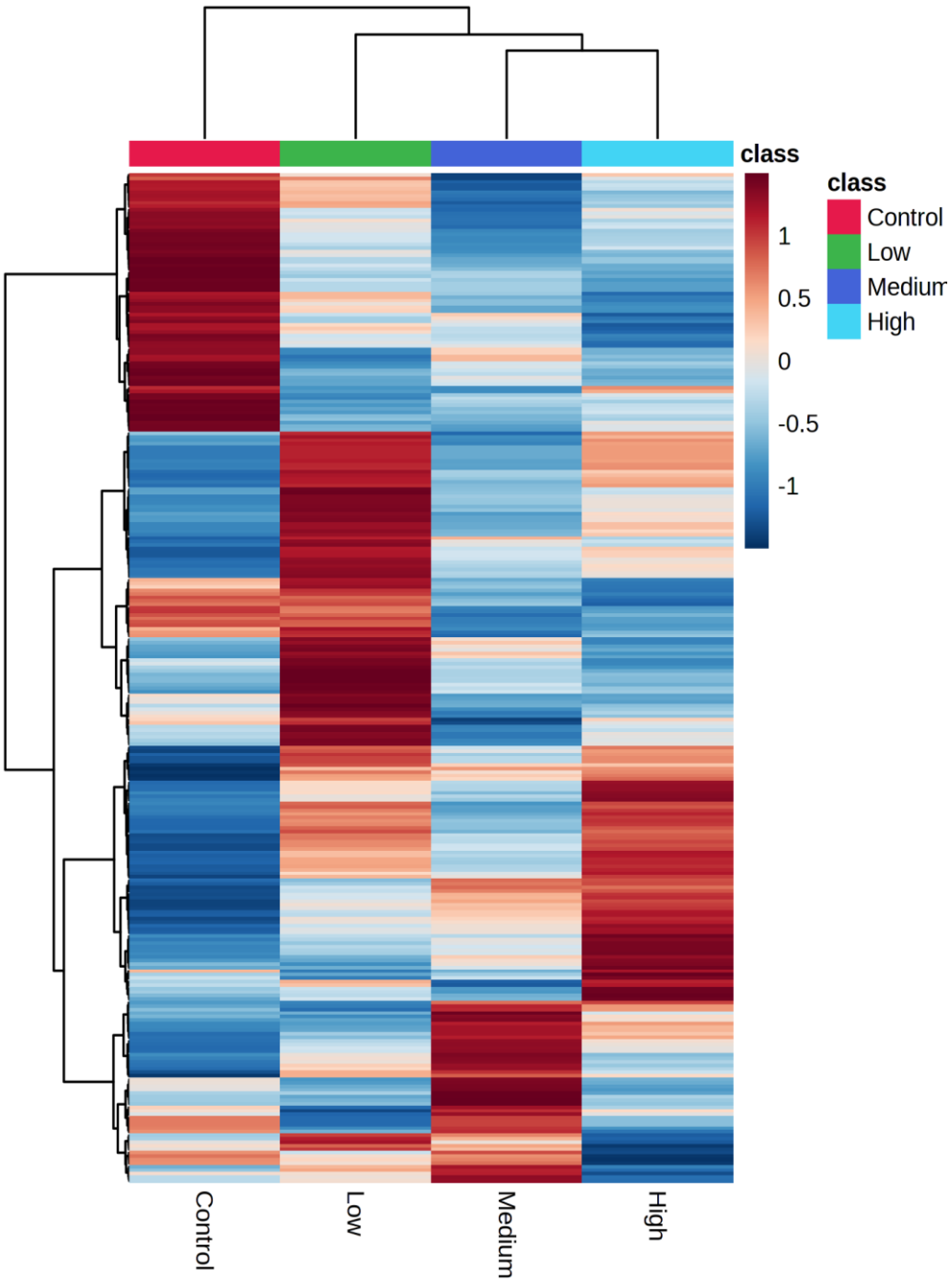

Figure 3. 10.Figure 3.10. Heatmap illustrating the abundance of the 289 significant proteins affected by PFOS exposure ($p < 0.05$). 289 proteins changed in abundance, the proteins are ranked by significance using a one-way ANOVA. The raw data were normalized and Ward's method was used for hierarchical clustering.

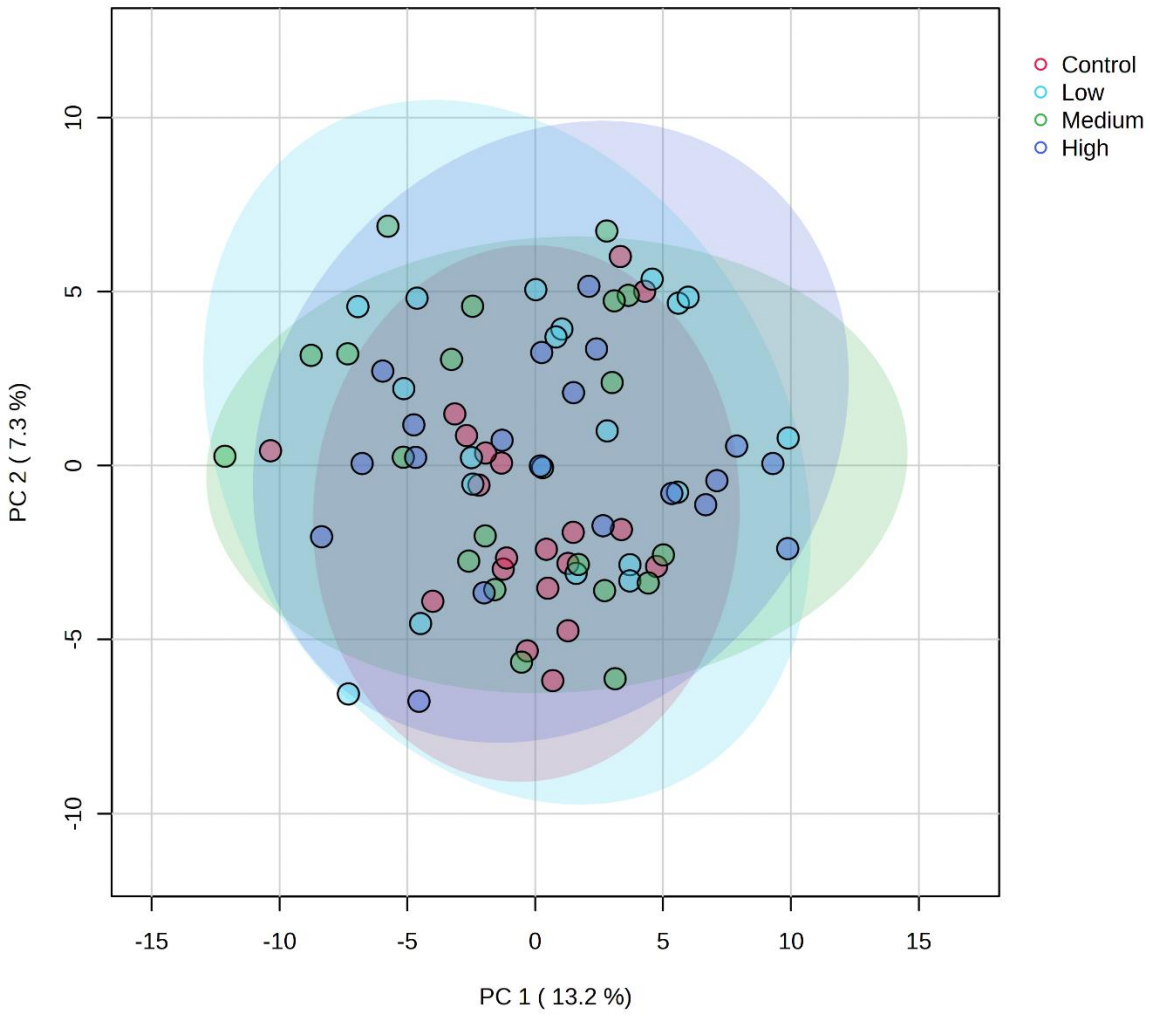

Figure 3. 11. Principal Component Analysis (PCA) of untargeted proteomics of snail whole body tissue exposed to various PFOS treatments. Each concentration is represented by a different colour. The ellipses of each represent the 95% confidence intervals. The normalized data are projected.

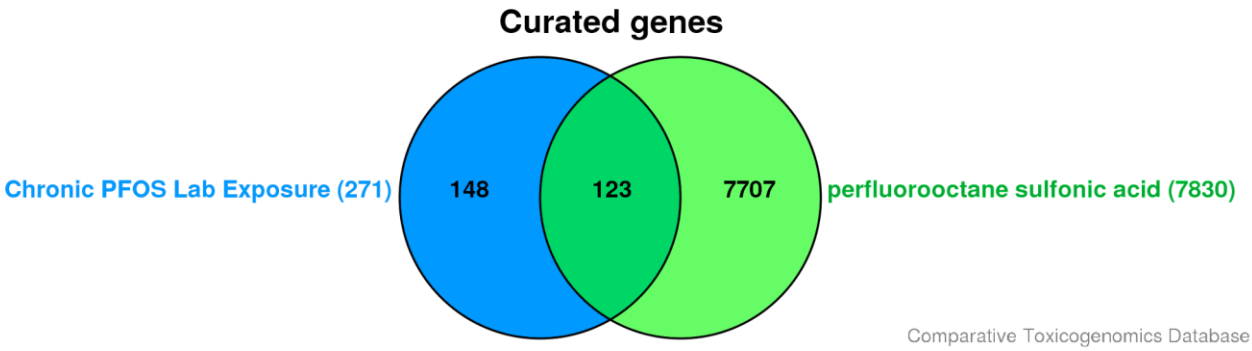

Figure 3. 12. Venn diagram representing the number of significant proteins from the PFOS laboratory exposure related to the chemical PFOS analyzed through the Comparative Toxicogenomic Database (CTD). 271 significant proteins ($p < 0.05$) were uploaded to the database and 148 were recognized as Human gene symbols. 123/7830 proteins were related to PFOS.

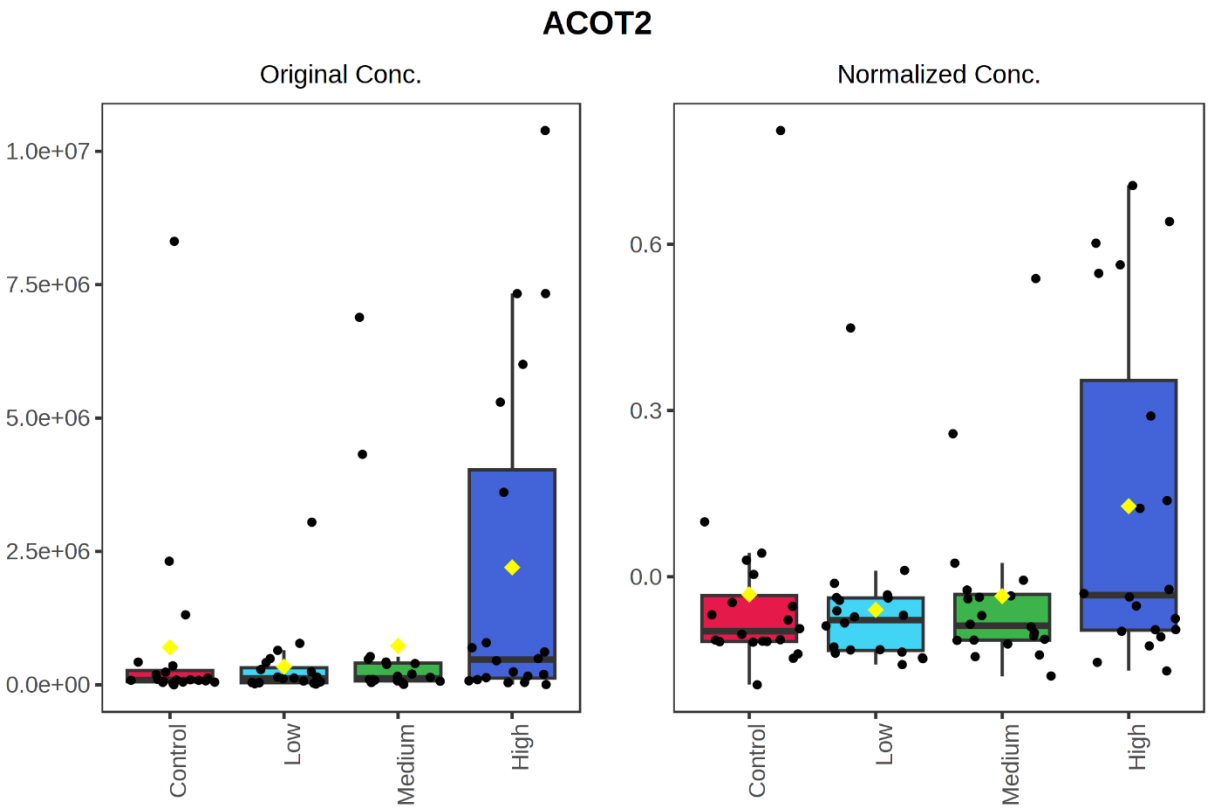

Figure 3. 13. Boxplot illustrating the Acot2 protein concentration in the various treatments. This is a significant protein ($p < 0.05$) where the original data on the left was normalized and projected on the right. The horizontal line represents the median of the treatments.

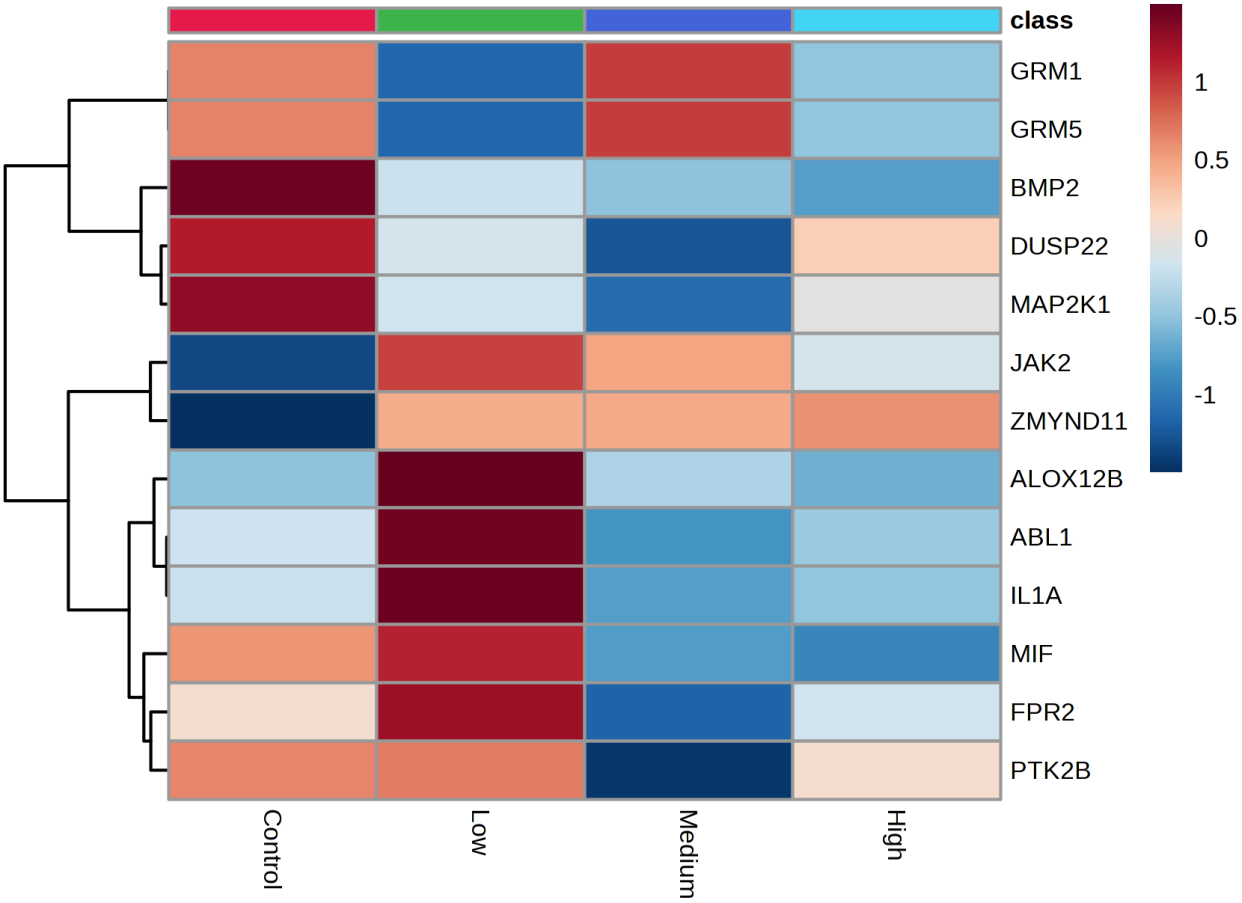

Figure 3. 14. Heatmap illustrating the abundance of the significant proteins related to p38MAPK pathway ($p < 0.05$). The raw data were normalized and Ward's method was used for hierarchical clustering.

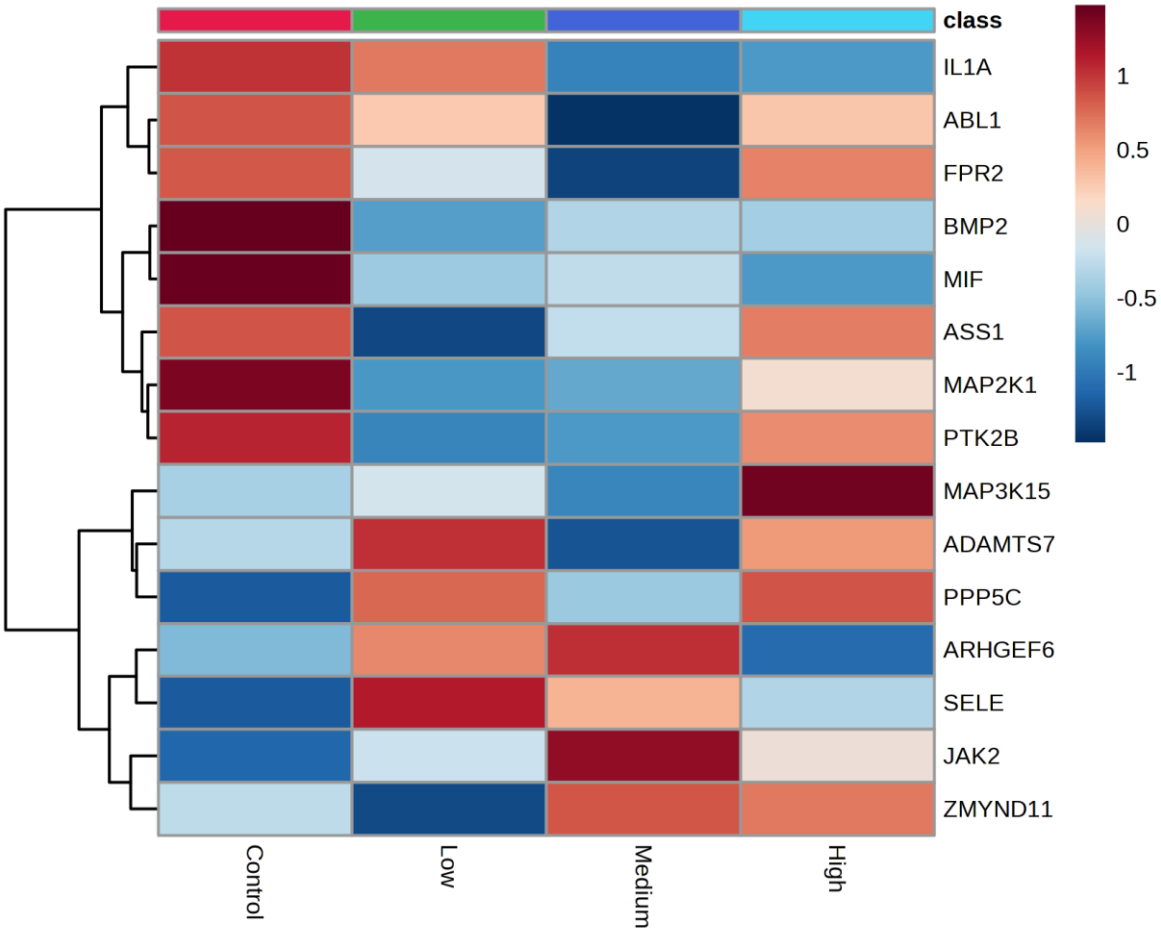

Figure 3. 15. Heatmap illustrating the abundance of the significant proteins related to ERK1/2 MAPK pathway ($p < 0.05$). The raw data were normalized and Ward's method was used for hierarchical clustering.

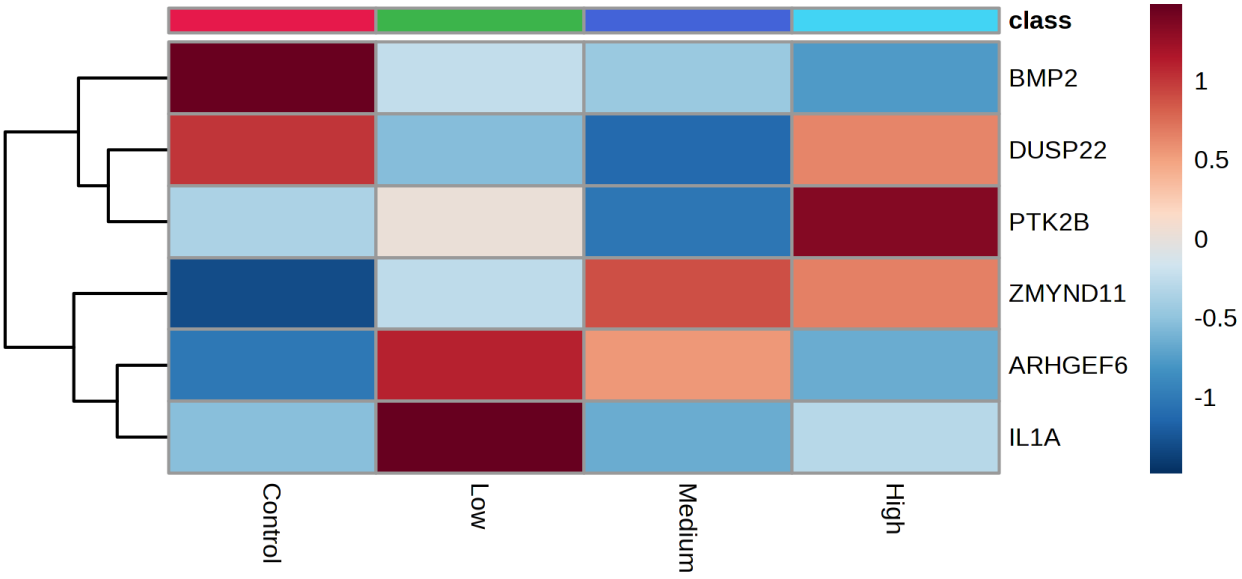

Figure 3. 16. Heatmap illustrating the abundance of the significant proteins related to the JNK pathway ($p < 0.05$). The raw data were normalized and Ward's method was used for hierarchical clustering.

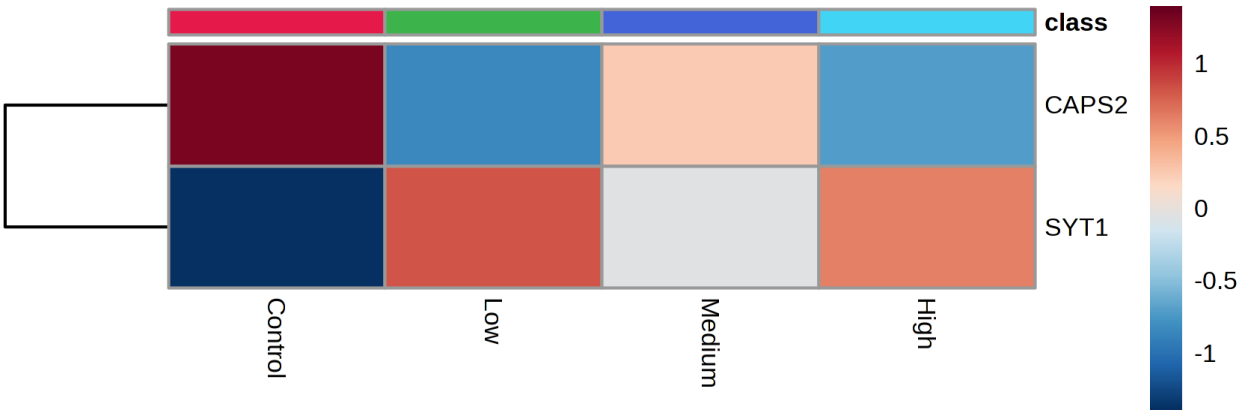

Figure 3. 17. Heatmap illustrating the abundance of the significant proteins related to calcium regulated pathways ($p < 0.05$). The raw data were normalized and Ward's method was used for hierarchical clustering.

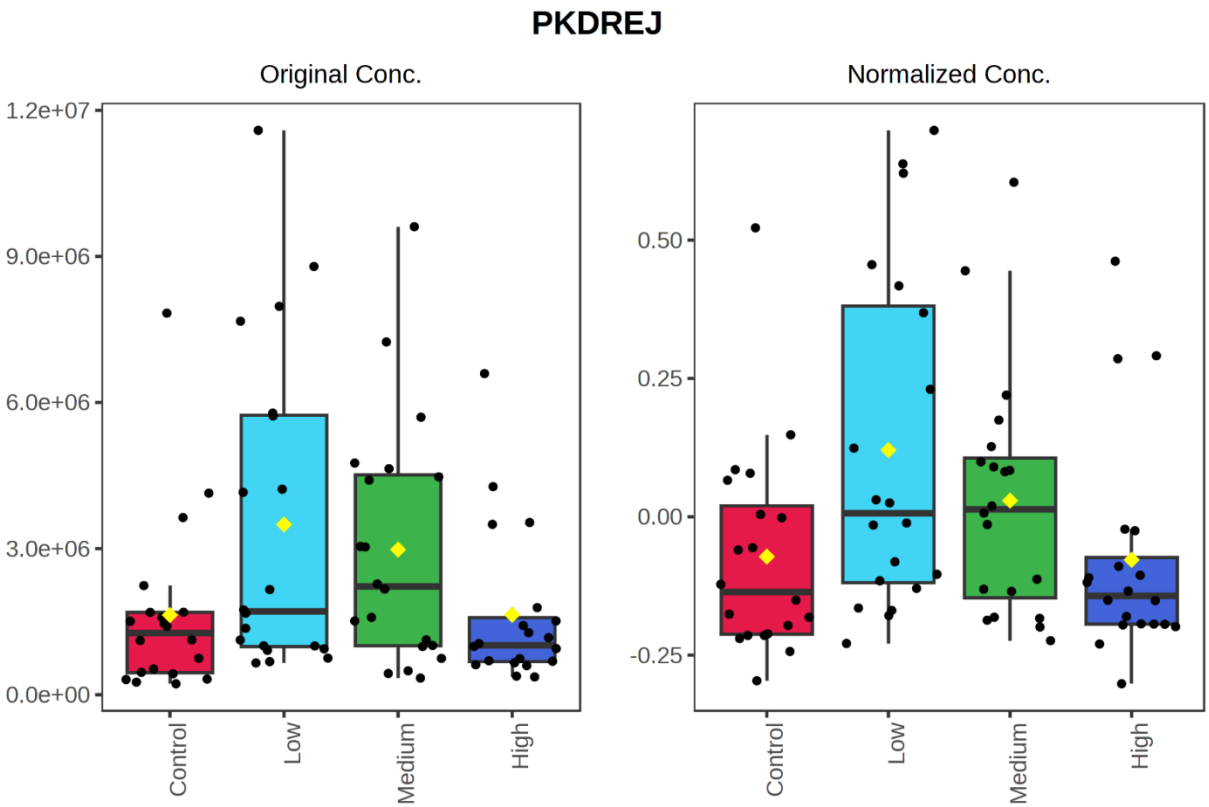

Figure 3. 18. A boxplot illustrating the Pkdrej protein abundance in the various treatments. This significant protein is related to the acrosomal reaction ($p < 0.05$), the original data on the left were normalized and projected on the right. The horizontal line represents the median of the treatments.

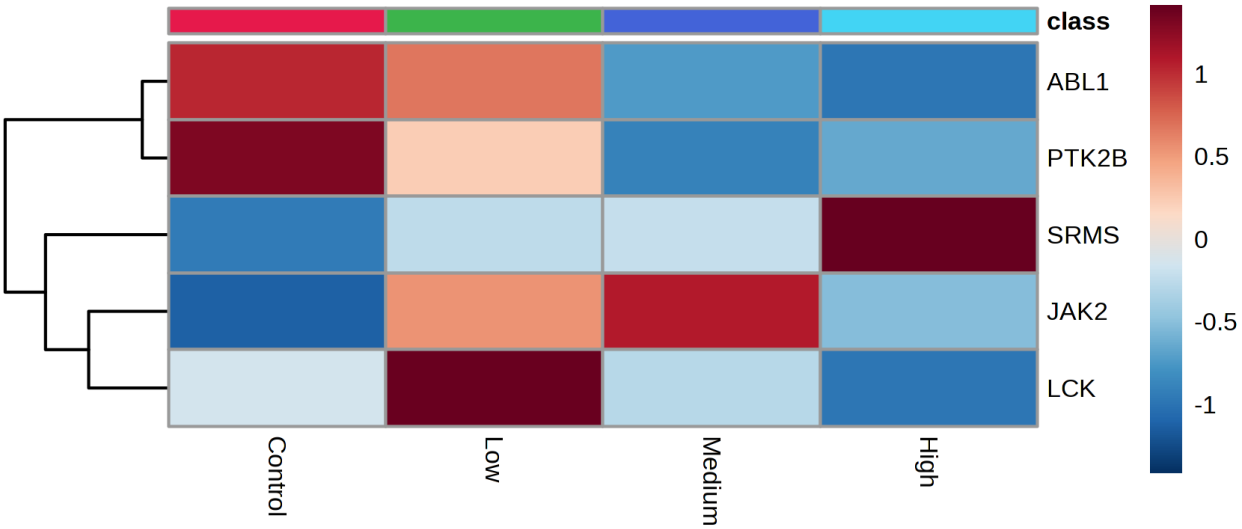

Figure 3. 19. Heatmap illustrating the abundance of the significant proteins related to the non-receptor tyrosine protein kinase protein class ($p < 0.05$). The raw data were normalized and Ward's method was used for hierarchical clustering

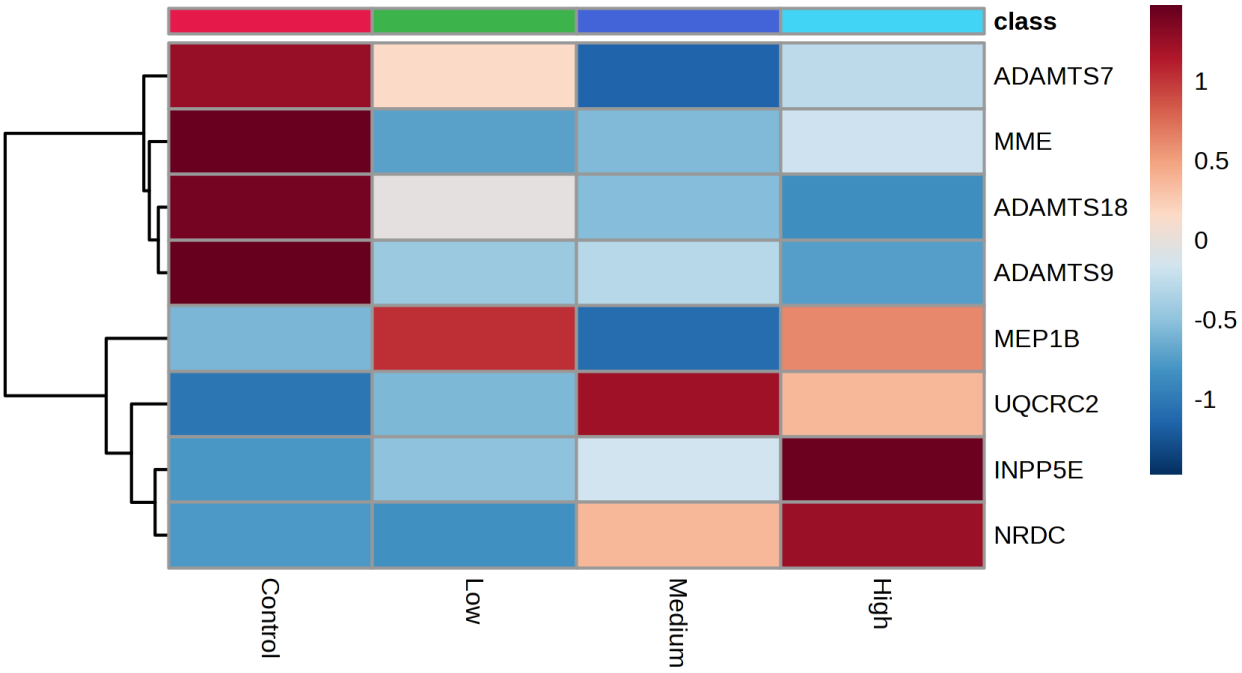

Figure 3. 20. Heatmap illustrating the abundance of the significant proteins related to the metalloprotease protein class ($p < 0.05$). The raw data was normalized and Ward's method was used for hierarchical clustering.

Table 3. 4. Proteins significantly affected from PFOS exposure that are related to pulmonary tissue types ($p<0.05$). G:profiler results of proteins related to specific cells based on The Human Protein Atlas.

Term Name	Term ID	Gene Set Size	G:Profiler Gene Set	Overlapping Genes	Proteins from Significant List Input related to
Nasopharynx; Respiratory Epithelial Cells [≥ Low]	HPA:0320101	5787	187	127	Slc38a6, Ccdc102b, Apex1, Inpp5e, Tango6, Mtif2, Rin2, Ppp5c, Lrp5, Ptprt, Met, Wdr13, Rps18, Rab11fip3, Lmnb2, Zng1b, Cep104, Lmna, Rangap1, Tp53bp2, Dusp22, Ccdc90b, Slc25a20, Adh5, Ttll4, Dpysl3, Mif, Ggta1, Atic, Psap, Golim4, Myo5b, Tmem19, Lrrc40, Klf5, Cenpe, Blzf1, Eif3e, Napepld, C1orf131, Alkbh8, Tubb4b, Gle1, Gtf3c6, Top3a, Wdr90, Ccdc125, Rprd1b, Hsp90b1, Nhlrc2, Nrf1, Acsf2, Adar, Gars1, Srm, MtCyb, Mprip, Kiaa0753, Uqcrc2, Trappc13, Abl1, Ewsr1, Adprh, Jak2, Ppwd1, Adamts9, Bin1, Galnt3, Rpl8, Irf2bpl, Rab11fip4, Rab3gap2, Srbd1, Shprh, Pus7, Ass1, Ifih1, Esco1, Acot2, Eif4enif1, Sae1, Chst12, Fut8, Slc10a3, Llgl1, Zdhhc4, Scarf1, Arsb, Ppp1r9b, Mlycd, Pld3, Clptm1l, Heatr5b, Ccnb2, Cep72, Bicral, Mia2, Muc5ac, Ano6, Pak1ip1, Rex1bd, Ddr1, Etnk1, Slc28a3, Znf800, Pcif1, Sele, Map2k1, Dek, Eif4e, Golga4, Tdrkh, Rpl6, Cdk5rap2, Xpr1, Mvp, Sirt6, Dpy19l3, Lgmn, Arhgef6, Rps15, Znf24, Rsf1, Usp22, Nsrp1, Calr, Zfx
Bronchus; Respiratory Epithelial Cells [≥ Low]	HPA:0060101	5931	187	128	Slc38a6, Ccdc102b, Apex1, Inpp5e, Tango6, Mtif2, Rin2, Ppp5c, Ube2q1, Lrp5, Ptprt, Myo1b, Met, Wdr13, Rps18, Rab11fip3, Lmnb2, Zng1b, Cep104, Lmna, Rangap1, Tp53bp2, Dusp22, Ccdc90b, Slc25a20, Adh5, Ttll4, Dpysl3, Ncam2, Mif, Ggta1, Atic, Psap, Prkci, Pgs1, Golim4, Myo5b, Lrrc40, Klf5,

Cenpe, Blzf1, Eif3e, Napepld, C1orf131, Alkbh8, Tubb4b, Gle1, Gtf3c6, Top3a, Wdr90, Ccdc125, Rprd1b, Hsp90b1, Nhlrc2, Nrf1, Acsf2, Adar, Gars1, Srm, MtCyb, Mprip, Kiaa0753, Uqcrc2, Trappc13, Abl1, Ewsr1, Adprh, Jak2, Ppwd1, Adamts9, Bin1, Galnt3, Rpl8, Irf2bpl, Rab11fip4, Rab3gap2, Srbd1, Pus7, Ass1, Ifih1, Esco1, Acot2, Eif4enif1, Sae1, Chst12, Fut8, Slc10a3, Lama1, Llgl1, Zdhhc4, Scarf1, Arsb, Ppp1r9b, Mlycd, Pld3, Clptm1l, Heatr5b, Ccnb2, Cep72, Bicral, Muc5ac, Pak1ip1, Mfsd6, Rex1bd, Ddr1, Etnk1, Slc28a3, Znf800, Pcif1, Dek, Eif4e, Golga4, Tdrkh, Rpl6, Cdk5rap2, Xpr1, Mvp, Sirt6, Dpy19l3, Lgmn, Arhgef6, Rps15, Znf24, Rsf1, Usp22, Nsrp1, Calr, Zfx

Table 3. 5. Significant proteins that were affected by PFOS exposure that are related to cancer types ($p < 0.05$). CTD results representing proteins related to cancerous types listed in decreasing order of number of annotated genes.

Disease Name	Disease ID	Disease Categories	# of Annotated Genes	Annotated Genes
Neoplasms	MESH:D009369	Cancer	59	Abcd2, Abl1, Ache, Adamts7, Adar, Aldh1a2, Alkbh8, Alox12b, Apex1, Bmp2, Cacna1d, Calr, Ccnb2, Cenpe, Clptm1l, Ddr1, Dek, Dll1, Eif3e, Eif4e, Ewsr1, F3, Fmn2, Galnt3, Golga4, Grm1, Hs3st5, Hsp90b1, Hspa8, Igfals, Il1a, Itih3, Jak2, Klf5, Lama1, Llgl1, Lmna, Lmntd1, Map2k1, Met, Mif, Mme, Myo5b, Nrf1, Ptk2b, Rangap1, Rpl6, Rps15, Sac3d1, Sftpd, Slc2a5, Srm, Srms, Tagln2, Tonsl, Tp53bp2, Ugt2b15, Wdr46, Znf595
Neoplasms by Site	MESH:D009371	Cancer	51	Abcd2, Abl1, Ache, Adar, Aldh1a2, Alkbh8, Alox12b, Apex1, Bmp2, Calr, Ccnb2, Cenpe, Clptm1l, Ddr1, Dek, Dll1, Eif3e, Ewsr1, F3, Fmn2, Galnt3, Golga4, Hsp90b1, Hspa8, Igfals, Il1a, Itih3, Jak2, Klf5, Lama1, Llgl1, Lmna, Lmntd1, Map2k1, Met, Mif, Mme, Myo5b, Ptk2b, Rpl6, Rps15, Sftpd, Slc2a5, Srm, Srms, Tagln2, Tonsl, Tp53bp2, Ugt2b15, Wdr46, Znf595
Neoplasms by Histologic Type	MESH:D009370	Cancer	36	Abl1, Ache, Alox12b, Apex1, Cacna1d, Calr, Ccnb2, Cenpe, Clptm1l, Ddr1, Eif3e, Eif4e, Ewsr1, F3, Fmn2, Grm1, Hs3st5, Hspa8, Igfals, Il1a, Itih3, Jak2, Klf5, Lmna, Map2k1, Met, Mif, Nrf1, Ptk2b, Rangap1, Rpl6, Sac3d1, Srm, Tagln2, Tonsl, Tp53bp2

Carcinoma	MESH:D002277	Cancer	26	Abl1, Ache, Alox12b, Apex1, Calr, Ccnb2, Cenpe, Clptm1l, Ddr1, Eif3e, Fmn2, Hspa8, Igfals, Il1a, Itih3, Klf5, Lmna, Map2k1, Met, Mif, Nrf1, Rpl6, Srm, Tagln2, Tonsl, Tp53bp2
Neoplasm, Glandular and Epithelial	MESH:D009375	Cancer	28	Abl1, Ache, Alox12b, Apex1, Cacna1d, Calr, Ccnb2, Cenpe, Clptm1l, Ddr1, Eif3e, Ewsr1, Fmn2, Hspa8, Igfals, Il1a, Itih3, Klf5, Lmna, Map2k1, Met, Mif, Nrf1, Rpl6, Srm, Tagln2, Tonsl, Tp53bp2
Prostatic Neoplasms	MESH:D011471	Cancer, Urogenital disease (male)	17	Ache, Aldh1a2, Alox12b, Apex1, Calr, Clptm1l, Ddr1, Ewsr1, Galnt3, Golga4, Hsp90b1, Jak2, Map2k1, Met, Mif, Mme, Ugt2b15
Genital Neoplasm, Male	MESH:D005834	Cancer, Urogenital disease (male)	17	Ache, Aldh1a2, Alox12b, Apex1, Calr, Clptm1l, Ddr1, Ewsr1, Galnt3, Golga4, Hsp90b1, Jak2, Map2k1, Met, Mif, Mme, Ugt2b15
Adenocarcinoma	MESH:D000230	Cancer	21	Abl1, Ache, Alox12b, Apex1, Ccnb2, Cenpe, Clptm1l, Ddr1, Eif3e, Fmn2, Hspa8, Igfals, Itih3, Klf5, Lmna, Map2k1, Met, Srm, Tagln2, Tonsl, Tp53bp2
Adenocarcinoma of Lung	MESH:D000077192	Cancer	8	Alox12b, Apex1, Clptm1l, Eif3e, Klf5, Lmna, Map2k1, Srm
Urogenital Neoplasms	MESH:D014565	Cancer, Urogenital disease (female), Urogenital disease (male)	20	Ache, Aldh1a2, Alox12b, Apex1, Calr, Clptm1l, Ddr1, Ewsr1, Fmn2, Galnt3, Golga4, Hsp90b1, Jak2, Klf5, Map2k1, Met, Mif, Mme, Tagln2, Ugt2b15

Lung Neoplasms	MESH:D008175	Cancer, Respiratory tract disease	15	Alox12b, Apex1, Clptm1l, Ddr1, Eif3e, Il1a, Klf5, Lmna, Lmntd1, Map2k1, Met, Mif, Sftpd, Srm, Znf595
Respiratory Tract Neoplasms	MESH:D012142	Cancer, Respiratory tract disease	15	Alox12b, Apex1, Clptm1l, Ddr1, Eif3e, Il1a, Klf5, Lmna, Lmntd1, Map2k1, Met, Mif, Sftpd, Srm, Znf595
Thoracic Neoplasms	MESH:D013899	Cancer	15	Alox12b, Apex1, Clptm1l, Ddr1, Eif3e, Il1a, Klf5, Lmna, Lmntd1, Map2k1, Met, Mif, Sftpd, Srm, Znf595
Breast Neoplasms	MESH:D001943	Cancer, Skin disease	13	Abl1, Ache, Adar, Alkbh8, Bmp2, Dek, Dll1, F3, Llgl1, Mif, Mme, Slc2a5, Tp53bp2
Digestive System Neoplasms	MESH:D004067	Cancer, Digestive system disease	22	Abcd2, Abl1, Ache, Alox12b, Apex1, Bmp2, Calr, Ccnb2, Cenpe, Hspa8, Igfals, Itih3, Jak2, Klf5, Lama1, Met, Myo5b, Rps15, Srms, Tagln2, Tonsl, Wdr46
Melanoma	MESH:D008545	Cancer	7	Apex1, Calr, Hs3st5, Map2k1, Met, Ptk2b, Sac3d1
Nevi and Melanomas	MESH:D018326	Cancer	7	Apex1, Calr, Hs3st5, Map2k1, Met, Ptk2b, Sac3d1
Urologic Neoplasms	MESH:D014571	Cancer, Urogenital disease (female), Urogenital disease (male)	8	Ache, Alox12b, Clptm1l, Fmn2, Jak2, Klf5, Met, Tagln2
Adenoma	MESH:D000236	Cancer	4	Cacna1d, Il1a, Met, Mif
Bronchial Neoplasms	MESH:D001984	Cancer, Respiratory tract disease	2	Clptm1l, Met
Carcinogenesis	MESH:D063646	Cancer, Pathology (process)	3	Abl1, Jak2, Met

Carcinoma, Bronchogenic	MESH:D002283	Cancer, Respiratory tract disease	2	Clptm1l, Met
Carcinoma, Hepatocellular	MESH:D006528	Cancer, Digestive system disease	8	Apex1, Ccnb2, Cenpe, Igfals, Itih3, Met, Tagln2, Tonsl
Carcinoma, Non-Small-Cell Lung	MESH:D002289	Cancer, Respiratory tract disease	2	Clptm1l, Met
Carcinoma, Renal Cell	MESH:D002292	Cancer, Urogenital disease (female), Urogenital disease (male)	5	Ache, Alox12b, Fmn2, Met, Tagln2
Carcinoma, Squamous Cell	MESH:D002294	Cancer	6	Calr, Hspa8, Il1a, Klf5, Met, Nrf1
Colorectal Neoplasms	MESH:D015179	Cancer, Digestive system disease	7	Abcd2, Ache, Alox12b, Bmp2, Calr, Klf5, Lama1
Cysts	MESH:D003560	Cancer, Pathology (anatomical condition)	3	Adamts7, Lmna, Tonsl
Endocrine Gland Neoplasms	MESH:D004701	Cancer, Endocrine system disease	4	Alox12b, Galnt3, Klf5, Met
Esophageal Neoplasms	MESH:D004938	Cancer, Digestive	3	Abl1, Calr, Met

		system disease		
Gastrointestinal Neoplasms	MESH:D005770	Cancer, Digestive system disease	13	Abcd2, Abl1, Ache, Alox12b, Apex1, Bmp2, Calr, Hspa8, Klf5, Lama1, Met, Rps15, Wdr46
Genital Neoplasms, Female	MESH:D005833	Cancer, Urogenital disease (female)	5	Alox12b, Clptm1l, Galnt3, Jak2, Met
Head and Neck Neoplasms	MESH:D006258	Cancer	7	Abl1, Calr, Clptm1l, Hspa8, Il1a, Klf5, Met
Intestinal Neoplasms	MESH:D007414	Cancer, Digestive system disease	7	Abcd2, Ache, Alox12b, Bmp2, Calr, Klf5, Lama1
Kidney Neoplasms	MESH:D007680	Cancer, Urogenital disease (female), Urogenital disease (male)	5	Ache, Alox12b, Fmn2, Met, Tagln2
Leukemia	MESH:D007938	Cancer	6	Abl1, Clptm1l, F3, Jak2, Map2k1, Met
Leukemia, Lymphoid	MESH:D007945	Cancer, Immune system disease, Lymphatic disease	2	Abl1, Clptm1l
Leukemia, Myeloid	MESH:D007951	Cancer	4	Abl1, F3, Jak2, Met

Leukemia, Myeloid, Acute	MESH:D015470	Cancer	3	F3, Jak2, Met
Liver Neoplasms	MESH:D008113	Cancer, Digestive system disease	12	Abl1, Apex1, Ccnb2, Cenpe, Igfals, Itih3, Jak2, Met, Myo5b, Srms, Tagln2, Tonsl
Liver Neoplasms, Experimental	MESH:D008114	Cancer, Digestive system disease	2	Jak2, Met
Lymphoma	MESH:D008223	Cancer, Immune system disease, Lymphatic disease	2	Eif4e, Rangap1
Lymphoma, Non-Hodgkin	MESH:D008228	Cancer, Immune system disease, Lymphatic disease	2	Eif4e, Rangap1
Mammary Neoplasms, Animal	MESH:D015674	Animal disease, Cancer	3	Ddr1, Mif, Rpl6
Mammary Neoplasms, Experimental	MESH:D008325	Cancer	3	Ddr1, Mif, Rpl6
Mesothelioma	MESH:D008654	Cancer	3	Il1a, Met, Mif
Mesothelioma, Malignant	MESH:D000086002	Cancer, Respiratory tract disease	3	Il1a, Met, Mif

Mouth Neoplasms	MESH:D 009062	Cancer, Mouth disease	2	Clptm1l, Hspa8
Neoplasm Invasiveness	MESH:D 009361	Cancer, Pathology (process)	6	Alkbh8, Calr, Dek, Eif4e, Met, Tp53bp2
Neoplasm Metastasis	MESH:D 009362	Cancer, Pathology (process)	2	Dek, Met
Neoplasms, Bone Tissue	MESH:D 018213	Cancer	3	Ewsr1, Grm1, Met
Neoplasms, Connective and Soft Tissue	MESH:D 018204	Cancer	4	Ewsr1, Grm1, Il1a, Met
Neoplasms, Connective Tissue	MESH:D 009372	Cancer, Connective tissue disease	4	Ewsr1, Grm1, Il1a, Met
Neoplasms, Experimental	MESH:D 009374	Cancer	7	Abl1, Calr, Ddr1, Jak2, Met, Mif, Rpl6
Neoplasms, Germ Cell and Embryonal	MESH:D 009373	Cancer	9	Alox12b, Apex1, Calr, Ewsr1, Hs3st5, Map2k1, Met, Ptk2b, Sac3d1
Neoplasms, Mesothelial	MESH:D 018301	Cancer	3	Il1a, Met, Mif
Neoplasms, Nerve Tissue	MESH:D 009380	Cancer	8	Apex1, Calr, Ewsr1, Hs3st5, Map2k1, Met, Ptk2b, Sac3d1
Neoplasms, Neuroepithelial	MESH:D 018302	Cancer	2	Ewsr1, Met
Neoplasms, Squamous Cell	MESH:D 018307	Cancer	5	Calr, Hspa8, Klf5, Met, Nrf1

Neoplastic Processes	MESH:D009385	Cancer, Pathology (process)	9	Abl1, Alkbh8, Calr, Dek, Eif4e, Ewsr1, Jak2, Met, Tp53bp2
Neuroectodermal Tumors	MESH:D017599	Cancer	8	Apex1, Calr, Ewsr1, Hs3st5, Map2k1, Met, Ptk2b, Sac3d1
Neuroectodermal Tumors, Primitive	MESH:D018242	Cancer	2	Ewsr1, Met
Neuroendocrine Tumors	MESH:D018358	Cancer	7	Apex1, Calr, Hs3st5, Map2k1, Met, Ptk2b, Sac3d1
Osteosarcoma	MESH:D012516	Cancer	2	Ewsr1, Met
Ovarian Cysts	MESH:D010048	Cancer, Endocrine system disease, Urogenital disease (female)	3	Adamts7, Lmna, Tonsl
Ovarian Neoplasms	MESH:D010051	Cancer, Endocrine system disease, Urogenital disease (female)	3	Alox12b, Galnt3, Met
Pancreatic Neoplasms	MESH:D010190	Cancer, Digestive system disease, Endocrine system disease	2	Alox12b, Klf5

Pleural Neoplasms	MESH:D 010997	Cancer, Respiratory tract disease	3	Il1a, Met, Mif
Polycystic Ovary Syndrome	MESH:D 011085	Cancer, Endocrine system disease, Urogenital disease (female)	3	Adamts7, Lmna, Tonsl
Sarcoma	MESH:D 012509	Cancer	3	Ewsr1, Il1a, Met
Skin Neoplasms	MESH:D 012878	Cancer, Skin disease	2	Il1a, Ptk2b
Stomach Neoplasms	MESH:D 013274	Cancer, Digestive system disease	6	Apex1, Bmp2, Hspa8, Met, Rps15, Wdr46
Urinary Bladder Neoplasms	MESH:D 001749	Cancer, Urogenital disease (female), Urogenital disease (male)	4	Ache, Clptm1l, Jak2, Klf5
Uterine Cervical Neoplasms	MESH:D 002583	Cancer, Urogenital disease (female)	2	Clptm1l, Jak2
Uterine Neoplasms	MESH:D 014594	Cancer, Urogenital disease (female)	2	Clptm1l, Jak2

3.6 Laboratory Whole Snail Tissue Metabolomics

Through spectra processing, 1947 metabolites were identified. PFOS exposure had a significant effect on snail metabolites (ANOVA, Fisher's LSD, p-value of < 0.05). A heatmap displayed the 133 metabolites that were significantly different (Figure 3.21). A PCA plot representing the ordinal treatments of the metabolomic data displayed low variability within the treatments (Figure 3.22). The most variation was seen in the control group that changes along the principal component one axis. However, this variation is probably due to the control outlier observed outside of the ellipse. There were also two more outliers observed within the high treatment. To reiterate, although the outliers were not ideal, the data was still valid due to sample replicates and randomization throughout. In addition, 472 level-two identification metabolites were uploaded to the Metaboanalyst Enrichment Analysis tool and revealed that the top three processes affected were - Riboflavin metabolism ($p = 0.045$), Carnitine synthesis ($p = 0.0574$), and Beta oxidation of very long chain fatty acids ($p = 0.152$) (Figure 3.23).

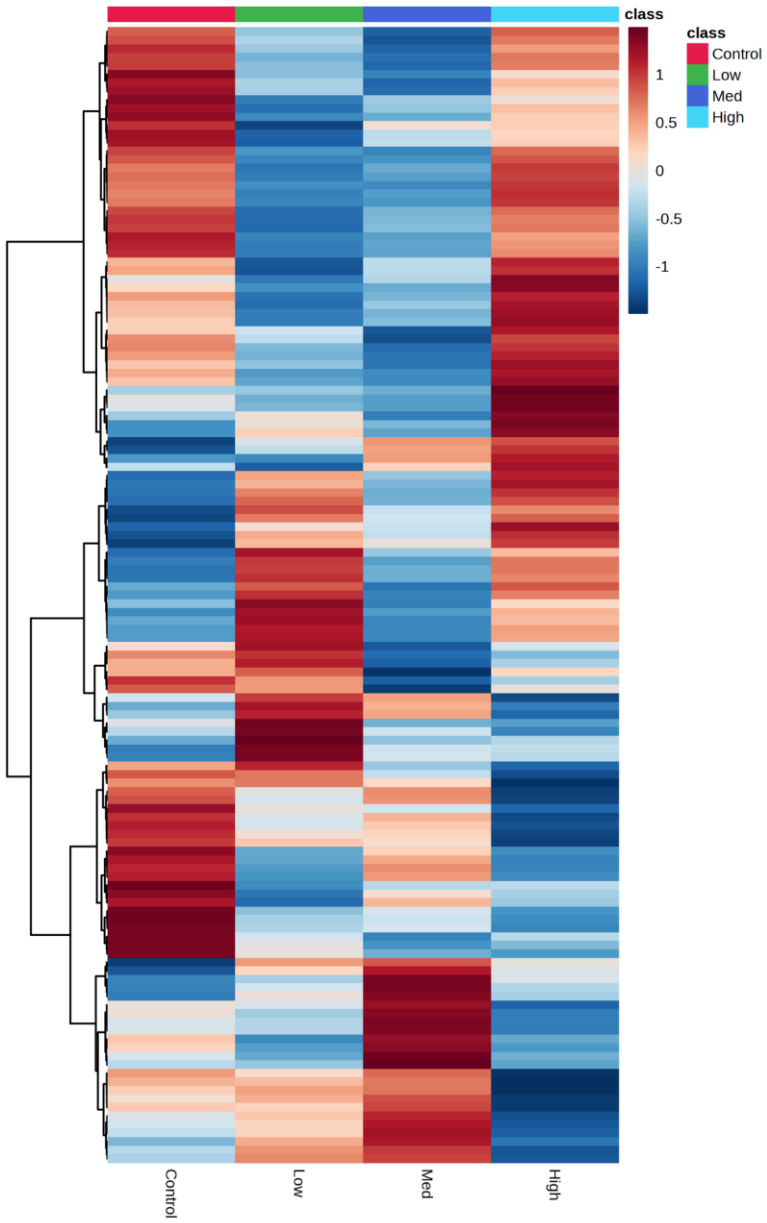

Figure 3. 21. Heatmap illustrating the abundance of the 133 significant metabolites affected by PFOS exposure. 133 metabolites changed in abundance, the metabolites are ranked by significance using a one-way ANOVA. The raw data were normalized and Ward's method was used for hierarchical clustering.

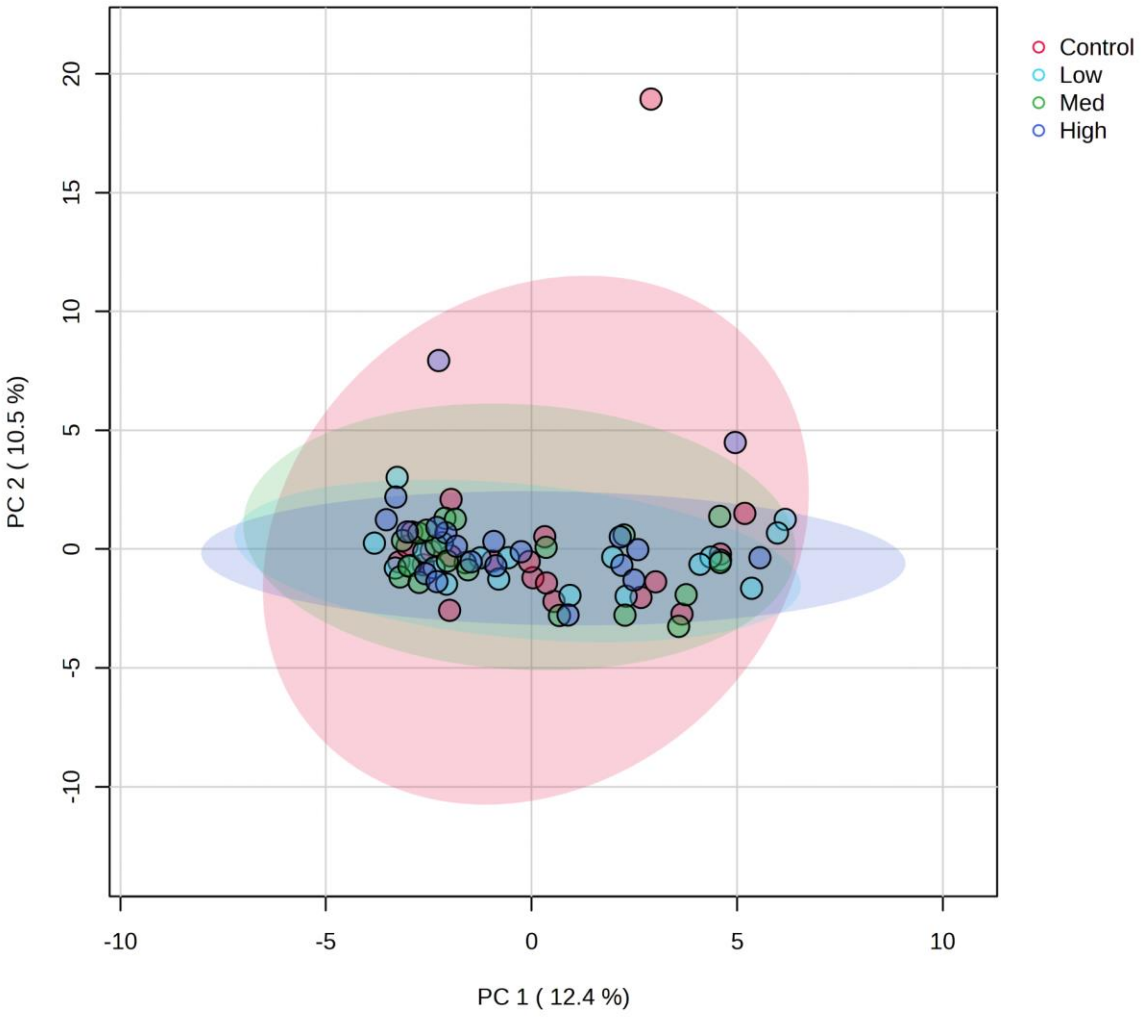

Figure 3. 22. PCA of untargeted metabolomics of snail whole-body tissue exposed to various PFOS treatments. Each concentration is represented by a different colour. The ellipses of each represent the 95% confidence intervals. The normalized data are projected.

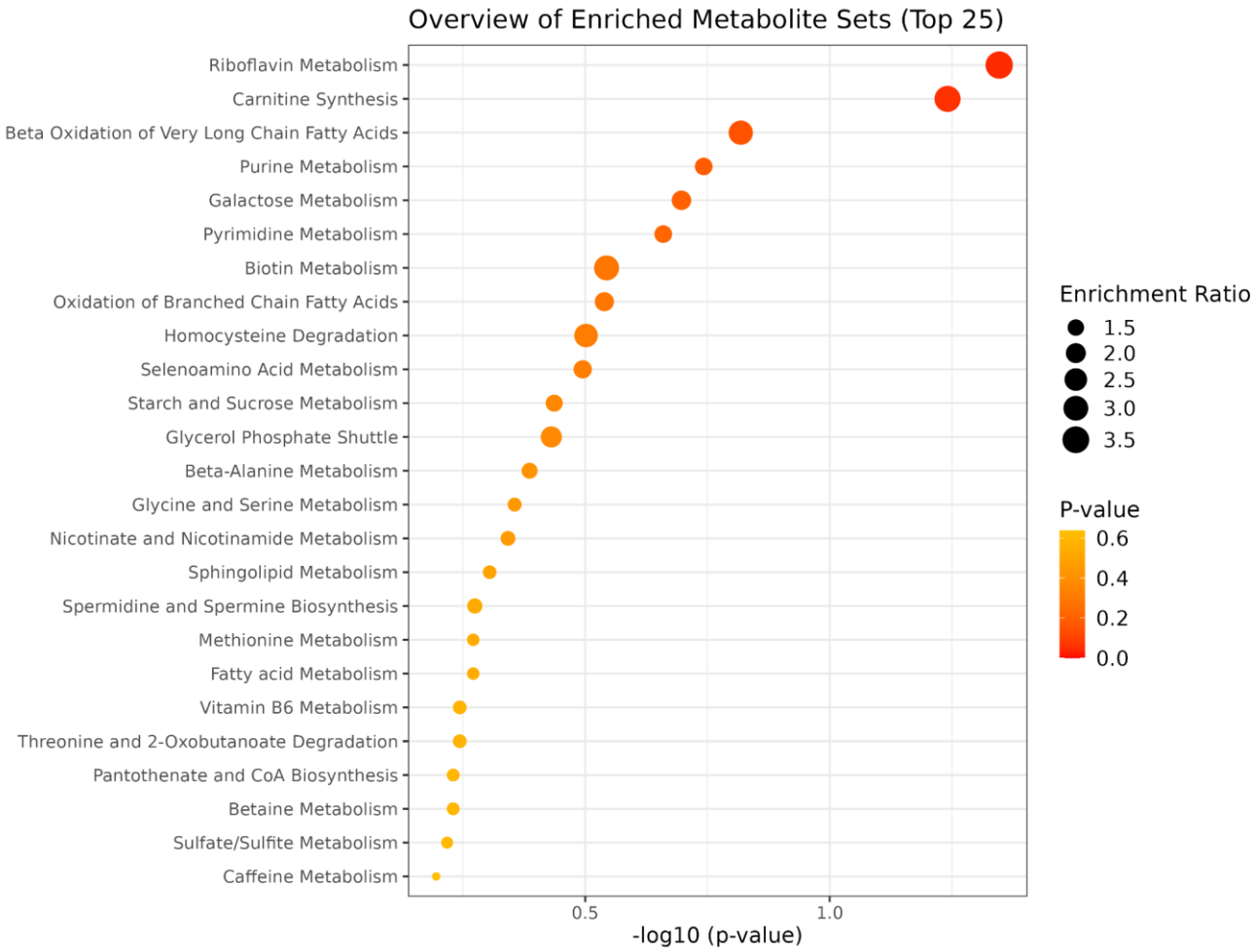

Figure 3. 23. Dot plot of enrichment analysis displaying the top 25 metabolite processes affected by PFOS exposure. P-values and enrichment ratios are represented by colour and size, respectively.

Chapter 4. Discussion

4.1 Field PFOS Concentrations

Within the field component of this study, water and sediment samples were collected from a reference site and contaminated site for PFAS analysis. PFOS water concentrations (mean ± standard deviation) were 0.002 µg/L ± 0 and 0.072 µg/L ± 0.01 for the reference and contaminated sites, respectively. In a previous study conducted in 2011, water samples from Lake Niapenco – the contaminated site, were also collected. The PFOS concentrations were determined to be 0.049 ± 7.4 µg/L for linear-PFOS (99 m/z) and 0.0449 ± 5.2 µg/L for linear-PFOS (80 m/z) (de Solla et al., 2012). Lower levels were reported in the 2011 study as compared to our present data, however, this can be due to spatial and temporal differences between the studies. Notably, in 11 years we can see that PFOS is persistent and remains within aquatic environments for a long time. This is due to the chemical characteristic of PFAS being extremely stable via the C-F bond and the resistance to degradation (Lei et al., 2020). Furthermore, in the present study, sediment samples from the contaminated site had the highest PFOS concentration (6.811 ± 7.096 µg/L). Similar trends were seen for surface sediment samples that were collected in 2010, 2011, and 2015 with higher concentrations being detected closer to the inlet of Lake Niapenco (Bhavsar et al., 2016).

It is not a surprising outcome to have recorded high levels of PFAS in the tested site. In the past, Lake Niapenco has been a documented site of PFAS contamination with reported PFOS concentrations being some of the highest worldwide (Bhavsar et al., 2016). The contaminated sampling site is located downstream of the southern side of the John C.

Munro International Airport, where PFOS-based AFFF was utilized (de Solla et al., 2012). It is a known historical firefighting training property that has released 15 000L of PFOS-based AFFF each year between 1985 and 1994 (Gewurtz et al., 2014).

The Federal Water Quality Guideline (FWQG) for the protection of freshwater organisms for PFOS is 6.8 µg/L. The PFOS water concentrations in the contaminated site were below the stated guidelines with an average of 0.072 µg/L. The same conclusions were observed in a 2016 publication (Bhavsar et al., 2016). Contrastingly, the U.S. EPA has established a drinking water advisory of 0.07 µg/L of PFOS based on reproductive and developmental effects. The advisory is applied to the sum of PFOS and PFOA. Our numerical data exceeds the U.S. EPA advisory with a sum of 0.096 ± 0.011 µg/L. The U.S. EPA advisory is in accordance with the Australian Department of Health guidelines, whereas the World Health Organization and European Union have not developed regulatory limits for PFOS in drinking water.

4.2 Laboratory PFOS Concentrations

The measured concentrations proved to be lower than the desired nominal concentrations; for example, the low, medium, and high stock solutions were 60%, 108%, and 56% of the nominal concentration. In the residual solutions the low, medium, and high solutions measured 65%, 52%, and 89% of the nominal. These lower measured concentrations were possibly due to equipment and human error while producing the stock solution. However, even with the lower than desired measured nominal concentrations, we still observed a change in protein and metabolite abundance. This proves that PFOS had effects below the lowest observable effect concentration (LOEC). As previously mentioned, the Canada FWQG for PFOS determined that 6.8 µg/L is the guideline for

protection of freshwater organisms (CEPA, 2018). This guideline was calculated from a species sensitivity distribution using long-term toxicity data from amphibian, fish, invertebrate, and plant species (CEPA, 2018). The low treatment group in our data was below the FWQG, but the medium and high treatment groups exceeded this guideline.

No relationships between PFOS exposure, survival, length, weight, and reproductive output were identified, as there were no significant differences between the control and treatment groups, suggesting that the tested concentrations were not high enough to elicit toxicological effects on the measured endpoints. However, this research does demonstrate that PFOS had the ability to bio-concentrate within snail tissue. It was observed that lower concentrations provided a higher bio-concentration factor, indicating that PFOS tissue concentrations do not increase proportionally and instead are dependent on the concentration. This trend has also been observed in other studies that investigated BCF of PFAS, including PFOS (Inoue et al., 2012).

4.3 Laboratory Proteomics

4.3.1 Acyl-CoA Thioesterase 2

Acot2 is a protein-coding gene that was identified within the significant gene list produced from the laboratory chronic exposure. Acot2 is found in the mitochondria and is responsible for hydrolyzing acyl-CoA to the free fatty acid and Coenzyme A (CoASH) (Hunt, Rautanen, Westin, Svensson, & Alexson, 2006). According to the CTD, this protein is within the top ten proteins that are known to interact with PFOS (Davis et al., 2023) . Overall, the database highlighted eleven different published articles that all reported PFOS exposure resulted in increased expression of Acot2. A study conducted by Marques et al.,

2020 that introduced ~0.36 mg/kg/day of PFOS through a dietary route noted an increase of the Acot2 protein with greater than 5-fold induction. In the present study, we observed an increase in abundance of Acot2 only in the snails exposed to the high treatment. It is possible that this observation was only noted in the high treatment group as the low treatment group was below the FWQG and the medium group only slightly exceeds the guideline. Comparing the previously mentioned study to ours, the PFOS dietary exposure concentration was closest to our high treatment group, where we observed similar results. Marques et al., (2020) importantly notes that this protein is related to lipid catabolism, fatty acid metabolism, and lipid synthesis pathways (Marques et al., 2020).

4.3.2 Significant Protein Class: NRTKs and MMPs

Our data indicated that the significant proteins represented two protein classes – non-receptor tyrosine kinase (NRTKs) and matrix metalloproteinases (MMPs), also known as metalloprotease. We observed 127 out of 289 significant proteins related to Nasopharynx respiratory epithelial cells and 128 out of 289 related to the bronchial epithelial cells suggesting that PFOS is targeting proteins responsible for pulmonary pathways.

Protein tyrosine kinases (PTKs) are a family of enzymes that are responsible for catalyzing the transfer of the γ (gamma) phosphate of ATP to tyrosine residues located on protein substrates (Hubbard & Till, 2000). The phosphorylation of tyrosine residues allows for binding sites to be created for downstream signaling proteins to bind to (Hubbard & Till, 2000). PTKs are known to regulate a plethora of biological processes such as cell proliferation, migration, differentiation, and survival (Blaukat, 2007). Furthermore, this

protein class plays an important role in the development of diseases such as immunodeficiency, atherosclerosis, psoriasis, osteoporosis, diabetes, and cancer (Blaukat, 2007). PTKs are divided into two main families, which are the receptor tyrosine kinase (RTKs) and NRTKs.

MMPs are a family of zinc-dependent extracellular matrix endopeptidases (Cabral-Pacheco et al., 2020). These proteins have the ability to break down collagen and remodel components of the extracellular matrix. Such cellular processes play a role in physiologic tissue remodeling and wound repair (Cabral-Pacheco et al., 2020). Furthermore, these enzymes can cleave peptide bonds, thus changing cell-matrix and cell-cell interactions, as well as activation or inactivation of growth factors, cytokines, and cell-surface receptors (Sternlicht & Werb, 2001). MMPs have the ability to influence processes including inflammatory diseases, embryonic development, and cancer (Nelson, Fingleton, Rothenberg, & Matrisian, 2000).

According to Aschner et al., (2014) NRTKs and MMPs are two protein classes that have been observed to play a role in Acute Lung Injury, which is now classified as Acute Respiratory Distress Syndrome in Humans, a progressive lung condition characterized by arterial hypoxemia, shortness of breath, and respiratory failure (Matthay & Zemans, 2011). Some clinical disorders associated with Acute Respiratory Distress Syndrome include pneumonia, sepsis, gastric aspiration, and respiratory trauma (Matthay & Zemans, 2011). These protein classes represent potential biomarkers and targets for therapeutic intervention (Aschner, Zemans, Yamashita, & Downey, 2014). A Disintegrin and Metalloproteinases (ADAMs) are a part of the MMPs family and are commonly expressed in lung cells (Dreymueller, Uhlig, & Ludwig, 2015). ADAMs have been

known to play a pivotal role in mediating cell-specific acute lung inflammation (Dreymueller et al., 2015). They are also able to modify cell surfaces to regulate various functions through enzymatic cleaving and releasing from the plasma membrane (Primakoff & Myles, 2000). This function is notably observed in the release of tumor necrosis factor α (TNF-α) that is a cytokine involved in inflammatory response (Primakoff & Myles, 2000). An article reported an increase in abundance of Adam8, Adam9, Adam15, and Adam33 during acute or chronic lung inflammation (Dreymueller et al., 2015). In our dataset, A Disintegrin and Metalloproteinase with Thrombospondin motifs (ADAMTSs) were present. Notably, Adamts7, Adamts9, and Adamts18 were found within the significant proteins of our dataset, and all experienced a decrease in protein abundance. The different observed trends may be due to the proteins in our dataset being ADAMTSs and not ADAMs. ADAMTSs and ADAMs are closely related families of proteolytic enzymes (Przemyslaw, Boguslaw, Elzbieta, & Malgorzata, 2013). The ADAMs family of proteins contain both transmembrane and secreted proteins, while the ADAMTSs family only have proteins in the secreted forms, and mostly process extracellular matrix components (Blobel & Apte; Przemyslaw et al., 2013).

Furthermore, research has identified a link between pulmonary injury, which is linked to ALI, and ski wax exposure. Ski wax is often used in winter sports to optimize sporting equipment, however professional ski-waxers are known to have PFAS within their human serum (Freberg et al., 2010). A 2010 study tested 13 professional ski-waxers and found elevated levels of 11 perfluorinated carboxylic and 8 perfluorinated sulfonic acids in their serum (Freberg et al., 2010). The highest concentrations within the serum samples were of PFOA, followed by PFOS and PFNA (Freberg et al., 2010). Scandinavian literature

found that smoking ski-wax-contaminated cigarettes led to a case of pulmonary edema (Ström & Alexandersen, 1990). Other studies described that aerosolized Teflon particles from other waterproofing agents such as waterproofing aerosols and leather protectors caused lung toxicity in mice (Laliberté, Sanfaçon, & Blais, 1995; SMILKSTEIN et al., 1993; Yamashita & Tanaka, 1995). In 1997, a study investigated the relationship between ski wax and pulmonary function by exposing humans to ski-wax vapors. It was concluded that the inhalation exposure showed impaired carbon monoxide diffusion capacity (Hoffman, Clifford, & Varkey, 1997). Diffusion capacity of the lungs for carbon monoxide (DLCO) is a test performed to assess lung function; a decreased or low DLCO is indicative of poor lung health and relative to potential pulmonary disease (Modi & Cascella, 2020; Nakazawa, Shimizu, Mogi, & Kuwano, 2018). Lastly, in 1998, there was a documented case study of a patient with Acute Respiratory Distress Syndrome caused by ski wax (Bracco & Favre, 1998). The U.S EPA have banned the use of fluorinated ski wax in all competitions across North America for the 2020-2021 winter season (EPA, 2022). Moreover, the International Ski and Snowboard Federation has prohibited C8-fluorocarbon products from being used at their events (EPA, 2022).

Prior research has indicated that there is a relationship between PFAS and Acute Lung Injury. We have specifically seen this link through PFAS containing ski wax and humans. In our study we have identified potential biomarkers of Acute Lung Injury which are proteins belonging to the classes of NRTKs and MMPs. Some proteins related to NRTKs such as Abl1 and Ptk2b experienced a decrease, while Srms, Jak2, and Lck experienced an increase in abundance. Proteins related to MMPs displayed distinct trends. Mme, Adamts7, Adamts9, and Adamts18 decreased in protein abundance across all

treatments. In the high treatment group Mep1b, Uqcrc2, Inpp5e, and Nrdc increased in protein abundance. Acute Lung Injury is characterized by excessive inflammatory responses which leads to the accumulation of protein rich edema fluid (Aschner et al., 2014). NRTKs and MMPs play a role in controlling and inducing signaling pathways thus resulting in inflammatory responses, specifically these proteins interact bidirectionally as NRTKs trigger the secretion of MMPs (Aschner et al., 2014).

4.3.3 Mitogen Activated Protein Kinase (Sperm/Fertility)

The mitogen-activated protein kinases (MAPKs) are a group of protein kinases that are responsible for regulating diverse cellular processes such as motility, differentiation, cell proliferation, and survival (Cargnello & Roux, 2011). The three main components of MAPKs are the p38MAPK, ERK1/2, and JNK pathways (Cargnello & Roux, 2011) . Activation of these three main signaling pathways in Sertoli cells, cells that are necessary for spermatogenesis, have been linked with environmental toxicant-induced blood-testis barrier (BTB) disruption (Wong & Cheng, 2011). Sertoli cells have been identified in the freshwater snail *Biomphalaria glabrata* and play a role in spermatogenesis (de Jong-Brink, Boer, Hommes, & Kodde, 1977). In addition, a paper published in 1984 mentions that the hermaphroditic gonads of freshwater snails, such as *Lymnaea stagnalis*, utilize tight junctions in the blood testis barrier (Jong-Brink, With, Hurkmans, & Sassen, 1984). In regards to reproductive functions, MAPKs in the testes are responsible for regulating spermatogenesis, sperm hyperactivation, and acrosome reaction (Almog & Naor, 2010). Environmental toxicants, such as PFOS, can induce unregulated activation of MAPKs leading to pathophysiological effects on Sertoli and Leydig cells in the testes (Wong & Cheng, 2011).

It must be noted that activation of the p38 and ERK1/2 signaling pathways play a vital role in regulating tight and gap junctions while also influencing the redistribution of junction proteins in Sertoli cells (Wong & Cheng, 2011). PFOS targets Sertoli cells thus disrupting the BTB integrity and function leading to PFOS-induced male reproductive toxicity (Qiu et al., 2013). According to Qiu et al., (2013) PFOS decreased junction proteins, and increased proteins related to MAPK, p38 and ERK1/2 signaling pathways. These conclusions were determined using a p38 MAPK-selective inhibitor on male mice Sertoli cells. When PFOS was exposed to Sertoli cells, there was a loss of junction proteins and a deficiency of Sertoli cell junction barrier integrity (Qiu et al., 2013). However, the selective inhibitor was able to mitigate these outcomes, confirming that Sertoli cells in the BTB play a role in reproductive dysfunction induced by PFOS (Qiu et al., 2013). In our data set, multiple proteins related to the p38 MAPK displayed an increase in abundance in the low group. Specifically, Jak2, Zmynd11, Alox12b, Abl1, Il1a, Mif, Fpr2, and Ptk2b, found within our significant protein list, experienced an increase in abundance. Some proteins related to the ERK1/2 pathway also displayed an increase in abundance. Map3k15, increased in abundance in the high treatment, whereas Adamts7 and Ppp5c increased in the low and high treatment groups. Arhgef6 and Sele increased in the low and medium groups. Lastly, Jak2, and Zmynd11 increased in the medium and high treatment groups. This increase in MAPK p38 and the ERK1/2 pathways are consistent with other studies and suggests that PFOS exposure could affect the reproductive function of freshwater snails.

As previously mentioned, the JNK pathway also plays a pivotal role in reproductive processes. Environmental toxicants, such as the heavy metal cadmium, have been documented to increase apoptosis, polyubiquitination of proteins, and detachment of

gonocytes from Rat Sertoli cells (Yu, Hong, & Faustman, 2008). Moreover, a study that investigated MAPKs-mediated oxidative stress pathways in zebrafish embryos exposed to PFOS determined that this toxicant significantly altered JNK gene expression (Shi & Zhou, 2010). When sulforaphane was used to chemically inhibit the expression of MAPKs, there was a significant upregulation of Jnk1 and p38b (Shi & Zhou, 2010). These significant changes were observed in zebrafish exposed to 400 μg/L and 1000 μg/L of PFOS (Shi & Zhou, 2010). In our dataset, 4 out of the 6 proteins related to the JNK pathway experienced an increase in protein abundance in varying treatment groups. Ptk2b increased in the high treatment, Zmynd11 increased in the medium and high treatment, Arhgef6 increased in the low and medium treatments, and Il1A only increased in the low treatment. Due to previous research, it is probable that PFOS exposure is causing an increase in JNK pathway protein abundance, resulting in apoptosis of reproductive cells.

Acrosome reaction and calcium are factors unrelated to MAPKs, but also play a role in reproduction. The penultimate step of maturation of spermatozoa entails ensuring that the sperm is competent for fertilization (Ickowicz, Finkelstein, & Breitbart, 2012). This occurs via various biochemical and physiological modifications (Ickowicz et al., 2012). The ultimate step of fertilization is the acrosome reaction, which is an exocytotic process driven by an influx of Ca^{2+} that allows for the spermatozoon to pass through the zona pellucida and essentially allow for fusion of the sperm and egg (Florman, Tombes, First, & Babcock, 1989; Ickowicz et al., 2012). Pkdrej was a protein found within our significant protein list that relates to acrosome reaction. This protein is located within the head of sperm which interacts with the zona pellucida (Butscheid et al., 2006). Although little is known about this protein, it has been characterized in humans, mice, and sea urchin

(Butscheid et al., 2006). Notably, in sea urchin, Pkdrej homologues are likely to be involved in fertilization processes and in the induction of acrosome reaction (Butscheid et al., 2006). PFOS exposure resulted in an increase of Pkdrej abundance in the low and medium treatment groups, while the high treatment group closely resembled control abundance levels. In terms of calcium-related proteins, Caps2 experienced a decrease, and Syt1 experienced an increase in protein abundance across all treatment groups. One study concluded that signaling pathways involving tyrosine phosphorylation via PTK are negatively regulated by calcium in mouse epididymal spermatozoa (Ecroyd, Asquith, Jones, & Aitken, 2004). This suggests that the significant changes in PTK (NRTKs) and Ca^{2+} due to PFOS-exposure can negatively impact sperm production and thus have reproductive implications.

4.3.4 Cancer

By investigating changes in protein abundance, it is possible to identify cancer-related profiles. There is currently a concern, as PFAS has been linked to a plethora of health issues and diseases, including cancer. A two-year dietary exposure to ammonium perfluorooctanoate– a type of PFOA salt, caused a significant increase in Leydig cell tumors within the testes of male rats (Butenhoff, Kennedy, Chang, & Olsen, 2012). This is related to our study as we observed that Sertoli cells may be a potential PFOS target. PFOS and PFOA are also associated with hepatocellular adenomas in rats (Seacat et al., 2003). Furthermore, although it is difficult to determine the cause of cancer in humans, an increase in bladder cancer has been observed in individuals who are exposed to PFOS (Alexander, Olsen, Burris, Mandel, & Mandel, 2003). Our significant proteins were related to multiple types of potential cancers including various neoplasia, carcinoma,

leukemia, sarcoma, and ovarian cancers. Grm1 is a type of glutamate receptor that may play a role in tumor growth (Nord et al., 2014). An increase of Grm1 was documented in an aggressive bone tumor causing cancer (Nord et al., 2014). This protein was seen within our dataset; however it did not follow the same trend. Instead, the low and high treatments experienced a decrease in protein abundance while the medium treatment closely resembled the control. Although we are not seeing Grm1 follow the same trend, it was still identified as a significantly altered protein due to PFOS exposure. Therefore, it is possible that this protein could exhibit cancerous effects. Lastly, an increase of abundance in MMPs was present in lung tumors compared to non-malignant lung tissue (Merchant et al., 2017). As previously mentioned, MMPs were a class of significant proteins identified in our dataset. Although the cancerous effects of Grm1 and MMPs were not observed in PFOS exposure, these proteins could potentially be cancer biomarkers, an avenue that needs to be further explored.

4.4 Laboratory Metabolomics

At the metabolome level, riboflavin metabolism, carnitine synthesis, and beta oxidation of very long chain fatty acids were the top three enriched metabolite pathways.

4.4.1 Riboflavin Metabolism

In the present study, there were three annotated metabolites related to riboflavin found within our dataset which were Quinone, Dimethylbenzimidazole, and 7-Hydroxy-6-methyl-8-ribityl lumazine. Riboflavin, commonly known as Vitamin B_2, is known to play a role in a variety of metabolic pathways (Balasubramaniam & Yaplito-Lee, 2020). This essential vitamin can only be obtained through exogenous sources via the diet in the form

of free riboflavin or as flavoproteins such as flavin adenine dinucleotide (FAD) and flavin mononucleotide (FMN), which must be released from their bound carrier proteins (Balasubramaniam & Yaplito-Lee, 2020). In the stomach, the molecules will undergo protein denaturation and hydrolysis using FAD and FMN pyrophosphatase resulting in molecules used for energy metabolism (Balasubramaniam & Yaplito-Lee, 2020). This results in free riboflavin being transported into enterocytes by a Solute Carrier Family 52 Member 3 (*SLC52A3*), a carrier-mediated transporter, which functions to absorb riboflavin from the diet (Barile, Giancaspero, Leone, Galluccio, & Indiveri, 2016). The riboflavin available in the plasma is either bound to albumin and immunoglobulins, or converted into its coenzyme forms, whereas unbound riboflavins are hydrolyzed and excreted via urine in the form of free riboflavin (Balasubramaniam & Yaplito-Lee, 2020). Excess ingested riboflavin is removed from the body as there is little to no storage (Balasubramaniam & Yaplito-Lee, 2020) . It has been documented that even at supra-pharmacological doses, riboflavin has relatively low toxicity (Barile et al., 2016). The function of riboflavin as a diet supplement has been studied in multiple fish species such as rainbow trout (*Oncorhynchus mykiss*) and grass carp (*Ctenopharyngodon idella*) (Jiang et al., 2019; Woodward, 1982). This exogenous exposure resulted in a profound effect on growth, carcass composition, and biological processes such as antioxidant defense and enzymatic intestinal activity. Studies have documented that a riboflavin deficiency caused loss of appetite, stunted growth, and increased fish mortality (Phillips Jr & Brockway, 1957).

As previously mentioned, one aspect of riboflavin metabolism is the binding of the vitamin to albumin in the plasma for transport and energy metabolism. Serum albumin is one of the most abundant proteins in the plasma and is responsible for acting as a carrier

protein and binding large numbers of ligands such as amino acids, vitamins, and fatty acids (Zhang, Chen, Fei, Ma, & Gao, 2009). According to Zhang et al., (2009) PFOS exposure negatively affects the binding of riboflavin to serum albumin. Specifically, a more than 30% reduction in the binding ratio of riboflavin to serum albumin was observed (Zhang et al., 2009). It is probable that PFOS competes for the binding sites and the conformational changes of serum albumin are unfavorable for riboflavin (Zhang et al., 2009). The reduction of riboflavin binding to serum albumin suggests an inhibition of the riboflavin being transported through the body and thus decreasing energy metabolism and leading to riboflavin deficiency (Zhang et al., 2009).

In previous studies investigating hydrophilic vitamins in freshwater snails using traditional chemical assays, riboflavin (Vitamin B_2) was quantified in *Biomphalaria alexandrina*, *Bulinus truncatus*, and *Lymnaea truncatula* (Ponder, Fried, & Sherma, 2004). Another study using thin layer chromatographic analysis also identified and quantified riboflavin in the freshwater snail *Helisoma trivolvis* (Ponder et al., 2004). In the current study, snails were fed a consistent diet of shrimp pellets (Omega One® Sinking Catfish Pellets) and organic spinach leaves, which both contain riboflavin.

In this study PFOS exposure resulted in a decrease of dimethylbenzimidazole metabolite abundance in the low and medium group. This metabolite is a component of Vitamin B_{12} and is known to increase Vitamin B_{12} production (Wang, Zhang, Wang, Liu, & Liu, 2018). Furthermore, 7-Hydroxy-6-methyl-8-ribityl lumazine displayed an increase of metabolite abundance in the low and medium treatments. This metabolite is known to act as an inhibitor of riboflavin synthase, which is an enzyme that is used in the final step to produce riboflavin (Fischer et al., 2003). Lastly, there was no change in quinone

metabolite abundance. This suggests that PFOS is decreasing a potential metabolite that increases riboflavin production and is instead increasing a riboflavin inhibitor, thus resulting in a decrease of riboflavin metabolism.

4.4.2 Carnitine Synthesis

L-Carnitine (L-trimethyl-3-hydroxy-ammoniabutanoate) is an endogenous compound obtained from food sources, but is also synthesized in the liver and kidneys of humans using essential amino acids such as lysine and methionine (Vaz & Wanders, 2002). In order to regulate normal mitochondrial function, the carnitine acyltransferase pathway is used to remove excess acyl groups (Sharma & Black, 2009). A primary role of L-carnitine is in the transport of long chain fatty acids across the inner membrane of the mitochondria, and is an essential cofactor for B-oxidation of long-chain fatty acids (Cao et al., 2009). Interestingly, L-carnitine has protective characteristics for certain cells against toxicity (Chen et al., 2009). L-carnitine has been noted to inhibit apoptosis caused by antibiotic-induced reactive oxygen species and pathways, as well as apoptosis occurring in renal tubular cells in mice (Chen et al., 2009).

When renal tubular cells were exposed to PFOS it caused a decrease in cell viability. However, these degenerative effects were reversed with a treatment of L-carnitine (Y. G. Lee et al., 2022). It is known that PFOS has concentration-dependent effects on mitochondrial bioenergetics, which results in decreased ATP production, cell respiration, and an increase of proton leakage (Y. G. Lee et al., 2022). A study described that a pretreatment of 10 mM of L-carnitine mitigated these mitochondrial function effects resulting in an increase of ATP production and cellular respiration of renal tubular cells affected by 100-µM PFOS (Lee et al., 2022). Lastly, L-carnitine is known to protect renal

tubular cells from PFOS-mediated apoptosis (Y. G. Lee et al., 2022). PFOS exposure produces reactive oxygen species through the increased activation of the ERK 1/2 cascade thus leading to autophagy activation and eventually renal tubular cell apoptosis (Y. G. Lee et al., 2022). However, autophagy activation and apoptosis in renal tubular cells can be attenuated by the exposure of L-carnitine (Y. G. Lee et al., 2022). Overall, L-carnitine can mitigate the effects of PFOS-induced injury to renal tubular cells.

As previously discussed, proteins related to the ERK1/2 pathway had significantly altered abundances. PFOS exposure resulted in an increase of protein abundance in Map3k15, Adamts7, Ppp5c, Arhgef6, Sele, Jak2, and Zmynd11. In our dataset, L-carnitine, L-lysine, and N6,N6,N6-Trimethyl-L-lysine were found within our metabolite dataset and related to L-carnitine synthesis. These metabolites increased in abundance as L-carnitine increased in the medium treatment, L-lysine in the low and medium treatment, and N6,N6,N6-Trimethyl-L-lysine in the low. It is possible that the increase of metabolite abundance related to L-carnitine synthesis could play a role in mitigating PFOS-induced cellular degradation.

4.4.3 Beta oxidation of very long chain fatty acids

Beta-oxidation of very-long-chain fatty acids – which are composed of 24-26 carbon units, can occur in the mitochondria or peroxisomes (Talley & Mohiuddin, 2020). This oxidation essentially regulates the cell's energy requirements by breaking down fatty acids. Mitochondrial beta-oxidation of very-long-chain fatty acids converts free fatty acid molecules to acyl-CoA, which are then transported to the mitochondrial matrix using carnitine-specific transferase enzymes (Ribas & Vargas, 2022). In the mitochondrial matrix, an oxidation reaction catalyzed by multiple enzymes produces acetyl-CoA, utilized

in the Krebs cycle to further undergo complete oxidation (Ribas & Vargas, 2022). Peroxisomal beta-oxidation is similar to that of mitochondrial beta-oxidation however, some enzymatic steps differ**.** Notably, very-long-chain fatty acids are not dependent on carnitine-based molecules for transport into the peroxisomes (Talley & Mohiuddin, 2020). To be specific, due their size, very-long-chain fatty acids do not have the ability to pass organelle membranes via diffusion, and therefore are substrate-dependent (Talley & Mohiuddin, 2020). An experiment investigated the effects of hepatotoxicity elicited by PFOS and measured the rate of beta-oxidation to determine that the rates of total (peroxisomal and mitochondrial) and peroxisomal beta-oxidation were significantly higher in mice exposed to 5 or 10 mg/kg PFOS (Wan et al., 2012). In contrast, the mitochondrial beta-oxidation rates were lower in all PFOS-exposed mice compared to the control (Wan et al., 2012). An increase of both peroxisomal and mitochondrial beta-oxidation were observed in other studies assessing exposure to PFOS and PFOA (Bjork, Lau, Chang, Butenhoff, & Wallace, 2008; Kennedy et al., 2004).

In our dataset, a metabolite set enrichment analysis identified beta-oxidation of very-long-chain fatty acid pathways as an enriched group. Two metabolites related to this pathway were found within our dataset, that being L-carnitine and L-acetylcarnitine. These two metabolites are used in beta-oxidation as carriers to transport long-chain fatty acids. PFOS is known to play a role in beta-oxidation and subsequently lipid metabolism, as it mediates the activation of peroxisome proliferator-activated receptor-alpha (Ppar-a) (Bjork et al., 2008). In the present study, only Peroxisome Proliferator Activated Receptor Gamma (Ppar-g) was identified, however not at significant levels. Although we did not identify proteins related to peroxisome proliferator-activated receptors (PPARs), it is possible we

are seeing downstream effects within our metabolite data. In our data the low and medium treatment increased in abundance but the high treatment decreased in abundance of L-carnitine. We observed the opposite for L-acylcarnitine, with a decrease in the low and medium groups and increase in the high group. These findings suggest that PFOS exposure can also be reflected at the metabolome level. Acot2 was a protein identified in our dataset that is utilized in beta-oxidation of lipids in the mitochondria (Moffat et al., 2014). When Acot2 is in high abundance, higher beta-oxidation in hepatocytes occurs (Bekeova et al., 2023). Therefore, PFOS exposure may be causing proteome changes, thus resulting in an enrichment of metabolites related to beta-oxidation.

Chapter 5. Conclusion

This work contributes to important ecotoxicological information of PFAS and, namely PFOS. In this study, we exposed freshwater snails to PFAS *in-situ* at environmentally relevant concentrations. The field site selected is at ecological risk due to the PFAS contamination from historical usage of AFFF at a nearby airport. Apical endpoint evaluations revealed that the conditions did not significantly affect survival, growth, or reproduction. However, this site was contaminated over three decades ago, yet elevated levels of PFAS still persist, which demonstrates how recalcitrant this class of compounds is. Additionally, we exposed snails to PFOS in a controlled laboratory setting and also determined that apical endpoints were not affected to PFOS at the exposure concentrations selected. Nevertheless, we observed that PFOS has the ability to bioconcentrate within snail tissue even at relatively low concentrations.

Through proteomic and metabolomic approaches, we demonstrated that the proteome and metabolome of freshwater snails are sensitive to PFOS exposure at sublethal concentrations. The changed proteins represented NRTK, MMP, and MAPK pathways which play a role in acute lung injury and reproductive dysfunction. Specifically, NRTKs and MMPs are potential biomarkers that have been identified and are characteristic of biological pathways related to lung injury. In addition, altered proteins were also related to various potential types of cancer such as neoplasms, carcinoma, and leukemia. At the metabolome level, enrichment analysis provided mechanistic insight that PFOS exposure is affecting riboflavin metabolism, carnitine synthesis, and beta oxidation of very long chain fatty acids.

Although there has been a voluntary phase-out of some PFAS, the present work remains relevant, as these chemicals remain in our aquatic environments, thus posing a risk of exposure to aquatic species. Furthermore, our data helps fill knowledge gaps by understanding molecular level effects, especially at concentrations below the no-observed effect concentration. ‘Omic technology provides a multitude of detailed information, further studies using targeted approaches and developing standardized targeted assays should be investigated to validate these findings.

This research provides an understanding of PFAS mixtures and PFOS exposure repercussions on apical endpoints, tissue burden, and molecular-level response. These data will assist in the assessment of ecological risk and the necessity of more toxicological testing to be completed to confirm and gain further insight into the impact of these forever chemicals.

Reference List

Ahrens, L. (2011). Polyfluoroalkyl compounds in the aquatic environment: a review of their occurrence and fate. *Journal of Environmental Monitoring, 13*(1), 20-31.

Alexander, B., Olsen, G., Burris, J., Mandel, J., & Mandel, J. (2003). Mortality of employees of a perfluorooctanesulphonyl fluoride manufacturing facility. *Occupational and environmental medicine, 60*(10), 722-729.

Alm, R. R., & Stern, R. M. (1992). Aqueous film-forming foamable solution useful as fire extinguishing concentrate. In: Google Patents.

Almog, T., & Naor, Z. (2010). The role of Mitogen activated protein kinase (MAPK) in sperm functions. *Molecular and cellular endocrinology, 314*(2), 239-243.

Armitage, J., Cousins, I. T., Buck, R. C., Prevedouros, K., Russell, M. H., MacLeod, M., & Korzeniowski, S. H. (2006). Modeling global-scale fate and transport of perfluorooctanoate emitted from direct sources. *Environmental Science & Technology, 40*(22), 6969-6975.

Aschner, Y., Zemans, R. L., Yamashita, C. M., & Downey, G. P. (2014). Matrix metalloproteinases and protein tyrosine kinases: potential novel targets in acute lung injury and ARDS. *Chest, 146*(4), 1081-1091. doi:10.1378/chest.14-0397

Backe, W. J., Day, T. C., & Field, J. A. (2013). Zwitterionic, cationic, and anionic fluorinated chemicals in aqueous film forming foam formulations and groundwater from US military bases by nonaqueous large-volume injection HPLC-MS/MS. *Environmental Science & Technology, 47*(10), 5226-5234.

Balasubramaniam, S., & Yaplito-Lee, J. (2020). Riboflavin metabolism: role in mitochondrial function. *J. Transl. Genet. Genom, 4*, 285-306.

Barile, M., Giancaspero, T. A., Leone, P., Galluccio, M., & Indiveri, C. (2016). Riboflavin transport and metabolism in humans. *Journal of inherited metabolic disease, 39*, 545-557.

Bekeova, C., Han, J. I., Xu, H., Kerr, E., Blackburne, B., Lynch, S. C., . . . Beld, J. (2023). Acyl-CoA thioesterase-2 facilitates beta-oxidation in glycolytic skeletal muscle in a lipid supply dependent manner. *bioRxiv*, 2023.2006. 2027.546724.

Bhavsar, S. P., Fowler, C., Day, S., Petro, S., Gandhi, N., Gewurtz, S. B., . . . Morse, D. (2016). High levels, partitioning and fish consumption based water guidelines of perfluoroalkyl acids downstream of a former firefighting training facility in Canada. *Environment International, 94*, 415-423. doi:https://doi.org/10.1016/j.envint.2016.05.023

Bjork, J. A., Lau, C., Chang, S. C., Butenhoff, J. L., & Wallace, K. B. (2008). Perfluorooctane sulfonate-induced changes in fetal rat liver gene expression. *Toxicology, 251*(1), 8-20. doi:https://doi.org/10.1016/j.tox.2008.06.007

Blaukat, A. (2007). Tyrosine Kinases. In S. J. Enna & D. B. Bylund (Eds.), *xPharm: The Comprehensive Pharmacology Reference* (pp. 1-4). New York: Elsevier.

Blobel, C. P., & Apte, S. *ADAMs and ADAMTSs*: Encyclopedia of Respiratory Medicine. 2022:568-73. doi: 10.1016/B978-0-12-801238-3.11698-8. Epub 2021 Sep 17.

Bracco, D., & Favre, J.-B. (1998). Pulmonary Injury After Ski Wax Inhalation Exposure. *Annals of emergency medicine, 32*(5), 616-619. doi:https://doi.org/10.1016/S0196-0644(98)70043-5

Buck, R. C., Franklin, J., Berger, U., Conder, J. M., Cousins, I. T., De Voogt, P., . . . van Leeuwen, S. P. (2011). Perfluoroalkyl and polyfluoroalkyl substances in the environment: terminology, classification, and origins. *Integrated environmental assessment and management, 7*(4), 513-541.

Butenhoff, J. L., Kennedy, G. L., Chang, S.-C., & Olsen, G. W. (2012). Chronic dietary toxicity and carcinogenicity study with ammonium perfluorooctanoate in Sprague–Dawley rats. *Toxicology, 298*(1), 1-13. doi:https://doi.org/10.1016/j.tox.2012.04.001

Butscheid, Y., Chubanov, V., Steger, K., Meyer, D., Dietrich, A., & Gudermann, T. (2006). Polycystic kidney disease and receptor for egg jelly is a plasma membrane protein of mouse sperm head. *Molecular Reproduction and Development: Incorporating Gamete Research, 73*(3), 350-360.

Cabral-Pacheco, G. A., Garza-Veloz, I., Castruita-De la Rosa, C., Ramirez-Acuña, J. M., Perez-Romero, B. A., Guerrero-Rodriguez, J. F., . . . Martinez-Fierro, M. L. (2020). The Roles of Matrix Metalloproteinases and Their Inhibitors in Human Diseases. *Int J Mol Sci, 21*(24). doi:10.3390/ijms21249739

Cao, Y., Wang, Y.-x., Liu, C.-j., Wang, L.-x., Han, Z.-w., & Wang, C.-b. (2009). Comparison of pharmacokinetics of L-carnitine, Acetyl-L-carnitine and Propionyl-Lcarnitine after single oral administration of L-carnitine in healthy volunteers. *Clinical and Investigative Medicine (Online), 32*(1), E13-19.

Cargnello, M., & Roux, P. P. (2011). Activation and function of the MAPKs and their substrates, the MAPK-activated protein kinases. *Microbiol Mol Biol Rev, 75*(1), 50-83. doi:10.1128/mmbr.00031-10

CEPA. (2018). *Canadian Environmental Protection Act, 1999 Federal Environmental Quality Guidelines Perfluorooctane Sulfonate (PFOS).*

Chen, H.-H., Sue, Y.-M., Chen, C.-H., Hsu, Y.-H., Hou, C.-C., Cheng, C.-Y., . . . Chen, T.-H. (2009). Peroxisome proliferator-activated receptor alpha plays a crucial role in l -carnitine anti-apoptosis effect in renal tubular cells. *Nephrology Dialysis Transplantation, 24*(10), 3042-3049. doi:10.1093/ndt/gfp258

Clarke, A. H. (1981). The freshwater molluscs of Canada. *(No Title).*

Covich, A. P., Palmer, M. A., & Crowl, T. A. (1999). The role of benthic invertebrate species in freshwater ecosystems: zoobenthic species influence energy flows and nutrient cycling. *BioScience, 49*(2), 119-127.

Davis, Wiegers, Johnson, Sciaky, Wiegers, & Mattingly. (2023). Comparative Toxicogenomics database (CTD): update 2023. *Nucleic acids research, 51*(D1), D1257-D1262.

Davis, K. L., Aucoin, M. D., Larsen, B. S., Kaiser, M. A., & Hartten, A. S. (2007). Transport of ammonium perfluorooctanoate in environmental media near a fluoropolymer manufacturing facility. *Chemosphere, 67*(10), 2011-2019.

de Jong-Brink, M., Boer, H. H., Hommes, T. G., & Kodde, A. (1977). Spermatogenesis and the role of Sertoli cells in the freshwater snail Biomphalaria glabrata. *Cell Tissue Res, 181*(1), 37-58. doi:10.1007/bf00222773

de Solla, S. R., De Silva, A. O., & Letcher, R. J. (2012). Highly elevated levels of perfluorooctane sulfonate and other perfluorinated acids found in biota and surface water downstream of an international airport, Hamilton, Ontario, Canada.

Environment International, 39(1), 19-26. doi:https://doi.org/10.1016/j.envint.2011.09.011

DeWitt, J. C. (2015). *Toxicological effects of perfluoroalkyl and polyfluoroalkyl substances*. Retrieved from

Dreymueller, D., Uhlig, S., & Ludwig, A. (2015). ADAM-family metalloproteinases in lung inflammation: potential therapeutic targets. *American Journal of Physiology-Lung Cellular and Molecular Physiology, 308*(4), L325-L343.

Easton, S. (2008). *Canada's Chemicals Management Plan (CMP).* Paper presented at the Presentation at the Meeting of the Great Lakes Binational Toxics Strategy Substance Working Group, Chicago, IL, April.

Ecroyd, H., Asquith, K. L., Jones, R. C., & Aitken, R. J. (2004). The development of signal transduction pathways during epididymal maturation is calcium dependent. *Developmental biology, 268*(1), 53-63. doi:https://doi.org/10.1016/j.ydbio.2003.12.015

EPA, U. (2021). Draft Method 1633 Analysis of Per- and Polyfluoroalkyl Substances (PFAS) in Aqueous, Solid, Biosolids, and Tissue Samples by LC-MS/MS. In.

EPA, U. (2022). *Violations May Put Ski Wax Users at Risk from Illegal Perfluoroalkyl Substances*. (305S21001). Retrieved from https://www.epa.gov/system/files/documents/2022-01/pfasskiwax.pdf.

Fischer, M., Schott, A. K., Kemter, K., Feicht, R., Richter, G., Illarionov, B., . . . Bacher, A. (2003). Riboflavin synthase of Schizosaccharomyces pombe. Protein dynamics revealed by 19F NMR protein perturbation experiments. *BMC Biochem, 4*, 18. doi:10.1186/1471-2091-4-18

Florman, H. M., Tombes, R. M., First, N. L., & Babcock, D. F. (1989). An adhesion-associated agonist from the zona pellucida activates G protein-promoted elevations of internal Ca2+ and pH that mediate mammalian sperm acrosomal exocytosis. *Developmental biology, 135*(1), 133-146.

Flynn, R. W., Chislock, M. F., Gannon, M. E., Bauer, S. J., Tornabene, B. J., Hoverman, J. T., & Sepúlveda, M. S. (2019). Acute and chronic effects of perfluoroalkyl substance mixtures on larval American bullfrogs (Rana catesbeiana). *Chemosphere, 236*, 124350.

Freberg, B. I., Haug, L. S., Olsen, R., Daae, H. L., Hersson, M., Thomsen, C., . . . Ellingsen, D. G. (2010). Occupational Exposure to Airborne Perfluorinated Compounds during Professional Ski Waxing. *Environmental Science & Technology, 44*(19), 7723-7728. doi:10.1021/es102033k

George, S. E., Baker, T. R., & Baker, B. B. (2023). Nonlethal detection of PFAS bioaccumulation and biomagnification within fishes in an urban-and wastewater-dominant Great Lakes watershed. *Environmental Pollution, 321*, 121123.

Gewurtz, S. B., Bhavsar, S. P., Petro, S., Mahon, C. G., Zhao, X., Morse, D., . . . Drouillard, K. (2014). High levels of perfluoroalkyl acids in sport fish species downstream of a firefighting training facility at Hamilton International Airport, Ontario, Canada. *Environment International, 67*, 1-11. doi:https://doi.org/10.1016/j.envint.2014.02.005

Glüge, J., Scheringer, M., Cousins, I. T., DeWitt, J. C., Goldenman, G., Herzke, D., . . . Wang, Z. (2020). An overview of the uses of per-and polyfluoroalkyl substances (PFAS). *Environmental Science: Processes & Impacts, 22*(12), 2345-2373.

Gonzalez, D., Thompson, K., Quinones, O., Dickenson, E., & Bott, C. (2021). Assessment of PFAS fate, transport, and treatment inhibition associated with a simulated AFFF release within a WASTEWATER treatment plant. *Chemosphere, 262*, 127900.

Hawkins, C. P., & Furnish, J. K. (1987). Are snails important competitors in stream ecosystems? *Oikos*, 209-220.

Hoffman, M. D., Clifford, P. S., & Varkey, B. (1997). Acute effects of ski waxing on pulmonary function. *Medicine and science in sports and exercise, 29*(10), 1379-1382.

Horgan, R. P., & Kenny, L. C. (2011). 'Omic'technologies: genomics, transcriptomics, proteomics and metabolomics. *The Obstetrician & Gynaecologist, 13*(3), 189-195.

Hubbard, S. R., & Till, J. H. (2000). PROTEIN TYROSINE KINASE STRUCTURE AND FUNCTION. *Annual review of biochemistry, 69*(1), 373-398. doi:10.1146/annurev.biochem.69.1.373

Huryn, A. D., Benke, A. C., & Ward, G. M. (1995). Direct and indirect effects of geology on the distribution, biomass, and production of the freshwater snail Elimia. *Journal of the North American Benthological Society, 14*(4), 519-534.

Huset, C. A., Chiaia, A. C., Barofsky, D. F., Jonkers, N., Kohler, H.-P. E., Ort, C., . . . Field, J. A. (2008). Occurrence and mass flows of fluorochemicals in the Glatt Valley watershed, Switzerland. *Environmental Science & Technology, 42*(17), 6369-6377.

Ickowicz, D., Finkelstein, M., & Breitbart, H. (2012). Mechanism of sperm capacitation and the acrosome reaction: role of protein kinases. *Asian journal of andrology, 14*(6), 816.

Inoue, Y., Hashizume, N., Yakata, N., Murakami, H., Suzuki, Y., Kikushima, E., & Otsuka, M. (2012). Unique Physicochemical Properties of Perfluorinated Compounds and Their Bioconcentration in Common Carp Cyprinus carpio L. *Archives of Environmental Contamination and Toxicology, 62*(4), 672-680. doi:10.1007/s00244-011-9730-7

ISO. (2019). Water quality — Determination of perfluoroalkyl and polyfluoroalkyl substances (PFAS) in water — Method using solid phase extraction and liquid chromatography-tandem mass spectrometry (LC-MS/MS). In.

Jiang, W.-D., Chen, L., Liu, Y., Feng, L., Wu, P., Jiang, J., . . . Zhou, X.-Q. (2019). Impact and consequences of dietary riboflavin deficiency treatment on flesh quality loss in on-growing grass carp (Ctenopharyngodon idella). *Food & Function, 10*(6), 3396-3409.

Johnson, P. D., Bogan, A. E., Brown, K. M., Burkhead, N. M., Cordeiro, J. R., Garner, J. T., . . . Pip, E. (2013). Conservation status of freshwater gastropods of Canada and the United States. *Fisheries, 38*(6), 247-282.

Jong-Brink, M., With, N., Hurkmans, P., & Sassen, M. (1984). A morphological enzyme-cytochemical and physiological study of the blood-gonad barrier in the hermaphrodite snail Lymnaea stagnalis. *Cell Tissue Res, 235*, 593-600. doi:10.1007/BF00226957

Kennedy, G. L., Butenhoff, J. L., Olsen, G. W., O'Connor, J. C., Seacat, A. M., Perkins, R. G., . . . Farrar, D. G. (2004). The Toxicology of Perfluorooctanoate. *Critical Reviews in Toxicology, 34*(4), 351-384. doi:10.1080/10408440490464705

Kissa, E. (2001). *Fluorinated surfactants and repellents* (Vol. 97): CRC Press.

Laliberté, M., Sanfaçon, G., & Blais, R. (1995). Acute pulmonary toxicity linked to use of a leather protector. *Annals of emergency medicine, 25*(6), 841-844.

Lee, J. W., Choi, K., Park, K., Seong, C., Do Yu, S., & Kim, P. (2020). Adverse effects of perfluoroalkyl acids on fish and other aquatic organisms: A review. *Science of the Total Environment, 707*, 135334.

Lee, Y. G., Chou, H. C., Chen, Y. T., Tung, S. Y., Ko, T. L., Buyandelger, B., . . . Juan, S. H. (2022). L-Carnitine reduces reactive oxygen species/endoplasmic reticulum stress and maintains mitochondrial function during autophagy-mediated cell apoptosis in perfluorooctanesulfonate-treated renal tubular cells. *Sci Rep, 12*(1), 4673. doi:10.1038/s41598-022-08771-3

Lei, Y.-J., Tian, Y., Sobhani, Z., Naidu, R., & Fang, C. (2020). Synergistic degradation of PFAS in water and soil by dual-frequency ultrasonic activated persulfate. *Chemical Engineering Journal, 388*, 124215.

Liang, X., Martyniuk, C. J., & Simmons, D. B. (2020). Are we forgetting the "proteomics" in multi-omics ecotoxicology? *Comparative Biochemistry and Physiology Part D: Genomics and Proteomics, 36*, 100751.

Marques, E., Pfohl, M., Auclair, A., Jamwal, R., Barlock, B. J., Sammoura, F. M., . . . Slitt, A. L. (2020). Perfluorooctanesulfonic acid (PFOS) administration shifts the hepatic proteome and augments dietary outcomes related to hepatic steatosis in mice. *Toxicol Appl Pharmacol, 408*, 115250. doi:10.1016/j.taap.2020.115250

Martin, J. W., Mabury, S. A., Solomon, K. R., & Muir, D. C. (2013). Progress toward understanding the bioaccumulation of perfluorinated alkyl acids. *Environmental Toxicology and Chemistry, 32*(11), 2421-2423.

Martyniuk, C. J., & Simmons, D. B. (2016). Spotlight on environmental omics and toxicology: a long way in a short time. In (Vol. 19, pp. 97-101): Elsevier.

Matthay, M. A., & Zemans, R. L. (2011). The acute respiratory distress syndrome: pathogenesis and treatment. *Annu Rev Pathol, 6*, 147-163. doi:10.1146/annurev-pathol-011110-130158

Merchant, N., Nagaraju, G. P., Rajitha, B., Lammata, S., Jella, K. K., Buchwald, Z. S., . . . Ali, A. N. (2017). Matrix metalloproteinases: their functional role in lung cancer. *Carcinogenesis, 38*(8), 766-780. doi:10.1093/carcin/bgx063

Milley, S. A., Koch, I., Fortin, P., Archer, J., Reynolds, D., & Weber, K. P. (2018). Estimating the number of airports potentially contaminated with perfluoroalkyl and polyfluoroalkyl substances from aqueous film forming foam: A Canadian example. *Journal of environmental management, 222*, 122-131.

Modi, P., & Cascella, M. (2020). Diffusing capacity of the lungs for carbon monoxide.

Moffat, C., Bhatia, L., Nguyen, T., Lynch, P., Wang, M., Wang, D., . . . Claypool, S. M. (2014). Acyl-CoA thioesterase-2 facilitates mitochondrial fatty acid oxidation in the liver [S]. *Journal of lipid research, 55*(12), 2458-2470.

Moody, C. A., Martin, J. W., Kwan, W. C., Muir, D. C., & Mabury, S. A. (2002). Monitoring perfluorinated surfactants in biota and surface water samples following an accidental release of fire-fighting foam into Etobicoke Creek. *Environmental Science & Technology, 36*(4), 545-551.

Nakazawa, S., Shimizu, K., Mogi, A., & Kuwano, H. (2018). Low diffusing capacity, emphysema, or pulmonary fibrosis: who is truly pulling the lung cancer strings? *J Thorac Dis, 10*(2), 600-602. doi:10.21037/jtd.2017.12.145

Nelson, A. R., Fingleton, B., Rothenberg, M. L., & Matrisian, L. M. (2000). Matrix metalloproteinases: biologic activity and clinical implications. *J Clin Oncol, 18*(5), 1135-1149. doi:10.1200/jco.2000.18.5.1135

Nord, K. H., Lilljebjörn, H., Vezzi, F., Nilsson, J., Magnusson, L., Tayebwa, J., . . . Szuhai, K. (2014). GRM1 is upregulated through gene fusion and promoter swapping in chondromyxoid fibroma. *Nature genetics, 46*(5), 474-477.

O'Connor, W., Partridge, G., Fielder, S., Woolley, L., & Palanisami, T. (2020). Evaluation of practical technologies for Per-and Polyfluoroalkyl Substance (PFAS) remediation in marine fish hatcheries.

OECD. (2013). Synthesis paper on per-and polyfluorinated chemicals (PFCs). *Organisation for Economic Cooperation and Development (OECD)*.

OECD. (2016). *Test No. 243: Lymnaea stagnalis Reproduction Test*.

Patterson, S. D., & Aebersold, R. H. (2003). Proteomics: the first decade and beyond. *Nature genetics, 33*(3), 311-323.

Paul, A. G., Jones, K. C., & Sweetman, A. J. (2009). A first global production, emission, and environmental inventory for perfluorooctane sulfonate. *Environmental Science & Technology, 43*(2), 386-392.

Phillips Jr, A. M., & Brockway, D. R. (1957). The nutrition of trout: IV. Vitamin requirements. *The Progressive Fish-Culturist, 19*(3), 119-123.

Pino, L. K., Just, S. C., MacCoss, M. J., & Searle, B. C. (2020). Acquiring and analyzing data independent acquisition proteomics experiments without spectrum libraries. *Molecular & Cellular Proteomics, 19*(7), 1088-1103.

Place, B. J., & Field, J. A. (2012). Identification of novel fluorochemicals in aqueous film-forming foams used by the US military. *Environmental Science & Technology, 46*(13), 7120-7127.

Ponder, E., Fried, B., & Sherma, J. (2004). Thin-layer chromatographic analysis of hydrophilic vitamins in standards and from Helisoma trivolvis snails. *Acta chromatographica, 14*, 70-81.

Prevedouros, K., Cousins, I. T., Buck, R. C., & Korzeniowski, S. H. (2006). Sources, fate and transport of perfluorocarboxylates. *Environmental Science & Technology, 40*(1), 32-44.

Primakoff, P., & Myles, D. G. (2000). The ADAM gene family: surface proteins with adhesion and protease activity. *Trends in Genetics, 16*(2), 83-87. doi:10.1016/S0168-9525(99)01926-5

Prosser, R. S., Rodriguez-Gil, J. L., Solomon, K. R., Sibley, P. K., & Poirier, D. G. (2017). Effects of the herbicide surfactant MON 0818 on oviposition and viability of eggs of the ramshorn snail (Planorbella pilsbryi). *Environmental Toxicology and Chemistry, 36*(2), 522-531.

Przemyslaw, L., Boguslaw, H. A., Elzbieta, S., & Malgorzata, S. M. (2013). ADAM and ADAMTS family proteins and their role in the colorectal cancer etiopathogenesis. *BMB Rep, 46*(3), 139-150. doi:10.5483/bmbrep.2013.46.3.176

Qiu, L., Zhang, X., Zhang, X., Zhang, Y., Gu, J., Chen, M., . . . Wang, S.-L. (2013). Sertoli cell is a potential target for perfluorooctane sulfonate–induced reproductive dysfunction in male mice. *toxicological sciences, 135*(1), 229-240.

Ribas, G. S., & Vargas, C. R. (2022). Evidence that oxidative disbalance and mitochondrial dysfunction are involved in the pathophysiology of fatty acid oxidation disorders. *Cellular and Molecular Neurobiology, 42*(3), 521-532.

Rijnders, J., Bervoets, L., Prinsen, E., Eens, M., Beemster, G. T., AbdElgawad, H., & Groffen, T. (2021). Perfluoroalkylated acids (PFAAs) accumulate in field-exposed snails (Cepaea sp.) and affect their oxidative status. *Science of the Total Environment, 790*, 148059.

Schultz, M. M., Higgins, C. P., Huset, C. A., Luthy, R. G., Barofsky, D. F., & Field, J. A. (2006). Fluorochemical mass flows in a municipal wastewater treatment facility. *Environmental Science & Technology, 40*(23), 7350-7357.

Seacat, A. M., Thomford, P. J., Hansen, K. J., Clemen, L. A., Eldridge, S. R., Elcombe, C. R., & Butenhoff, J. L. (2003). Sub-chronic dietary toxicity of potassium perfluorooctanesulfonate in rats. *Toxicology, 183*(1-3), 117-131.

Sharma, S., & Black, S. M. (2009). Carnitine homeostasis, mitochondrial function and cardiovascular disease. *Drug Discovery Today: Disease Mechanisms, 6*(1-4), e31-e39.

Shi, X., & Zhou, B. (2010). The Role of Nrf2 and MAPK Pathways in PFOS-Induced Oxidative Stress in Zebrafish Embryos. *toxicological sciences, 115*(2), 391-400. doi:10.1093/toxsci/kfq066

Simmons, D. B., Cowie, A. M., Koh, J., Sherry, J. P., & Martyniuk, C. J. (2019). Label-free and iTRAQ proteomics analysis in the liver of zebrafish (Danio rerio) following dietary exposure to the organochlorine pesticide dieldrin. *Journal of proteomics, 202*, 103362.

Sinclair, G. M., Long, S. M., & Jones, O. A. (2020). What are the effects of PFAS exposure at environmentally relevant concentrations? *Chemosphere, 258*, 127340.

Smilkstein, M., Burton, B., Keene, W., Barnett, M., Hedberg, K., Fleming, D., & Jacobson, C. (1993). Acute Respiratory Illness Linked To Use of Aerosol Leather Conditioner-Oregon, 1992 (Reprinted From Mmwr, Vol 41, Pg 965-967, 1993). *Jama-Journal Of The American Medical Association, 269*(5), 568-569.

Sternlicht, M. D., & Werb, Z. (2001). How matrix metalloproteinases regulate cell behavior. *Annu Rev Cell Dev Biol, 17*, 463-516. doi:10.1146/annurev.cellbio.17.1.463

Ström, E., & Alexandersen, O. (1990). Lungeskade i forbindelse med smøring av ski. *Tidsskr Nor Laegeforen, 110*, 3614-3616.

Sunderland, E. M., Hu, X. C., Dassuncao, C., Tokranov, A. K., Wagner, C. C., & Allen, J. G. (2019). A review of the pathways of human exposure to poly-and perfluoroalkyl substances (PFASs) and present understanding of health effects. *Journal of exposure science & environmental epidemiology, 29*(2), 131-147.

Talley, J. T., & Mohiuddin, S. S. (2020). Biochemistry, fatty acid oxidation.

Vaz, F. M., & Wanders, R. J. (2002). Carnitine biosynthesis in mammals. *Biochemical Journal, 361*(3), 417-429.

Wan, H., Zhao, Y., Wei, X., Hui, K., Giesy, J., & Wong, C. K. (2012). PFOS-induced hepatic steatosis, the mechanistic actions on β-oxidation and lipid transport. *Biochimica et Biophysica Acta (BBA)-General Subjects, 1820*(7), 1092-1101.

Wang, D., Zhang, B., Wang, J., Liu, H., & Liu, J. (2018). Effects of dietary 5, 6-dimethylbenzimidazole supplementation on vitamin B12 supply, lactation

performance, and energy balance in dairy cows during the transition period and early lactation. *Journal of dairy science, 101*(3), 2144-2147.

Wong, E. W. P., & Cheng, C. Y. (2011). Impacts of environmental toxicants on male reproductive dysfunction. *Trends in Pharmacological Sciences, 32*(5), 290-299. doi:https://doi.org/10.1016/j.tips.2011.01.001

Woodward, B. (1982). Riboflavin supplementation of diets for rainbow trout. *The Journal of Nutrition, 112*(5), 908-913.

Xia, J., Psychogios, N., Young, N., & Wishart, D. S. (2009). MetaboAnalyst: a web server for metabolomic data analysis and interpretation. *Nucleic acids research, 37*(suppl_2), W652-W660.

Yamashita, M., & Tanaka, J. (1995). Pulmonary collapse and pneumonia due to inhalation of a waterproofing aerosol in female CD-I Mice. *Journal of Toxicology: Clinical Toxicology, 33*(6), 631-637.

Yu, X., Hong, S., & Faustman, E. M. (2008). Cadmium-induced activation of stress signaling pathways, disruption of ubiquitin-dependent protein degradation and apoptosis in primary rat Sertoli cell-gonocyte cocultures. *toxicological sciences, 104*(2), 385-396.

Zhang, X., Chen, L., Fei, X. C., Ma, Y. S., & Gao, H. W. (2009). Binding of PFOS to serum albumin and DNA: insight into the molecular toxicity of perfluorochemicals. *BMC Mol Biol, 10*, 16. doi:10.1186/1471-2199-10-16

Appendix.

Appendix A. PCA of water parameters collected from YSI Probes

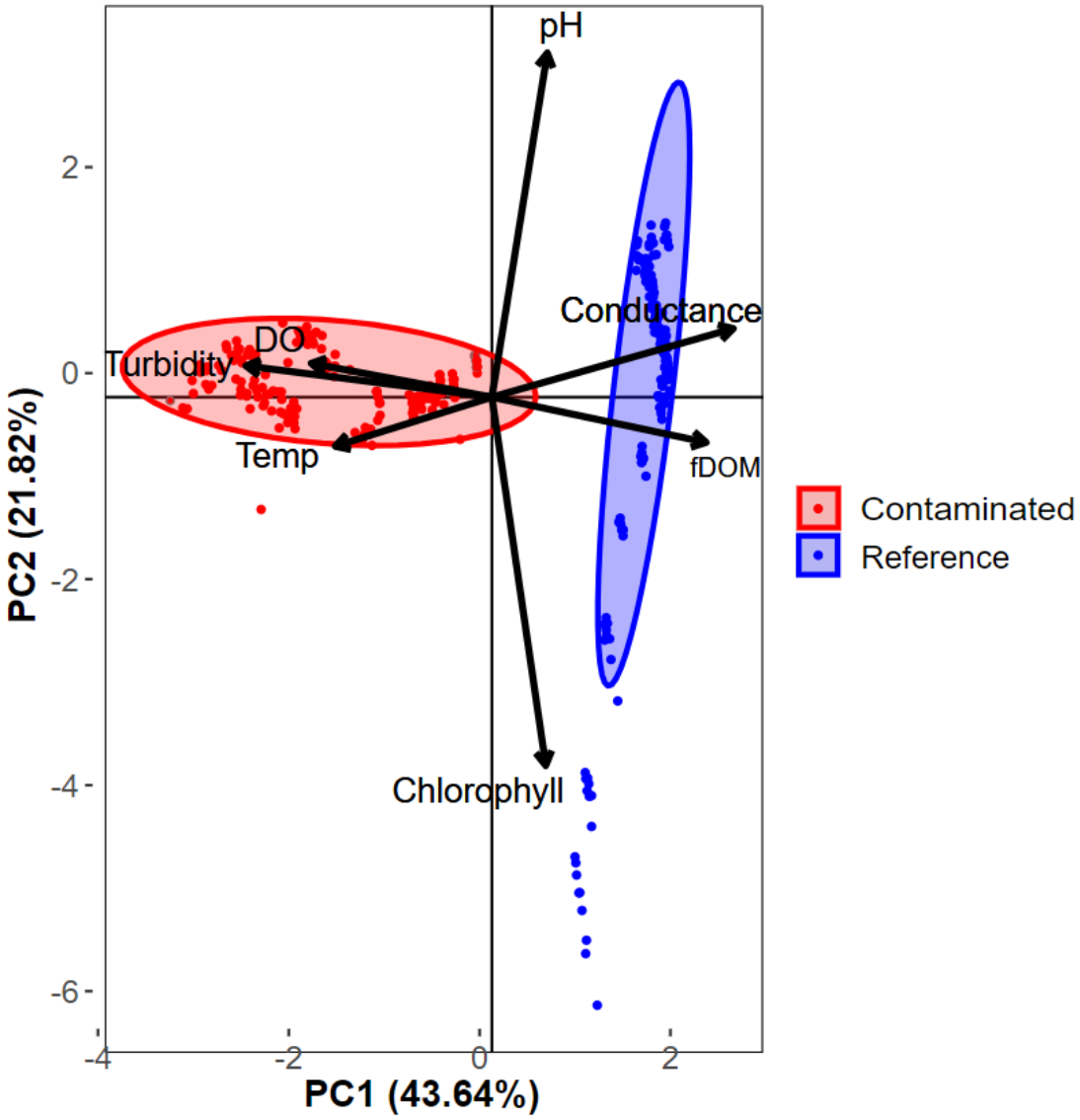

Appendix B. Burlington-National Lab for Environmental Testing Water Chemistry Analysis

Note:

645.1 – Bisphenol A Replacement Products 2022-23 refers to the name of the project which the analysis was financially coded under by the National Laboratories for Environmental Testing (Environment and Climate Change Canada, Burlington, ON).

Nebo Road refers to the Reference site.

Binbrook refers to the Contaminated site.

Burlington-National Lab for Environmental Testing
867 Lakeshore Road
Burlington, ON
L7S 1A1

Report of Analysis

645.1-Bisphenol A Replacement Products 2022-23

Ève Gilroy
Water Science & Technology
Aquatic Contaminants Research

867 Lakeshore Road
Burlington, ON
L7S 1A1

Work Order: B22F157

Reported: 2022-09-15
Printed: 2022-09-15

Authorization: Mlvosevic

Mirjana Ivosevic For Pat Falletta
Manager, NLET

The results reported pertain only to the samples as received and tested by the Environment and Climate Change Canada (ECCC) laboratory indicated in the report. To ensure that parts of this certificate of analysis are not taken out of context, this certificate shall not be reproduced, except in full, without approval of the laboratory.

These ECCC laboratories are accredited by the Canadian Association for Laboratory Accreditation (CALA) to the standard ISO/IEC 17025 for each of the reported analytes, except where indicated by an asterisk (*). Please refer to the CALA website (www.cala.ca) to view the full Scope(s) of Accreditation.

ABSTRACT

Unit	Description
mg/L	milligram per litre
pH	pH units

Qualifier	Description
1	Holding Time Exceeded
3	Result has been rechecked
NA	Not Applicable
P	Pass
*	Non-Accredited Analysis/Analyte

SAMPLE DESCRIPTION †

Lab ID	Client ID	Station ID	Matrix	Sampled YYYY/MM/DD/HH:MM-TZ	Date Received	Sample Type
B22F157-01	*2022-CMP-01 NEBO ROAD*		Water	2022-06-30 13:26 EST	2022-06-30	Pooled
B22F157-02	*2022-CMP-02 Binbrook*		Water	2022-06-30 13:26 EST	2022-06-30	Pooled

† All information included herein is supplied by the submitter and transcribed from the submission sheet into this portion of the report.

REFERENCES

Method ID	Laboratory Method	Reference
B0002W	B_Alk_pH_Cond_Water-PC Titrate	NLET SOP: Analysis of Conductivity, pH and Alkalinity ...
B0257W	B_Ca_Mg_Na_K_Si_Water- ICPOES	NLET SOP: Analysis of Ca, Mg, Na, K and SiO2 in Waters..
B0255W	B_DIC_DOC_Water-UV Digest IR	NLET SOP: Analysis of Dissolved Organic and Inorganic Carbon ....
B0252W	B_F_Cl_NO3_SO4-Water-Chemical Suppress IC	NLET SOP: Analysis of F, Cl, NO3 and SO4 in Waters ..
B0250W	B_NH3_Water-Color Phenate CFA	NLET SOP: Analysis of Ammonia Nitrogen in Waters by Automated CFA ..
B0262W	B_NO3-NO2_Water- Color Cd Reduction CFA	NLET SOP: Analysis of Nitrate-Nitrite Nitrogen in Waters by Automated CFA..
B0268W	B_TKN_TKNDiss-Water-Blck DigestPhenate Color CFA	NLET SOP: Analysis of TKN in Precipitation, Surface and Ground Waters...
B0271W	B_TP_Diss_Par_InBotDigest-Water-Color AscAcid CFA	NLET SOP: Analysis of Total Phosphorous in Waters by Auto-CFA ..
B0012W	B_TSS_VSS_Water-Gravimetry	NLET SOP: Determination of Total and Volatile Suspended Solids in Water

SAMPLE RESULTS

Physical and Aggregate Properties (Water)

		Lab ID:	B22F157-01	B22F157-02	-	-	-	-
		Client ID:	2022-CMP-01 NEBO ROAD	2022-CMP-02 Binbrook	-	-	-	-
Method - B_Alk_pH_Cond_Water-PC Titrate								
Alkalinity, Total (CaCO3)	mg/L		156	152	-	-	-	-
pH	pH		7.65	7.96	-	-	-	-
Alkalinity, Gran (CaCO3)	mg/L		Not Applicable/Non applicable	Not Applicable/Non applicable	-	-	-	-
Alkalinity, phenolphthalein	mg/L		Not Applicable/Non applicable	Not Applicable/Non applicable	-	-	-	-
Method - B_Ca_Mg_Na_K_Si_Water- ICPOES								
Hardness	mg/L		177	189	-	-	-	-
Method - B_TSS_VSS_Water-Gravimetry								
Solids, Total Suspended (TSS)	mg/L		60.0	112	-	-	-	-

Major Ions (Water)

		Lab ID:	B22F157-01	B22F157-02	-	-	-	-
		Client ID:	2022-CMP-01 NEBO ROAD	2022-CMP-02 Binbrook	-	-	-	-
Method - B_Ca_Mg_Na_K_Si_Water- ICPOES								
Calcium	mg/L		49.4	47.8	-	-	-	-
Magnesium	mg/L		13.1	17.0	-	-	-	-
Sodium	mg/L		80.6	90.9	-	-	-	-
Potassium	mg/L		2.31	3.16	-	-	-	-
Silica	mg/L		1.86	5.28	-	-	-	-
Method - B_F_Cl_NO3_SO4-Water-Chemical Suppress IC								
Fluoride	mg/L		0.36	0.28	-	-	-	-
Chloride	mg/L		123	136	-	-	-	-
Sulfate	mg/L		22.0	39.5	-	-	-	-

Nutrients (Water)

		Lab ID:	B22F157-01	B22F157-02	-	-	-	-
		Client ID:	2022-CMP-01 NEBO ROAD	2022-CMP-02 Binbrook	-	-	-	-
Method - B_DIC_DOC_Water-UV Digest IR								
Carbon, Dissolved Organic	mg/L		10.1	13.3	-	-	-	-
Carbon, Dissolved Inorganic	mg/L		37.0 [1]	34.8 [1]	-	-	-	-
Method - B_NH3_Water-Color Phenate CFA								
Ammonia as N	mg/L		0.079	0.095	-	-	-	-
Method - B_NO3-NO2_Water- Color Cd Reduction CFA								
Nitrate/Nitrite as N	mg/L		0.018	0.013	-	-	-	-
Method - B_TKN_TKNDiss-Water-Blck DigestPhenate Color CFA								
Nitrogen, Total Kjeldahl *	mg/L		0.826 [1] [3]	1.50 [1]	-	-	-	-
Method - B_TP_Diss_Par_InBotDigest-Water-Color AscAcid CFA								
Phosphorus, Total	mg/L		0.266	0.258	-	-	-	-

QUALITY CONTROL RESULTS

Burlington-National Lab for Environmental Testing

Accuracy

The accuracy of a methodology used to produce sample data is determined by the analysis of quality control samples. These samples are purchased from certified reference suppliers or created in-house from stock standards.

The results of the accuracy quality control data are reported as Percent Recovery (% Rec) and are as follows:

Major Ions
BJG0027 - BJG0027-BS1

Parameter	Result	Unit	Expected	% Rec	% Limits	Notes
Calcium	77.5	mg/L	77.800	99.6	95-105	
Magnesium	48.0	mg/L	47.500	101	95-105	
Sodium	59.7	mg/L	59.000	101	93-107	
Potassium	11.2	mg/L	11.200	100	95-105	
Silica	15.2	mg/L	15.000	101	95-105	

Major Ions
BJG0027 - BJG0027-BSD1

Parameter	Result	Unit	Expected	% Rec	% Limits	Notes
Calcium	78.3	mg/L	77.800	101	95-105	
Magnesium	48.1	mg/L	47.500	101	95-105	
Sodium	59.9	mg/L	59.000	102	93-107	
Potassium	11.3	mg/L	11.200	101	95-105	
Silica	15.3	mg/L	15.000	102	95-105	

Major Ions
BJG0027 - BJG0027-SRM1

Parameter	Result	Unit	Expected	% Rec	% Limits	Notes
Calcium	0.51	mg/L	0.48800	105	90-110	
Magnesium	0.28	mg/L	0.29400	96.9	90-110	
Sodium	2.59	mg/L	2.6600	97.4	90-110	
Potassium	0.25	mg/L	0.25200	98.4	90-110	
Silica	0.87	mg/L	0.87500	99.7	90-110	

Major Ions
BJG0114 - BJG0114-BS1

Parameter	Result	Unit	Expected	% Rec	% Limits	Notes
Fluoride	0.77	mg/L	0.76700	101	80-120	
Chloride	20.0	mg/L	20.000	99.9	95-105	
Sulfate	40.8	mg/L	41.200	99.0	95-105	

Major Ions
BJG0114 - BJG0114-BSD1

Parameter	Result	Unit	Expected	% Rec	% Limits	Notes
Fluoride	0.77	mg/L	0.76700	101	80-120	
Chloride	20.1	mg/L	20.000	101	95-105	
Sulfate	41.1	mg/L	41.200	99.8	95-105	

Major Ions
BJG0114 - BJG0114-SRM1

Parameter	Result	Unit	Expected	% Rec	% Limits	Notes
Fluoride	0.02	mg/L	0.018000	107	80-120	
Chloride	3.75	mg/L	3.7900	98.9	90-110	
Sulfate	1.10	mg/L	1.1300	97.4	90-110	

QUALITY CONTROL RESULTS
(Continued)

Burlington-National Lab for Environmental Testing

Accuracy (Continued)

Major Ions
BJG0114 - BJG0114-SRM2

Parameter	Result	Unit	Expected	% Rec	% Limits	Notes
Fluoride	0.11	mg/L	0.11400	96.2	50-150	
Chloride	22.7	mg/L	22.800	99.7	90-110	
Sulfate	24.9	mg/L	25.000	99.7	90-110	

Major Ions
BJG0114 - BJG0114-SRM3

Parameter	Result	Unit	Expected	% Rec	% Limits	Notes
Fluoride	0.04	mg/L	0.040000	95.8	75-125	
Chloride	1.42	mg/L	1.4400	98.9	90-110	
Sulfate	2.42	mg/L	2.4300	99.5	90-110	

Major Ions
BJG0114 - BJG0114-SRM4

Parameter	Result	Unit	Expected	% Rec	% Limits	Notes
Fluoride	0.09	mg/L	0.10040	91.8	65-135	
Chloride	0.10	mg/L	0.099800	101	70-130	
Sulfate	0.12	mg/L	0.099900	120	30-170	

Major Ions
BJG0114 - BJG0114-SRM5

Parameter	Result	Unit	Expected	% Rec	% Limits	Notes
Fluoride	0.20	mg/L	0.20080	97.2	85-115	
Chloride	14.8	mg/L	14.970	99.0	95-105	
Sulfate	14.9	mg/L	14.985	99.2	90-110	

Major Ions
BJG0114 - BJG0114-SRM6

Parameter	Result	Unit	Expected	% Rec	% Limits	Notes
Fluoride	0.49	mg/L	0.50200	98.5	80-120	
Chloride	39.8	mg/L	39.920	99.7	95-105	
Sulfate	79.4	mg/L	79.920	99.4	95-105	

Major Ions
BJG0114 - BJG0114-SRM7

Parameter	Result	Unit	Expected	% Rec	% Limits	Notes
Fluoride	0.02	mg/L	0.018000	105	80-120	
Chloride	3.77	mg/L	3.7900	99.5	90-110	
Sulfate	1.11	mg/L	1.1300	97.8	90-110	

Major Ions
BJG0114 - BJG0114-SRM8

Parameter	Result	Unit	Expected	% Rec	% Limits	Notes
Fluoride	0.11	mg/L	0.11400	97.8	50-150	
Chloride	23.0	mg/L	22.800	101	90-110	
Sulfate	25.3	mg/L	25.000	101	90-110	

QUALITY CONTROL RESULTS
(Continued)

Burlington-National Lab for Environmental Testing

Accuracy (Continued)

Major Ions
BJG0114 - BJG0114-SRM9

Parameter	Result	Unit	Expected	% Rec	% Limits	Notes
Fluoride	0.04	mg/L	0.040000	97.2	75-125	
Chloride	1.44	mg/L	1.4400	100	90-110	
Sulfate	2.45	mg/L	2.4300	101	90-110	

Major Ions
BJG0114 - BJG0114-SRMA

Parameter	Result	Unit	Expected	% Rec	% Limits	Notes
Fluoride	0.09	mg/L	0.10040	92.8	65-135	
Chloride	0.10	mg/L	0.099800	101	70-130	
Sulfate	0.12	mg/L	0.099900	117	30-170	

Major Ions
BJG0114 - BJG0114-SRMB

Parameter	Result	Unit	Expected	% Rec	% Limits	Notes
Fluoride	0.20	mg/L	0.20080	97.3	85-115	
Chloride	14.9	mg/L	14.970	99.8	95-105	
Sulfate	15.0	mg/L	14.985	100	90-110	

Major Ions
BJG0114 - BJG0114-SRMC

Parameter	Result	Unit	Expected	% Rec	% Limits	Notes
Fluoride	0.50	mg/L	0.50200	99.9	80-120	
Chloride	40.2	mg/L	39.920	101	95-105	
Sulfate	80.3	mg/L	79.920	100	95-105	

Nutrients
BJF0194 - BJF0194-BS1

Parameter	Result	Unit	Expected	% Rec	% Limits	Notes
Ammonia as N	0.711	mg/L	0.70000	102	95-105	
Nitrate/Nitrite as N	1.04	mg/L	1.0542	99.1	95-105	

Nutrients
BJF0194 - BJF0194-BSD1

Parameter	Result	Unit	Expected	% Rec	% Limits	Notes
Ammonia as N	0.679	mg/L	0.70000	97.0	95-105	
Nitrate/Nitrite as N	1.07	mg/L	1.0542	101	95-105	

Nutrients
BJF0194 - BJF0194-SRM1

Parameter	Result	Unit	Expected	% Rec	% Limits	Notes
Ammonia as N	0.050	mg/L	0.052000	96.2	90-110	
Nitrate/Nitrite as N	0.022	mg/L	0.023000	95.7	70-130	

Nutrients
BJF0194 - BJF0194-SRM2

Parameter	Result	Unit	Expected	% Rec	% Limits	Notes
Ammonia as N	0.159	mg/L	0.15997	99.4	85-115	
Nitrate/Nitrite as N	0.051	mg/L	0.047984	106	85-115	

QUALITY CONTROL RESULTS
(Continued)

Burlington-National Lab for Environmental Testing

Accuracy (Continued)

Nutrients
BJG0060 - BJG0060-BS1

Parameter	Result	Unit	Expected	% Rec	% Limits	Notes
Carbon, Dissolved Organic	6.8	mg/L	6.8000	100	90-110	
Carbon, Dissolved Inorganic	27.4	mg/L	26.800	102	94-106	

Nutrients
BJG0060 - BJG0060-BSD1

Parameter	Result	Unit	Expected	% Rec	% Limits	Notes
Carbon, Dissolved Organic	6.8	mg/L	6.8000	99.8	90-110	
Carbon, Dissolved Inorganic	27.5	mg/L	26.800	103	94-106	

Nutrients
BJG0060 - BJG0060-SRM1

Parameter	Result	Unit	Expected	% Rec	% Limits	Notes
Carbon, Dissolved Organic	0.8	mg/L	0.82000	98.5	70-130	
Carbon, Dissolved Inorganic	1.9	mg/L	1.8300	105	70-130	

Nutrients
BJG0060 - BJG0060-SRM2

Parameter	Result	Unit	Expected	% Rec	% Limits	Notes
Carbon, Dissolved Organic	14.5	mg/L	15.000	96.8	95-105	

Nutrients
BJG0060 - BJG0060-SRM3

Parameter	Result	Unit	Expected	% Rec	% Limits	Notes
Carbon, Dissolved Organic	1.4	mg/L	1.4400	97.8	90-110	
Carbon, Dissolved Inorganic	21.0	mg/L	20.800	101	94-106	

Nutrients
BJG0084 - BJG0084-BS1

Parameter	Result	Unit	Expected	% Rec	% Limits	Notes
Phosphorus, Total	0.421	mg/L	0.40300	104	95-105	

Nutrients
BJG0084 - BJG0084-BSD1

Parameter	Result	Unit	Expected	% Rec	% Limits	Notes
Phosphorus, Total	0.415	mg/L	0.40300	103	95-105	

Nutrients
BJG0084 - BJG0084-SRM1

Parameter	Result	Unit	Expected	% Rec	% Limits	Notes
Phosphorus, Total	0.0090	mg/L	0.010125	88.9	85-115	

Nutrients
BJG0084 - BJG0084-SRM2

Parameter	Result	Unit	Expected	% Rec	% Limits	Notes
Phosphorus, Total	0.0397	mg/L	0.040150	98.9	90-110	

QUALITY CONTROL RESULTS
(Continued)

Burlington-National Lab for Environmental Testing

Accuracy (Continued)

Nutrients
BJG0084 - BJG0084-SRM3

Parameter	Result	Unit	Expected	% Rec	% Limits	Notes
Phosphorus, Total	0.0806	mg/L	0.080000	101	0-200	

Nutrients
BJG0183 - BJG0183-BS1

Parameter	Result	Unit	Expected	% Rec	% Limits	Notes
Nitrogen, Total Kjeldahl	0.341	mg/L	0.36448	93.6	92-108	

Nutrients
BJG0183 - BJG0183-BS2

Parameter	Result	Unit	Expected	% Rec	% Limits	Notes
Nitrogen, Total Kjeldahl	0.339	mg/L	0.36448	93.0	92-108	

Nutrients
BJG0183 - BJG0183-BS3

Parameter	Result	Unit	Expected	% Rec	% Limits	Notes
Nitrogen, Total Kjeldahl	0.345	mg/L	0.36448	94.7	92-108	

Nutrients
BJG0183 - BJG0183-BSD1

Parameter	Result	Unit	Expected	% Rec	% Limits	Notes
Nitrogen, Total Kjeldahl	0.347	mg/L	0.36448	95.2	92-108	

Nutrients
BJG0183 - BJG0183-SRM1

Parameter	Result	Unit	Expected	% Rec	% Limits	Notes
Nitrogen, Total Kjeldahl	0.085	mg/L	0.10000	85.0	70-130	

Nutrients
BJG0183 - BJG0183-SRM2

Parameter	Result	Unit	Expected	% Rec	% Limits	Notes
Nitrogen, Total Kjeldahl	0.666	mg/L	0.66406	100	90-110	

Nutrients
BJG0183 - BJG0183-SRM3

Parameter	Result	Unit	Expected	% Rec	% Limits	Notes
Nitrogen, Total Kjeldahl	0.091	mg/L	0.10000	91.0	70-130	

Nutrients
BJG0183 - BJG0183-SRM4

Parameter	Result	Unit	Expected	% Rec	% Limits	Notes
Nitrogen, Total Kjeldahl	0.688	mg/L	0.66406	104	90-110	

Nutrients
BJG0183 - BJG0183-SRM5

Parameter	Result	Unit	Expected	% Rec	% Limits	Notes
Nitrogen, Total Kjeldahl	0.087	mg/L	0.10000	87.0	70-130	

QUALITY CONTROL RESULTS
(Continued)

Burlington-National Lab for Environmental Testing

Accuracy (Continued)

Nutrients
BJG0183 - BJG0183-SRM6

Parameter	Result	Unit	Expected	% Rec	% Limits	Notes
Nitrogen, Total Kjeldahl	0.706	mg/L	0.66406	106	90-110	

Nutrients
BJG0183 - BJG0183-SRM7

Parameter	Result	Unit	Expected	% Rec	% Limits	Notes
Nitrogen, Total Kjeldahl	0.104	mg/L	0.10000	104	70-130	

Nutrients
BJG0183 - BJG0183-SRM8

Parameter	Result	Unit	Expected	% Rec	% Limits	Notes
Nitrogen, Total Kjeldahl	0.704	mg/L	0.66406	106	90-110	

Physical and Aggregate Properties
BJF0195 - BJF0195-BS1

Parameter	Result	Unit	Expected	% Rec	% Limits	Notes
Alkalinity, Total (CaCO3)	258	mg/L	253.00	102	95-105	
pH	8.39	pH	8.3600	100	90-110	
Alkalinity, phenolphthalein	4.79	mg/L	5.5000	87.1	40-160	

Physical and Aggregate Properties
BJF0195 - BJF0195-BSD1

Parameter	Result	Unit	Expected	% Rec	% Limits	Notes
Alkalinity, Total (CaCO3)	259	mg/L	253.00	102	95-105	
pH	8.44	pH	8.3600	101	90-110	
Alkalinity, phenolphthalein	6.30	mg/L	5.5000	115	40-160	

Physical and Aggregate Properties
BJF0195 - BJF0195-SRM1

Parameter	Result	Unit	Expected	% Rec	% Limits	Notes
pH	6.98	pH	6.8300	102	95-105	
Alkalinity, Gran (CaCO3)	6.78	mg/L	6.5200	104	90-110	

Physical and Aggregate Properties
BJF0195 - BJF0195-SRM4

Parameter	Result	Unit	Expected	% Rec	% Limits	Notes
pH	6.88	pH	6.8650	100	95-105	

Physical and Aggregate Properties
BJG0004 - BJG0004-BS1

Parameter	Result	Unit	Expected	% Rec	% Limits	Notes
Solids, Total Suspended (TSS)	65.4	mg/L	71.800	91.1	80-120	
Solids, Volatile Suspended (VSS)	<5.0	mg/L			80-120	

QUALITY CONTROL RESULTS
(Continued)

Burlington-National Lab for Environmental Testing

Accuracy (Continued)

Physical and Aggregate Properties
BJG0004 - BJG0004-BSD1

Parameter	Result	Unit	Expected	% Rec	% Limits	Notes
Solids, Total Suspended (TSS)	68.9	mg/L	71.800	96.0	80-120	
Solids, Volatile Suspended (VSS)	<5.0	mg/L			80-120	

QUALITY CONTROL RESULTS
(Continued)

Burlington-National Lab for Environmental Testing

Precision

The precision of sample data is measured by the analysis of replicate samples. The relative percent difference (% RPD) is an indicator as to the level of precision of the data. The level of % RPD can vary depending upon the parameter and methodology. Low % RPDs for concentrations above the limit of quantitation indicate good precision, however the % RPD will rise as results approach the detection limit.

The results of the precision quality control data are as follows:

Major Ions
BJG0027 - BJG0027-DUP1
Sample B22G009-07

Parameter	Result	Unit	Source Result	% RPD	% RPD Limits	Notes
Calcium	36.1	mg/L	35.5	1.68	10	
Magnesium	9.80	mg/L	9.81	0.102	10	
Sodium	13.2	mg/L	13.2	0.00	10	
Potassium	1.63	mg/L	1.64	0.612	10	
Silica	0.42	mg/L	0.42	0.237	10	

Major Ions
BJG0114 - BJG0114-DUP1
Sample B22F151-02

Parameter	Result	Unit	Source Result	% RPD	% RPD Limits	Notes
Fluoride	0.07	mg/L	0.07	1.57	10	
Chloride	8.69	mg/L	8.62	0.762	10	
Sulfate	15.3	mg/L	15.2	1.16	10	

Major Ions
BJG0114 - BJG0114-DUP2
Sample B22G035-03

Parameter	Result	Unit	Source Result	% RPD	% RPD Limits	Notes
Fluoride	0.09	mg/L	0.09	7.08	10	
Chloride	16.1	mg/L	16.1	0.287	10	
Sulfate	19.2	mg/L	19.2	0.257	10	

Nutrients
BJF0194 - BJF0194-DUP1
Sample B22F150-03

Parameter	Result	Unit	Source Result	% RPD	% RPD Limits	Notes
Ammonia as N	0.080	mg/L	0.076	5.13	10	
Nitrate/Nitrite as N	0.248	mg/L	0.244	1.63	10	

Nutrients
BJG0060 - BJG0060-DUP1
Sample B22F069-70

Parameter	Result	Unit	Source Result	% RPD	% RPD Limits	Notes
Carbon, Dissolved Organic	0.2	mg/L	0.2		10	
Carbon, Dissolved Inorganic	0.3	mg/L	0.3	5.51	10	

Nutrients
BJG0084 - BJG0084-DUP1
Sample B22F136-09

Parameter	Result	Unit	Source Result	% RPD	% RPD Limits	Notes
Phosphorus, Total	0.151	mg/L	0.170	12.0	15	

QUALITY CONTROL RESULTS
(Continued)

Burlington-National Lab for Environmental Testing

Precision (Continued)

Nutrients
BJG0084 - BJG0084-DUP2
Sample B22G017-07

Parameter	Result	Unit	Source Result	% RPD	% RPD Limits	Notes
Phosphorus, Total	0.0129	mg/L	0.0133	3.05	15	

Physical and Aggregate Properties
BJF0195 - BJF0195-DUP1
Sample B22F153-01

Parameter	Result	Unit	Source Result	% RPD	% RPD Limits	Notes
Alkalinity, Total (CaCO3)	202	mg/L	201	0.200	10	
pH	8.23	pH	8.13	1.16	10	
Alkalinity, Gran (CaCO3)	Not Applicable/Non applicable	mg/L	0.00		40	
Alkalinity, phenolphthalein	Not Applicable/Non applicable	mg/L	<0.10		40	

Physical and Aggregate Properties
BJF0195 - BJF0195-DUP2
Sample B22F157-01

Parameter	Result	Unit	Source Result	% RPD	% RPD Limits	Notes
Alkalinity, Total (CaCO3)	152	mg/L	156	2.46	10	
pH	7.99	pH	7.65	4.41	10	
Alkalinity, Gran (CaCO3)	Not Applicable/Non applicable	mg/L	Not Applicable/Non applicable		40	
Alkalinity, phenolphthalein	Not Applicable/Non applicable	mg/L	Not Applicable/Non applicable		40	

Physical and Aggregate Properties
BJG0004 - BJG0004-DUP1
Sample B22F154-05

Parameter	Result	Unit	Source Result	% RPD	% RPD Limits	Notes
Solids, Total Suspended (TSS)	<5.0	mg/L	<5.0		8.99	
Solids, Volatile Suspended (VSS)	Not Applicable/Non applicable	mg/L	<5.0		9.19	

Physical and Aggregate Properties
BJG0004 - BJG0004-DUP2
Sample B22F156-02

Parameter	Result	Unit	Source Result	% RPD	% RPD Limits	Notes
Solids, Total Suspended (TSS)	<5.0	mg/L	<5.0		8.99	
Solids, Volatile Suspended (VSS)	Not Applicable/Non applicable	mg/L	<5.0		9.19	

QUALITY CONTROL RESULTS
(Continued)

Burlington-National Lab for Environmental Testing

Precision (Continued)

Physical and Aggregate Properties

BJG0027 - BJG0027-DUP1

Sample B22G009-07

Parameter	Result	Unit	Source Result	% RPD	% RPD Limits	Notes
Hardness	130	mg/L	129	1.12	200	

QUALITY CONTROL RESULTS
(Continued)

Burlington-National Lab for Environmental Testing

Recovery

The recovery of a parameter is determined by spiking a sample with a known amount of analyte. Recovery checks for any interferences which may be present in the analysis of the samples. It can check the methodology used in any sample preparation prior to analysis. Recovery is also an indirect method of determining accuracy and precision.

The results of the recovery quality control data are reported as Percent Recovery (% Rec) and are as follows:

Major Ions
BJG0027 - BJG0027-MS1
Sample B22G009-07

Parameter	Expected	Result	Unit	Source Result	% Rec	% Rec Limits	Notes
Calcium	20.000	55.1	mg/L	35.5	98.0	90-110	
Magnesium	20.000	30.0	mg/L	9.81	101	91.6-108.4	
Sodium	20.000	33.1	mg/L	13.2	99.5	90-110	
Potassium	20.000	21.5	mg/L	1.64	99.3	91.6-108.4	
Silica	20.000	20.6	mg/L	0.42	101	91.6-108.4	

Major Ions
BJG0114 - BJG0114-MS1
Sample B22G023-11

Parameter	Expected	Result	Unit	Source Result	% Rec	% Rec Limits	Notes
Fluoride	0.50000	0.60	mg/L	0.09	101	92.5-107.5	
Chloride	15.000	30.8	mg/L	16.0	98.5	90-110	
Sulfate	15.000	33.8	mg/L	19.0	98.5	90-110	

Nutrients
BJF0194 - BJF0194-MS1
Sample B22F151-02

Parameter	Expected	Result	Unit	Source Result	% Rec	% Rec Limits	Notes
Ammonia as N	0.37200	0.373	mg/L	<0.005	100	85-115	
Nitrate/Nitrite as N	0.60000	0.945	mg/L	0.333	102	90-110	

Nutrients
BJG0060 - BJG0060-MS1
Sample B22A011-27

Parameter	Expected	Result	Unit	Source Result	% Rec	% Rec Limits	Notes
Carbon, Dissolved Organic	1.9800	6.5	mg/L	4.9	79.9	60-140	
Carbon, Dissolved Inorganic	4.9340	9.1	mg/L	4.2	98.9	92.5-107.5	

Nutrients
BJG0084 - BJG0084-MS1
Sample B22A011-35

Parameter	Expected	Result	Unit	Source Result	% Rec	% Rec Limits	Notes
Phosphorus, Total	0.020000	0.0763	mg/L	0.0564	99.5	90-110	

Nutrients
BJG0183 - BJG0183-MS1
Sample B22A011-19

Parameter	Expected	Result	Unit	Source Result	% Rec	% Rec Limits	Notes
Nitrogen, Total Kjeldahl	0.20000	0.183	mg/L	<0.014	91.5	80-120	

QUALITY CONTROL RESULTS
(Continued)

Burlington-National Lab for Environmental Testing

Blank

The blank sample lacks the parameters of interest, and is used to detect contamination during sample handling, preparation, and/or analysis.

The results of the blank quality control data are as follows:

Major Ions
BJG0027 - BJG0027-BLK1

Parameter	Result	Unit	Notes
Calcium	<0.01	mg/L	
Magnesium	<0.01	mg/L	
Sodium	<0.01	mg/L	
Potassium	<0.03	mg/L	
Silica	<0.01	mg/L	

Major Ions
BJG0027 - BJG0027-BLK2

Parameter	Result	Unit	Notes
Calcium	<0.01	mg/L	
Magnesium	<0.01	mg/L	
Sodium	<0.01	mg/L	
Potassium	<0.03	mg/L	
Silica	<0.01	mg/L	

Major Ions
BJG0114 - BJG0114-BLK1

Parameter	Result	Unit	Notes
Fluoride	<0.01	mg/L	
Chloride	<0.01	mg/L	
Sulfate	<0.01	mg/L	

Major Ions
BJG0114 - BJG0114-BLK2

Parameter	Result	Unit	Notes
Fluoride	<0.01	mg/L	
Chloride	<0.01	mg/L	
Sulfate	<0.01	mg/L	

Major Ions
BJG0114 - BJG0114-BLK3

Parameter	Result	Unit	Notes
Fluoride	<0.01	mg/L	
Chloride	<0.01	mg/L	
Sulfate	<0.01	mg/L	

Nutrients
BJF0194 - BJF0194-BLK1

Parameter	Result	Unit	Notes
Ammonia as N	<0.005	mg/L	
Nitrate/Nitrite as N	<0.005	mg/L	

QUALITY CONTROL RESULTS
(Continued)

Burlington-National Lab for Environmental Testing

Blank (Continued)

Nutrients
BJG0060 - BJG0060-BLK1

Parameter	Result	Unit	Notes
Carbon, Dissolved Organic	<0.2	mg/L	
Carbon, Dissolved Inorganic	<0.2	mg/L	

Nutrients
BJG0084 - BJG0084-BLK1

Parameter	Result	Unit	Notes
Phosphorus, Total	<0.0005	mg/L	

Nutrients
BJG0084 - BJG0084-BLK2

Parameter	Result	Unit	Notes
Phosphorus, Total	<0.0005	mg/L	

Nutrients
BJG0183 - BJG0183-BLK1

Parameter	Result	Unit	Notes
Nitrogen, Total Kjeldahl	<0.014	mg/L	

Nutrients
BJG0183 - BJG0183-BLK2

Parameter	Result	Unit	Notes
Nitrogen, Total Kjeldahl	<0.014	mg/L	

Nutrients
BJG0183 - BJG0183-BLK3

Parameter	Result	Unit	Notes
Nitrogen, Total Kjeldahl	<0.014	mg/L	

Nutrients
BJG0183 - BJG0183-BLK4

Parameter	Result	Unit	Notes
Nitrogen, Total Kjeldahl	<0.014	mg/L	

Physical and Aggregate Properties
BJF0195 - BJF0195-BLK1

Parameter	Result	Unit	Notes
Alkalinity, Total (CaCO3)	Not Applicable/Non applicable	mg/L	
pH	5.75	pH	P
Alkalinity, phenolphthalein	Not Applicable/Non applicable	mg/L	

QUALITY CONTROL RESULTS
(Continued)

Burlington-National Lab for Environmental Testing

Blank (Continued)

Physical and Aggregate Properties
BJG0004 - BJG0004-BLK1

Parameter	Result	Unit	Notes
Solids, Total Suspended (TSS)	<5.0	mg/L	
Solids, Volatile Suspended (VSS)	<5.0	mg/L	

Physical and Aggregate Properties
BJG0027 - BJG0027-BLK1

Parameter	Result	Unit	Notes
Hardness	<0.50	mg/L	

Physical and Aggregate Properties
BJG0027 - BJG0027-BLK2

Parameter	Result	Unit	Notes
Hardness	<0.50	mg/L	

Environment Canada / Environnement Canada

FORMULAIRE DE SOUMISSION D'ÉCHANTILLONS DU LEST

Laboratory / Laboratoire:

ELEMENT Client (Project) No. - No du projet (ENNOR)	Work Order No. - Numéro de demande d'analyse	Date/Time Rec'd - Date/Heure de réception	Temperature on Arrival - Température à l'arrivée (°C)	Courrier service - Service courrier	Tracking number - numéro de référence
845		JUN 30 2022			
Sampled by - Échantillonné par (F. Name, L. Name / Surnom, prénom)	Client Project Manager/Gestionnaire de projet (Client)	Submitter: Expéditeur (F. Name, L. Name / Surnom, prénom)	Submitter Email - Courriel de l'expéditeur	Submitter Tel - No. de tél. de l'expéditeur	Remarks, Site Description, Sample Descriptions, Preservation Comments, etc. / Remarques, Description du site, Description de l'échantillon, Commentaires sur la conservation etc.
	Evelyn Roy			( ) -	

Lab Sample No. / No du laboratoire	No. of containers / Nbre de récipients	Client / Field Sample No. / No d'échantillon du client	Client / Field Sample Alias No. / No d'échantillon alias du client (Alias)	Analyses Requested / Analyses demandées	ENVIRODAT Station ID / No de station ENVIRODAT	Sampled / Échantillonné: Date	Time/Heure	Time Zone / Fuseau horaire	Matrix / Matrice	Sample Type / Type d'échantillon	Perishable / Périssable / Agent de conservation	Remarks, Site Description, Sample Descriptions, Preservation Comments, etc. / Remarques, Description du site, Description de l'échantillon, Commentaires sur la conservation etc.
	(1-N)	(Required / Requis)	(Optional / Optionnel)	XX Metals-diss; XX DOC; XX Ammonia; XX Nitrate/Nitrite; XX TKN; XX TP; XX Cond, ALK, pH; XX Hardness-calc; XX TSS; XX Anions; XX Cations; XX	(LLNNLLNNNN)	(YYYY-MM-DD) (AAAA-MM-JJ)	(hh:mm)	e.g. EST	e.g. Water / Eau	ANI	Yes/No Oui/Non	(Optional / Optionnel)
1	8	2022 CMP-01		✓ ✓ ✓ ✓ ✓ ✓ ✓ ✓ ✓ ✓						*		F157 Nebo Rd Binbrook
2	8	2022 CMP-02		✓ ✓ ✓ ✓ ✓ ✓ ✓ ✓ ✓ ✓						*		

Metals Extraction/ Extraction des métaux	Metals in water/Métaux dans l'eau: Dissolved/Dissous ☐	Metals in water/Métaux dans l'eau: Extractable/Extractible ☐	Metals in water/Métaux dans l'eau Total/Totaux ☐	Metals in solid/Métaux dans solide: Extractable/Extractible ☐	Metals in solid/Métaux dans solide: Total Recoverable/Totaux récupérable ☐	Metals in solid/Métaux dans solide: Total/Totaux ☐

Sample Return/Retour d'échantillon: Will pick up sample after analysis complete/Collectera l'échantillon après l'analyse complétée ☐ Samples are non-hazardous and may be disposed after analysis completed / Les échantillons sont non-dangereux et peuvent être jetés après l'analyse complétée. ☐

Page 18 of 18 B22F157_1 Summary 2022 09 15 1425

Appendix C. Metabolomic Orbitrap Parameters

Appendix C1: HPLC gradient used for metabolomics.

Time (min)	%A[1]	%B[2]
0	100	0
15	0	100
17	0	100
20	100	0
24	100	0

[1] Solvent A: 90% Acetonitrile:10% Water, 10 mM ammonium formate, 0.1% formic acid

[2] Solvent B: 10 mM ammonium formate 0.1% formic acid.

Appendix C2: MS parameters for metabolomics

Heated-Electrospray Ionization Source	Setting
Heated-Electrospray Ionization Mode	Positive
Spray Voltage	3500 kV
Sheath Gas	60 Arb
Ion Transfer Tube Temperature	350°C

Vaporizer Temperature	400°C.
Aux Gas	5 Arb
Sweep Gas	2 Arb